Characterization of Optical Fibre Sensor Systems for Applications at High Temperatures

By

Yonghang Shen

Submitted for the degree of Doctor of Philosophy

to

City University

Measurement and Instrumentation Centre,
School of Engineering and
Mathematical Sciences
City University, London.

May 2005

Declaration

I declare that the work presented in this thesis, except those specifically declared, is all my own work carried out and finished at City University, London and Zhejiang University.

Table of Contents

Abstract

As a rapid progressing technical field, fibre-optic sensors based on different schemes can work properly over a wide temperature range and sense the change of many important parameters. In this thesis, two major types of fibre optic sensors are comprehensively investigated, which are the fibre thermometer based on the fluorescence lifetime detection scheme of some specific fluorescent materials and fibre optic sensors based on the wavelength interrogation scheme of some specific fibre Bragg gratings.

As well known, these two types of fibre optic sensors are normally most suitable for comparatively low or medium temperature range. Difficulties still exist for these two types of sensors to work properly at an extended higher temperature region. To enable these types of sensors to operate efficiently and stably at higher temperature regions, some key problems remain to be solved. The aim of the work in this thesis is to extend their working temperature range to above 800 ^{0}C by exploring some novel fluorescent materials and novel photosensitive optical fibres.

In the aspect of fluorescence based fibre thermometer, several types of fluorescent materials were tested to evaluate their fluorescence performance, and the Tm doped YAG crystal was finally chosen to act as the fluorescent sensing material in a new developed fibre thermometer after extensive test of its fluorescence characteristics. The experiments carried out in the laboratory confirmed that the crystal has a monotonic and smooth fluorescence lifetime decay characteristics from room temperature to 1200 ^{0}C and an observable strong fluorescence intensity over such a temperature range. A novel fibre thermometer has been developed by using the Tm doped YAG as the sensing material and a phase locked detection (PLD) circuit as the signal processing scheme. The results obtained after comprehensive tests performed in laboratory and industrial fields clearly indicate that the fibre thermometer has very good long term performance stability, fast dynamic response and high temperature measurement resolution.

In the aspect of FBG-based sensors, the focus has been on the development of novel photosensitive fibres, which can be used to fabricate strong FBGs with superior high temperature sustainability. By co-doping Sb or In into germanium doped silica fibres, several new photosensitive fibres have been developed by means of modified chemical vapour deposition

(MCVD) method. Strong gratings have been fabricated by exposing pieces of these fibres to the laser emission of an UV excimer laser working at 248 nm. Annealing tests on these gratings confirmed that the gratings were able to survive an annealing temperature of 800 ^{0}C or even 900 ^{0}C for 24 hours or more and still retain an observable reflectivity in the reflective spectrum. The results obtained from these tests fully show the potential of using these gratings in industrial applications.

Based on the extensive experimental tests on the photosensitivity of the fibres and on the high temperature sustainability of the gratings, the mechanisms concerned with the decay of the gratings and the photosensitivity of the fibres were further investigated. A novel theoretical model, named *cation hopping*, was presented to account for the experimental results obtained. According to this model, the vacancies existing in germanosilicate fibre are important in acquiring a high degree of photosensitivity, and the cations hopping away from the original localized positions during UV emission exposure are responsible for the changes in the refractive index.

As an important application of fibre optic sensors, heat flux measurement was performed by using both the fluorescent lifetime-based fibre thermometer and FBG-based fibre optic sensors. Results thus obtained show the great prospect of using these fibre sensors in actual industrial applications.

Acknowledgements

It would be definitely impossible to finish the work presented in this thesis without the enormous help and support from so many individuals and institutions. So great is the number in fact that I fear I may fail to recognize all who have contributed to this effort, but in gratitude I attempt to do so here.

Professor Kenneth T.V. Grattan, the chief supervisor of my thesis, is the first man I should mention. As the leading scientist in the field of fluorescence based fibre-optic thermometry, he has the full understanding and command on the development of the field. So many beneficial discussions have we made on the fluorescence and lifetime of some possible novel sensing materials, and these discussions result in finding of Tm:YAG crystal as applied finally in the related work of this thesis.

Dr. Tong Sun, the co-supervisor, is an energetic, smart and conscientious scholar. She seems always full of energy in exploring the essence of difficult issues and solving different problems. Her gifted feeling in the field of fibre Bragg grating enables us to enter the hall of high temperature sustainable gratings and the related photosensitive fibres.

Both Professor Grattan and Dr. Sun contribute financially to my research by permitting me to purchase time, materials and equipments. I thank them for their tireless funding raising efforts.

Professor Xu Liu at Zhejiang University, acting as my external supervisor, provides enormous assistance to the work I pursued at Zhejiang University. So many thanks to him for his kind help and enormous assistance.

Many thanks should be given to Dr. Zhiyi Zhang. His comprehensive investigation in the field of fluorescence-based fibre thermometry has set a solid foundation to the continued work.

Many thanks to Dr. Weizhong Zhao, Dr. Suchanda Pal, Dr. Jahnal Mandal, Dr. Jackson Yeo and all the guys in Measurement and Instrumentation Centre of City University, London. Their kind assistance let me spend smoothly the years of study at City University.

I thank Dr. John Milner for his kind help in my living when I was staying in London. I will never forget the grove in the northern part of London.

Finally, I should thank my parents, my wife and my daughter. Without their self-giving contributions, it would be impossible for me to complete this thesis. I do owe them a lot.

List of Illustrations

Chapter 1: Introduction

1.1 Fibre optic thermometry: an introduction

Temperature is one of the most important parameters to be measured in almost all industrial areas. The accurate measurement of temperature is essential to the efficiency and the safety of many industrial processes. Almost all chemical processes are temperature dependent and a considerable loss of efficiency may result from the use of incorrect temperature data. In some cases, the loss of control of temperature can result in catastrophic plant failure with significant damage and possible loss of life.

Although a wide variety of existing instruments is available for use either in industry or in the laboratory, innovative research and development activities in temperature monitoring continue, due to the ever excessive use of thermometers in the industrial, research and development and biological spheres. These environments can present a number of real difficulties for the determination of temperature. The region to be measured may be extremely hostile, moving or in a position where access is extremely difficult, or where the physical contact of a sensing probe may even be impossible, or where the presence of interference from other forms of electromagnetic noise excludes the use of electronic thermometers.

The fibre-optic thermometer is one type of modern instrument that can be used to measure temperature accurately in a variety of environments. For most applications, thermocouples will be adequate – for some, especially where there are issues of intrinsic safety or where thermocouples offer a poor lifetime due to the hostile conditions, a fibre optic probe may be the preferred solution. Such sensors are immune to the interfering effects of electro-magnetic radiation (often not the case with thermocouples) and may be lighter in weight and durable in use. They are safe to the environment to be measured as they require no electrical power at the sensor end of the system. As the small size of the fibre and its electrical, chemical and thermal inertness can allow for long-term location of the sensor deep inside complex equipment, they are capable of remote measurement. Over the past 25 years, research work on fibre-optic sensors has progressed steadily and a number of effective devices have been discussed in the literature [1].

There is a variety of techniques available for optical temperature measurement, as a result of the fact that there are essentially as many ways of making a temperature measurement optically as there are temperature-dependent optical properties. As the sensor can either be formed using the

fibre itself as the sensing medium (termed 'intrinsic sensing') or from a material or structure attached to the end of the fibre (termed 'extrinsic sensing'), the number of possible fibre optic temperature sensor devices is quite large. Extensive reviews have been given by Grattan[2,3] and Wickersheim [4] on various proposed sensor schemes.

For the practical applications of fibre-optic sensors, some basic considerations should be taken into account. Sensor fabrication should, as far as possible, be simple. The performance of the instrument should not just depend on which individual sensor is being used. Substitution of sensors should be quick and easy and ideally, the system should not require calibration before use or after sensor replacement. The sensor materials or structure should also be very stable over time, with repeated thermal excursions, and furthermore, the performance of the system has to be insensitive to optical signal changes such as those caused by fibre bending, light source degradation, variable connector losses, or changes in fibre transmission over time. Based on these considerations, several types of fibre thermometers seem to be of greater importance among the techniques presented in the literature. They are mainly based on blackbody radiation [5][6][7], on the fluorescence properties of materials [8][9][10], and on fibre Bragg gratings (FBGs) [11][12] respectively.

1.2 Aims and objectives of the work

As mentioned in the above section, research and development on the fibre thermometer has been, and is still, an active area of great importance. Research and development on novel advanced materials continues to improve the performance of corresponding sensing systems. Undoubtedly, further investigation and characterization of these novel advanced materials will extend the field of fibre optic applications.

In this work, the focus has been upon the development, evaluation and use of the fluorescence-based fibre thermometer and FBGs for applications at high temperatures. This is mainly due to the fact that the fluorescence-based fibre thermometer and the FBG -based thermometer are both optical signal intensity insensitive in principle, and thus offer excellent long-term stability and good spatial resolution. Both of them have found wide commercial applications [4][12].

However, both the fluorescence-based fibre thermometer and the FBG-based thermometer

are normally used over a comparatively low temperature range [13]. For the fluorescence-based fibre thermometer, the fluorescence efficiency generally decreases while the background blackbody radiance increases at higher temperatures, these combined effects always resulting in additional difficulty in accurately determining the fluorescence lifetime. For the FBG based thermometer, the periodical refractive index modulation pattern generally decays or even disappears completely at higher temperatures and thus results in weak peak reflectance, and thus difficulty in determining the peak wavelength.

It would be very important that the upper temperature limit of these fibre thermometers can be extended to expand the application scopes of these devices to a higher level. For the fluorescence based systems, this needs some special materials with reasonably high fluorescence efficiency at high temperatures to be found and developed for sensing probes. The signal processing scheme should be sensitive enough to detect the fluorescence accurately and to eliminate the effect of strong background blackbody radiation efficiently. For the FBG-based systems, the main work should be focused on the development of novel photosensitive fibres, into which strong FBGs sustainable to high temperature can be readily written. Thus, the corresponding signal processing scheme can readily determine the peak wavelength position from the reflectance spectrum. This is the main aim of this work.

The above is the main focus of this work which can be divided into two main categories. One lies in the field of fluorescence-based fibre thermometer, where the main objective has been to find some advanced fluorescence material through which the fluorescence lifetime measurement scheme can cover a wider temperature range from room temperature to above 1000 ^{0}C, expanding upon the existing techniques reported in this field. It is impossible for the well-known silica based fluorescence probe to operate at such a high temperature for a long time. Crystals doped with fluorescence ions would be the main candidates to allow the range to be expanded. Second, for the FBG-based temperature sensor, the main objective has been to develop some types of novel photosensitive fibres into which the FBG is written can still operate at a comparatively higher temperature of over 900 ^{0}C, a temperature close to the upper limit that the silica based fibre can operate for a long period. This will extend further the upper temperature limit of currently available FBGs fabricated by the normal UV laser illumination.

Thus in summary the major objective of the work, and contribution to new knowledge in the

field of fibre optic –based thermometry are

- the development, evaluation and testing of a new material-based fluorescence thermometer, extending the measuring range to 1200 ^{0}C using Tm-doped crystals
- the development and characterization of specialist photosensitive fibres for high temperature applications using fibre Bragg grating –based techniques
- the fabrication of antimony –doped fibre, indium doped fibre, bismuth doped fibre and their use in high temperature FBG-based temperature sensors
- modeling of the decay mechanism of high temperature sustainable FBGs
- evaluation of the temperature sensor developed in the industrial context
- publication of the results in the major journals internationally, and presentations at international conferences

1.3 Structure of the thesis

This thesis reflects the progress of the author's recent work in the field of fluorescence-based fibre thermometry and the FBG-based temperature sensors. The thesis, as a whole, consists of eight chapters. Chapter 1 begins with a brief introduction to the work included in the thesis, followed by the analysis of current techniques and existing problems, which sets the main aims and objectives of this work. Chapter 2 and Chapter 3 discuss in detail the technical background of this work, with particular focus on the field of fluorescence-based and FBG-based fibre thermometers. The details of the novel work on the fluorescence-based fibre thermometer will be discussed in Chapter 4, in which the Tm^{3+} doped YAG crystal was specifically chosen as the fluorescence substance to cover the desired working temperature range from room temperature to 1200 ^{0}C. A compact fibre thermometer suitable for industrial applications has been developed and evaluated. In Chapter 5, the work on the design and fabrication of novel photosensitive fibre is detailed. Tests on the performance of the fibres have confirmed that these fibres have reasonably good photosensitivity and are suitable for strong FBG fabrication. In Chapter 6, the investigation on the fabrication and characterization of FBGs written into different types of photosensitive fibres has revealed that the photosensitivity of the fibres may result from the ions doped into the fibre and the vacancies trapped in the fibre. A so-called *Cation Hopping* model is presented to account for the experimental results of the annealing of the FBGs at high temperatures.

Following Chapter 6, some industrial applications of these two types of fibre thermometers are introduced in Chapter 7. These also include the performance investigation of the fibre thermometers used for heat-flux measurement and in industrial process monitoring. Finally, conclusion of the work and some suggestions for future work are included in Chapter 8.

1.4 Summary

In this chapter, further to a brief introduction, the main objectives of the work are determined with the aim of extending the working temperature limit of both fluorescence-based fibre thermometer and the FBG-based fibre thermometer after a careful analysis of the current status of research work in these fields. The structure of thesis is also introduced in this chapter.

1.5 References

[1] K.T.V. Grattan, Z. Y. Zhang, Fibre Optic Fluorescence Thermometry, Chapman & Hall (1995)

[2] K.T.V. Grattan, Fibre optic techniques for temperature sensing. In: Fibre Optic Chemical Sensors and Biosensors, Vol.II, Ed. by O. S. Wolfbeis (London: CRC Press), pp151-192 (1991)

[3]K.T.V. Grattan, "The use of fibre optic techniques for temperature measurement." Measurement and Control, 20, pp32-39 (1987)

[4] K.A.Wickershiem, "Fibre optic thermometry: an overview". In: Temperature – its Measurement and Control in Science and Industry, Vol.6, Part 2 (New York: American Institute of Physics), pp711-714 (1992)

[5]R.R. Dils, "High-temperature optical fibre thermometer", J. Appl. Phys., 54, pp1198-1201 (1983)

[6]H. Amick, "Optical fibre sensors broaden temperature measurement limits". Research & Development, pp64-69 (1986)

[7] Accufibre, Inc. "Model 100 Multi-channel optical fibre thermometer system". Publicity Data. Accufibre, Inc., Beaverton, Oregon, USA. (1988)

[8] R.R.Sholes and J.G. Small, "Fluorescent decay thermometer with biological applications", Rev. Sci. Instrum. 51, pp882-884(1980)

[9] T. Bosselmann, A. Reule, and J. Schröder, "Fibre-optic temperature sensor using fluorescence decay time". In Proceedings of 2nd Conference on Optical Fibre Sensors (OFS'84). SPIE Proceedings, 514, pp151-154 (1984)

[10] K. T. V. Grattan, A.W. Palmer, "Infrared fluorescence 'decay-time' temperature sensor", Rev. Sci. Instrum., 56, pp1784-1787(1985)

[11] K.O. Hill, Y. Fujii, D. C. Johnson, and B. S. Kawasaki, "Photosensitivity in optical fibre waveguides: Application to reflection filter fabrication," Applied Physics Letters, 32, pp647-649 (1978)

[12] A. Othonos, "Fibre Bragg Gratings", Review of Scientific Instruments, 68, pp4309-4341 (1997).

[13] K.A. Wickersheim and M.H. Sun, "Fibreoptic thermometry and its applications", Journal of Microwave Power, 22, pp85-94 (1987)

Chapter 2: Technical Background to Fluorescence Lifetime -Based Fibre Thermometry

2.1 Fluorescence lifetime decay杓ased thermometry: principles of operation

2.1.1 Photoluminescence

Photoluminescence is the phenomenon of light emission, in addition to thermal radiation, from a material which is excited by some form of electromagnetic radiation incident, usually in the ultraviolet, visible or infrared regions of the spectrum. Such emission is the release of the energy gained from the absorption of the incident photon energy which may be either in the form of fluorescence or phosphorescence, or both, while the distinction between the two terms is often somewhat arbitrary [1]. In conformity with current usage in the application field discussed, the term *fluorescence* will be applied generally to all types of photoluminescence, and the corresponding luminescent materials will be termed as fluorescent materials or 'phosphors' thereafter.

It has been found that the fluorescent emission following the removal of excitation depends on the lifetime of the excited state involved in the emission. This emission usually decays in a manner that can be categorized by an exponential form and the time-constant of such an exponential decay may be used as a measure of the lifetime of the excited state, often termed the fluorescence lifetime or fluorescence decay time. In fluorescence thermometry, most materials used have relatively long fluorescence lifetimes ($>10^{-6}$ s), compared to many laser dyes, for example. This means that the fluorescence corresponds to the weakly allowed transitions between electronic energy levels of the fluorescent material. The material may emit light when returning from the excited to the ground state. Any reasonably effective competitive relaxation process can shorten the lifetime of the excited state. A variety of such competitive processes, some radiative and some non-radiative, exists. Hence all luminescent materials can be expected to exhibit a temperature-dependent fluorescence lifetime, and thus a temperature-dependent fluorescence intensity to some degree, over some part of the temperature spectrum. These are the thermal properties which are most efficacious for fluorescence thermometry.

There are several classes of potentially useful fluorescent materials now available. Most lamp phosphors and many solid state materials are insulating compounds containing ionic

'activators'. The spectra of the rare-earth activators resemble, to a first approximation, those of free ions, while the electronic spectra of the transition-metal activators differ from those of free ions quite significantly due to the strong interaction with the crystal fields of the host materials. Clearly, the choice of sensor materials determines the performance of a fluorescence-based thermometer to a great extent. To achieve stable operation, the sensor material should be chosen to be stable over a specified temperature range for a long operation lifetime.

2.1.2 Fluorescence lifetime decay-based thermometry

There are several fibre optic thermometry systems using the fluorescence technique that have been discussed over the past twenty years. Most of the earliest systems are based on the temperature-dependent fluorescence intensity of appropriate materials. Such systems include two early commercial systems, the Luxtron Model 1000, which utilized europium-activated lanthanum and gadolinium oxysulphide as alternate sensor materials [2], and the ASEA 1010 system, which used a small crystal of gallium arsenide sandwiched between gallium aluminum arsenide layers [3] as the active material.

Although a substantial number of intensity-based systems were built, it could be seen that the technique had certain limitations in terms of performance and cost [4]. These stem from the need for an additional 'referencing channel', e.g. involving the monitoring of the luminescence intensity at another wavelength, for the separation of the effects of thermally-induced changes in intensity from other non-thermal sources, such as fibre bending, the light source involved, and detector degradation, etc. As a result, a technique based on the measurement of fluorescence lifetime was developed [5, 6, 7] and it has been more widely used in the development of commercial fluorescence-based systems to date, although active research in intensity-based systems continues [8][9].

In the more successful fluorescence-based schemes, the temperature-dependent lifetime of the fluorescence emitted from an appropriate material is utilized. There is a range of fluorescent materials potentially useful for temperature sensing, and those with a relatively long lifetimes (> 10^{-6} s) have often been used so that special high-speed electronic components were not required and the design of the lifetime detection electronics could be simple and made available at low cost.

It is clear that by measuring the fluorescence lifetime, the corresponding temperature of the environment in which the fluorescence material is placed can be interrogated only if the temperature dependence of the fluorescence lifetime is monotonic and stable. For accurate measurement of the lifetime, several techniques have been developed and these can be classified into three major categories: the pulse measurement; the phase and modulation measurement; and the phase-locked detection method.

A. Pulse measurement of fluorescence lifetime

In the scheme using the pulse measurement, a technique called ***two-point time constant measurement*** is straightforward in principle and easy to realize [4,10,11]. The fundamental concept of this technique is illustrated in Figure 2.1. The approach is to compare the intensity level at two points along the exponential decay curve after the excitation pulse has been terminated. Since the fluorescence signal is measured after the excitation pulse is over, the detector optics do not have to be designed to discriminate strongly against stray light signals from the excitation source. However, a significant disadvantage of this type of system is that, in practice, the signal is only measured at two specific points and, as a result, the precision of system is limited.

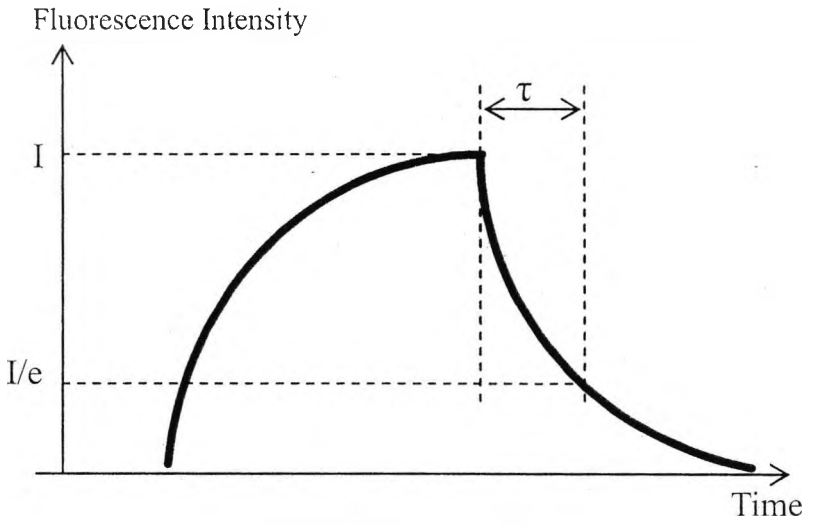

Figure 2.1 Two-point time constant measurement technique

Another technique named *the digital curve fit method* [12] is also used in this scheme and is expected to have better accuracy. In such a system, an unnamed fluorescent material is used, the excitation spectrum of the fluorescence material allows the use of a conventional excitation source,

e.g. a red LED or a laser diode. When the sensor is excited by the light pulses emitted from such an LED or laser diode, a periodic decaying luminescent signal is generated and a selected portion of each decay curve is digitalized, after the detected signal has been passed through a low noise, wide bandwidth amplifier. The digital samples, after correction for any offsets as shown in Figure 2.2, are then processed by a digital signal processor (DSP) to provide the best exponential curve by means of a least squares curve fitting technique. The exponential is first converted to a straight line by taking the natural logarithm of the digitized signal values. The slope of the best fitting straight line is proportional to the decay time of the luminescence and this value can be averaged further to reduce the effects of any noise present in the system.

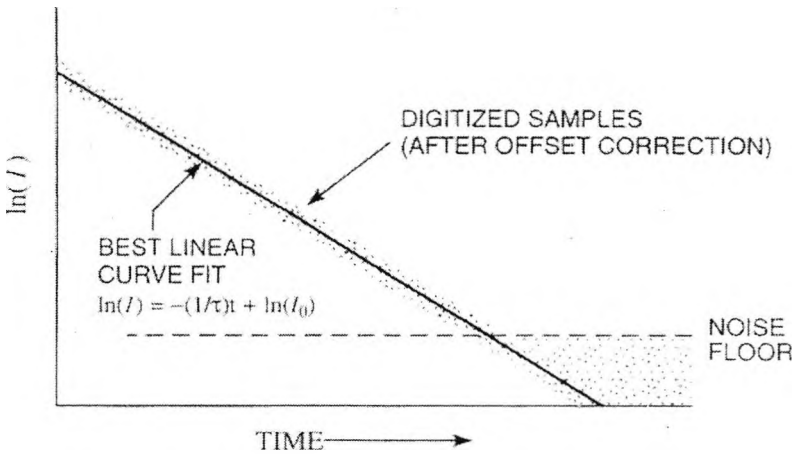

Figure 2.2 Illustration of linearized digital curve fit technique

For the scheme based on *the digital curve fit method*, an investigation of the errors caused by the baseline offset and the noise in the least-squares estimation of exponential lifetime has already been carried out by Dowell and Gillies [13]. It shows that the two-parameter estimation approach, which only estimates I_0 and τ and assumes a zero baseline (or dc) offset, such as that illustrated in Figure 2.2, is rather sensitive to small, residual baseline offsets. Therefore, it would appear that the performance of the digital-curve-fit technique relies strongly on the effectiveness of the correction of the dc offset in the processed signal. Thus, it requires a reiterative numerical algorithm, which increases the complexity of the programming required and prolongs the signal processing time.

B. Phase and modulation measurement

A schematic representation of *the phase and modulation measurement* approach is depicted in Figure 2.3. The intensity of the excitation light is sinusoidally modulated so that the fluorescence response from the sensor material is forced to follow the same sinusoidal law, but is lagging behind the excitation light by a phase shift, φ, which is expressed as

$$\tan\varphi = 2\pi f \tau \qquad (2\text{-}1)$$

Thus, the fluorescence lifetime τ can be derived from a measurement of the phase shift between the excitation signal and the fluorescence response, φ.

This technique potentially can offer high accuracy and is designed to be used in precision measurement instrumentation, as it is inherently insensitive to dc-offset and the ac-noise in the sinusoidal signal which can be substantially reduced by a variety of electronic devices, ranging from various electronic analogue filters and digital filters to the most effective lock-in amplifiers. Grattan et al. [14] have demonstrated the use of this technique in a ruby fluorescence-decay thermometer, where a high-power green LED was used as the excitation light source. Over the range from room temperature to 170 ^{0}C, a reasonably satisfactory measurement deviation was achieved under poor signal-to-noise ratio conditions. A similar system, reported by Augousti et al [15], used alexandrite as the sensor material and was shown capable to achieve a system accuracy of ± 1 ^{0}C over a range from 20 ^{0}C to 150 ^{0}C, with a response time of ~ 1 s.

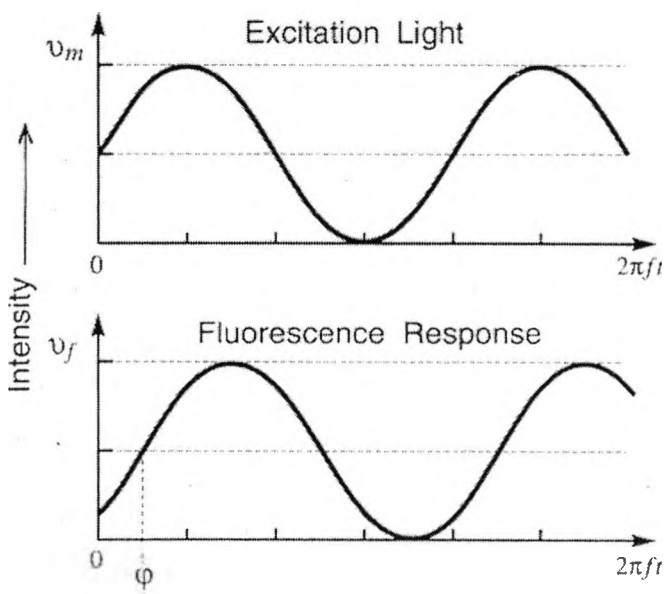

Figure 2.3 Phase and modulation measurement of fluorescence lifetime

However, since this kind of system requires the measurement of fluorescence during the

excitation period, it is highly sensitive to excitation light 'leakage' to the detector and the optics required to prevent such leakage (or reduce it to the necessary very low levels) can make such a system quite costly.

C. Phase-locked detection of fluorescence lifetime

The phase-locked detection approach was proposed by Zhang et al [16] to achieve a simple, inexpensive and versatile electronic signal processing system for the detection of fluorescence lifetime, and this has been successfully applied to several fibre-optic thermometer schemes. Although these schemes stem from the phase and modulation techniques, they differ from them in several important aspects. As shown in Figure 2.4, the excitation light source is modulated by a signal from a voltage-controlled oscillator (VCO). The fluorescence response signal from the sensor follows the variation of excitation light in intensity, but lags behind it by a phase shift, φ, which corresponds to the fluorescence lifetime as expressed in Equation (2-1). This signal is sent to a lock-in amplifier to mix with a reference signal derived from a VCO output with a phase lag of a fixed fraction, α, of the period. The resulting mixed signal is then filtered by a low-pass filter (LPF) and further integrated, with the resultant voltage signal being fed back to control the output frequency of the VCO. Consequently the VCO is driven at a frequency at which the integration of the mixed signal is zero. The period of this frequency is directly proportional to the lifetime and thus it makes measurement comparatively easy and potentially accurate.

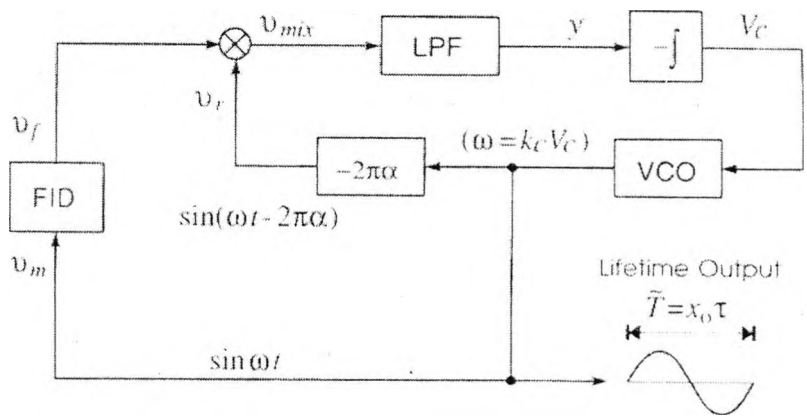

Figure 2.4 Phase-locked detection of fluorescence lifetime using single reference signal. FID:fluorescence inducing and detecting devices; υ_m: signal to modulate the output intensity of the excitation light source; υ_f: the fluorescence signal; LPF: low-pass electronic filter; VCO: voltage-controlled oscillator (Ref.16)

There have been several sensor systems developed using this phase-locked detection

scheme for fluorescence lifetime detection due to its accuracy in measurement and the flexible requirement for blocking the "leakage" of excitation light, which is obviously superior to the technique by *phase and modulation.* Thus this specific scheme has been used in this work for the detection of fluorescence lifetime, which has been detailed in Chapter 4.

2.2 Glass fibre -based fluorescence lifetime thermometry

2.2.1 Introduction

As mentioned in Section 2.1, the measurement of fluorescence lifetime decay has become one of the most important techniques in the field for temperature determination over the past twenty years. To meet the requirements of sensing probes in many different types of working environments, a range of fluorescence materials has been investigated comprehensively. They include rare-earth doped silica fibres, fluorescence oxide powders and a variety of rare-earth ion or transition metal ion doped crystals of high, optical grade, quality. In this section, the work described has been based on several fluorescent silica fibres, which are of major importance in industrial applications, such as Nd^{3+} or Er^{3+} doped silica fibres. Both the fluorescent crystals such as the Cr^{3+} doped alumina oxide (Ruby) and composite crystal fibres, which possess both the properties of the fibre and the fluorescent crystal, will be discussed in the following sections of this chapter.

Silica optical fibres are clearly one of the most important materials widely used in optic communication and fibre-optic sensing systems. For example, the specific silica fibres doped with rare-earth ions, have been used as the gain media, in applications of erbium doped fibre amplifiers (EDFA) and fibre lasers.

As a result, a wide range of doped glass fibres has been developed over the past twenty years, particularly for laser studies. The interaction of the rare-earth ion with the silica host within the fibre induces a spectral broadening of both the absorption and emission bands and therefore a change in the spectral characteristics over those for the material in a conventional laser host will occur. This allows the selection of slightly different wavelengths both for absorption and emission over what is found with the material when conventionally doped into bulk glasses. The concept of using a rare-earth doped fibre as the basis of an optical fibre amplifier was proposed as early as 1964 by Koester and Snitzer [17] and was demonstrated by Stone and Burrus in 1973 [18], using a

short 1cm fibre length, due to the high background loss of the fibres available at that time. The new technology of modified chemical vapor deposition (MCVD) has allowed the fabrication of doped fibres with low loss and Poole, Payne and Fermann [19] were able to fabricate fibres with high absorption at the excitation wavelengths and low loss at the laser wavelengths, ideal for laser studies. The first versions of such fibres had low concentrations of rare-earth ions to prevent clustering, and subsequently Ainslie et al [20] reported that by using Al_2O_3 as one of the core components, the problem of clustering could be eliminated. Rare-earth ions have been doped into a range of fibres, including silica and some exotic fluoride fibres. However, the most commonly available are based on silica and this section has been focused on the temperature characterization of Nd^{3+}-doped and Er^{3+}-doped silica-based fibres.

2.2.2 Neodymium doped silica fibre

Neodymium doped silica fibre is one of the most familiar fibres among all the doped fibres available. This is partly due to the fact that Nd^{3+} doped YAG is widely used as the gain medium in solid state lasers. The energy levels of the Nd^{3+} ion are well known, and the $^4F_{3/2}$ -$^4I_{11/2}$ transition results in the well-characterized laser line, seen in a variety of host materials and from it a series of absorption bands in the solid state laser arises. As shown in Figure 2.5, the absorption and emission spectra tend to broaden with respect to those in the bulk host materials, which make the excitation by solid state laser diodes in the 800 -820 nm region possible and had encouraged the early work on both sensors and lasers using neodymium-doped fibres.

The characteristics of neodymium doped silica fibres have been investigated throughly and several temperature sensors using the fluorescence decay of this type of fibres have been reported and are discussed below.

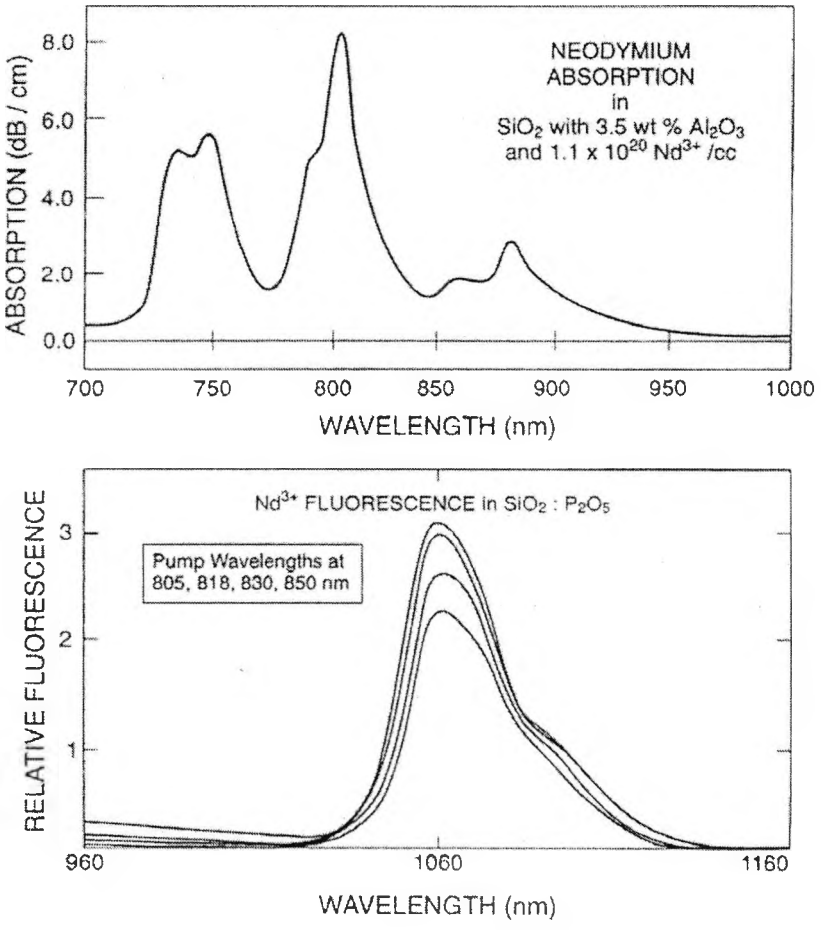

Figure 2.5 Absorption and emission spectra of neodymium in fibres and glasses (Ref.21)

Early research on the use of Nd^{3+}-doped optical fibre for temperature sensing was reported by Zhang et al [21]. The experimental setup for the measurement of the fluorescence lifetime is schematically depicted in Figure 2.6, where the phase-locked detection (PLD) method is employed for fluorescence signal processing [16], which directly converts the fluorescence signal into a TTL compatible frequency signal, whose period is directly proportional to the measured fluorescence lifetime. This frequency signal is transmitted to a desktop computer which is equipped with a counter-and-timer card to continuously monitor and record the lifetime measurements.

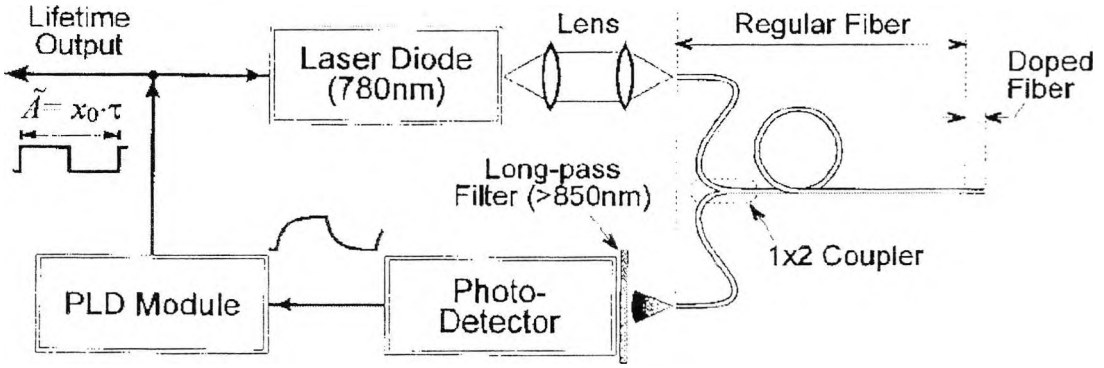

Figure 2.6 Schematic of the system for fluorescence lifetime measurement (after Ref.[21]).

The Nd^{3+}-doped optical fibre sample tested was based on an alumino–silicate glass supplied by Pirelli Cables Ltd. Its softening point was estimated to be 1450 °C. A high Nd^{3+} dopant concentration of 7.5 wt % was included by employing a special co-doping technique to achieve a strong fluorescence signal. As reported, such a heavy doping may result in concentration quenching and thus, a shortening of the fluorescence lifetime. This concentration quenching effect might be disadvantageous in some other applications, but here it does help to increase the temperature sensitivity of the fluorescence lifetime, an important feature for such sensor applications.

For the experimental setup reported, a piece of the doped fibre of 5 mm in length, was fusion spliced to the end of a 1 x 2 100/140 μm fibre coupler. The excitation was provided by a 780 nm laser diode in continuous (cw) output mode, and the power launched into one of the ends of the fibre coupler was estimated to be 1.5 mW. The induced fluorescence was detected at the other end of the coupler using a silicon-based avalanche detector, where an interference filter with a blocking characteristic from 650 to 850 nm was used to isolate the reflected excitation light from the detector. The length of the doped fibre was optimized.

The fluorescence lifetime dependence on temperature of this Nd^{3+} doped silica fibre probe had been calibrated with the result shown in Figure 2.7. Over the temperature range from -190 ^{0}C to 750 ^{0}C, the lifetime decreased monotonically from 410 μs to about 180 μs, showing an average temperature sensitivity of 0.25 μs/^{0}C. Further annealing tests on the performance stability of the probe had also shown that the probe was very stable at temperature below 750 ^{0}C after a test

period of 100 hours. However, similar tests at higher temperature, for example at 800 ^{0}C or 900 ^{0}C, would always result in some shift of the fluorescence lifetime. Thus, it seems clear that the probe based on the Nd^{3+} doped silica fibre is suitable for the temperature measurement over the wide temperature range below 750 ^{0}C.

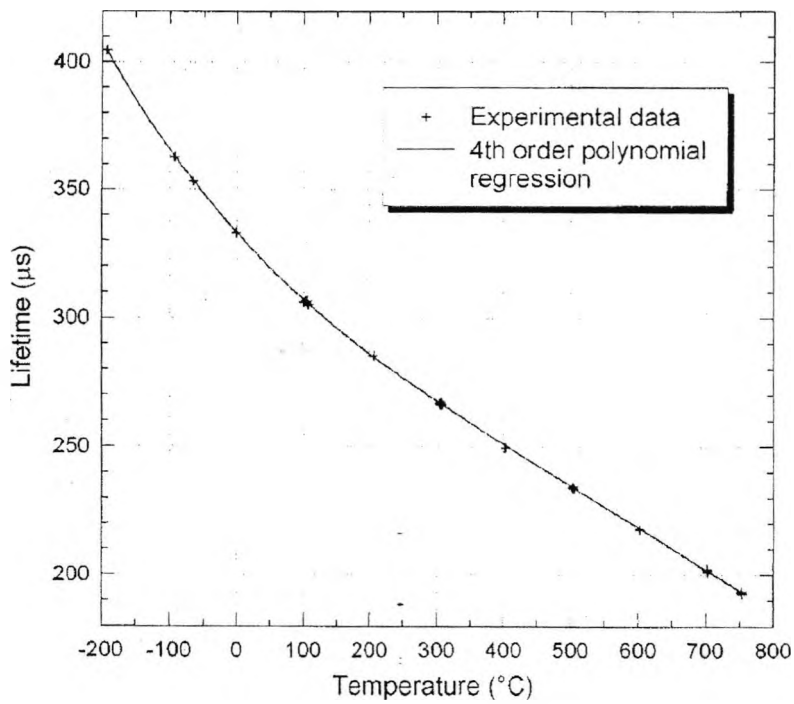

Figure 2.7 Fluorescence lifetime of the Nd^{3+}-doped fibre probe and its temperature sensitivity over the region from −190 °C to 750 °C, calibrated after the probe being annealed at 754 °C for more than 100 h (after Ref.21).

2.2.3. Erbium doped silica fibre

Erbium doped silica fibre is another most familiar fibre among all the doped fibres available, due to its well-known application in erbium doped fibre amplifier (EDFA). It seemed an obvious candidate in the search for an alternative fluorescent doped optical fibre to Nd, to find a material suitable for a temperature sensor probe which would operate up to even higher temperatures without showing hysteresis effects. First, the dopant erbium has a melting point which is much higher than that of neodymium and its atomic weight is also much higher. These indicate that the erbium dopant would behave more stably at high temperatures, both chemically and physically, by being less reactive and mobile within silica (SiO_2, the host material of the optical fibre) than the smaller and lighter Nd dopant. Second, due to the rapid developments in the

field of optical fibre amplifiers for telecommunications use, Er-doped fibres are commercially available with a wide range of doping concentrations.

The energy level structure of erbium (Er^{3+}) ions and the fluorescence properties of this fibre at room temperature are well-known [22]. Er^{3+} ions have several absorption bands centreed at wavelengths of 514, 650, 800, 980, and 1480 nm over the visible to infrared region, as is illustrated by its electronic level diagram shown in Figure 2.8a. Those bands which are clearly observed from the absorption spectrum of an Er-doped fibre are shown in Figure 2.8b, and a variety of light sources can be used for the excitation of Er fluorescence whose spectrum is depicted in Figure 2.8c. Almost all these absorption bands have been used as pumping wavelengths in successful demonstrations of Er fibre lasers. The most popular pump band for the Er fibre laser is at 980 nm as it is free of excited state absorption and thus results in a higher slope efficiency for the laser system.

The fluorescence characteristics at elevated temperatures of erbium doped silica fibres have been extensively studied by Zhang et al.[22]. The optoelectronic arrangement used for the measurement of fluorescence characteristics of Er-doped fibres is illustrated in Fig. 2.9. The doped fibre under test is fusion spliced to a plain 1550 nm single-mode fibre. The latter fibre is connected to the 980/1550 nm arm of a 980/1550 nm wavelength division multiplexer (WDM) which has an isolation of 23 dB against 970–990 nm and 26 dB against 1540–1560 nm in the 1550 and 980 nm arms, respectively. The sensor head, along with part of the transmission fibre, was loosely placed inside a fused quartz sheath, to minimize any stress caused by mismatch between the fibre and the sheath. The test probe created is inserted into a thermostatically controlled calibration oven and placed at the centre of the oven.

The excitation light from a laser diode (LD) is coupled into the 980 nm arm of a 980/1550 nm WDM. More than 90% of the Er fluorescence passed to the 980/1550 nm arm of the WDM, in the band 1540–1560 nm as is shown in Figure 2.8(c), was guided into the 1550 nm arm. It was detected by an InGaAs photodiode with a spectral response from 1100 to 1700 nm. The detected fluorescence decay signal was processed using the phase-locked detection technique or recorded for waveform analysis by a desktop computer via an analog-to-digital converter (A/D). Apart from the use of a thermostatically-controlled oven for the calibration of the doped fibres, a water bath was also used to obtain a controlled temperature with reference to the water freezing point (0 ^{0}C).

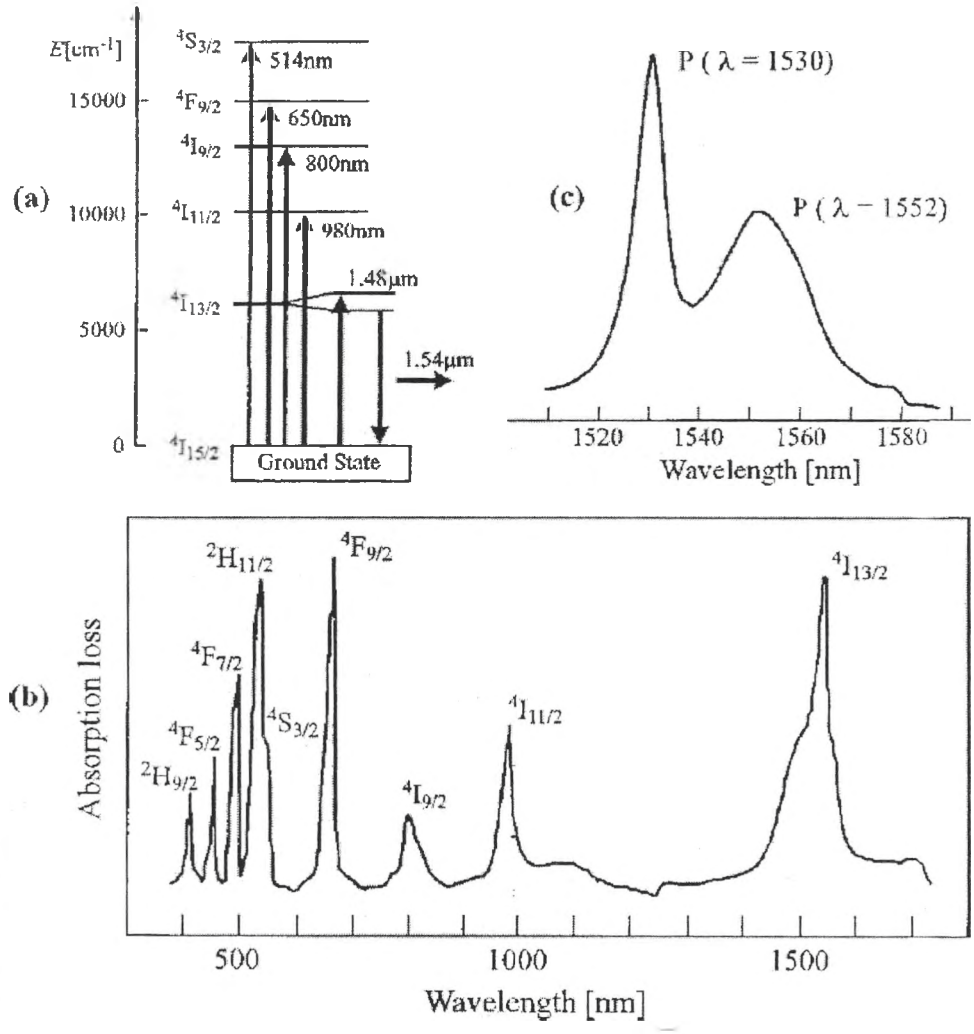

Figure 2.8 (a) Electronic level scheme of Er^{3+} ions; (b) absorption spectrum of the Er-doped fibre; (c) fluorescence emission spectrum of the Er-doped fibre (after Ref.22)

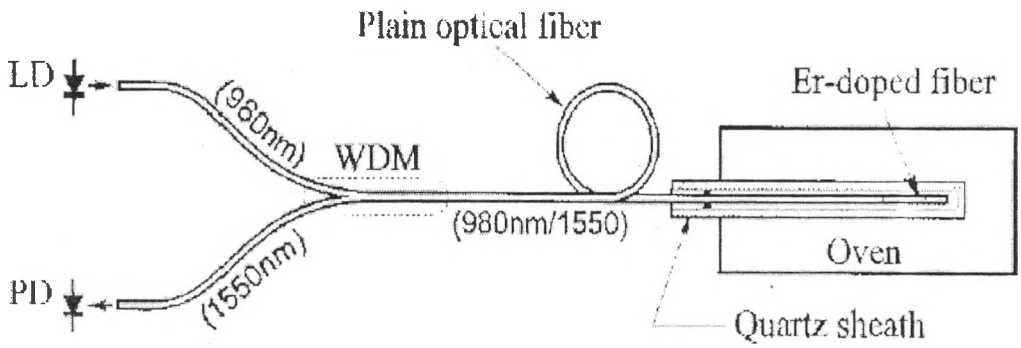

Figure 2.9 Optoelectronics arrangement for the measurement of fluorescence characteristics of Er-doped fibres. WDM: wavelength division multiplexer; LD: laser diode; PD: photodiode (after Ref.22).

The value of maximum intensity, I_{max} for the Er fibre doped at 4370 ppm is significantly lower than those for its counterparts with lower levels of Er concentration due to the concentration quenching effect. However, for short lengths of fibres (e.g., < 100 cm), the higher the Er dopant, the stronger the fluorescence intensity that is obtainable under the same excitation power.

The fluorescence lifetimes of the 200 and 4370 ppm Er-doped fibres may relate to the length of Er-doped samples, due likely to the existence of re-absorption of the Er band at 1540–1560 nm, which traps and then releases the fluorescence emission and hence prolongs the observed fluorescence lifetime. The longer the doped fibre and the higher the activator concentration, the stronger is the fluorescence trapping effect. Consequently, the length dependence of the fluorescence lifetime is more obvious with fibres of high Er concentration. As is shown in Figure 2.10, a significant correlation between the fluorescence lifetime and the length of the fibre can be seen with the 4370 ppm Er-doped fibre.

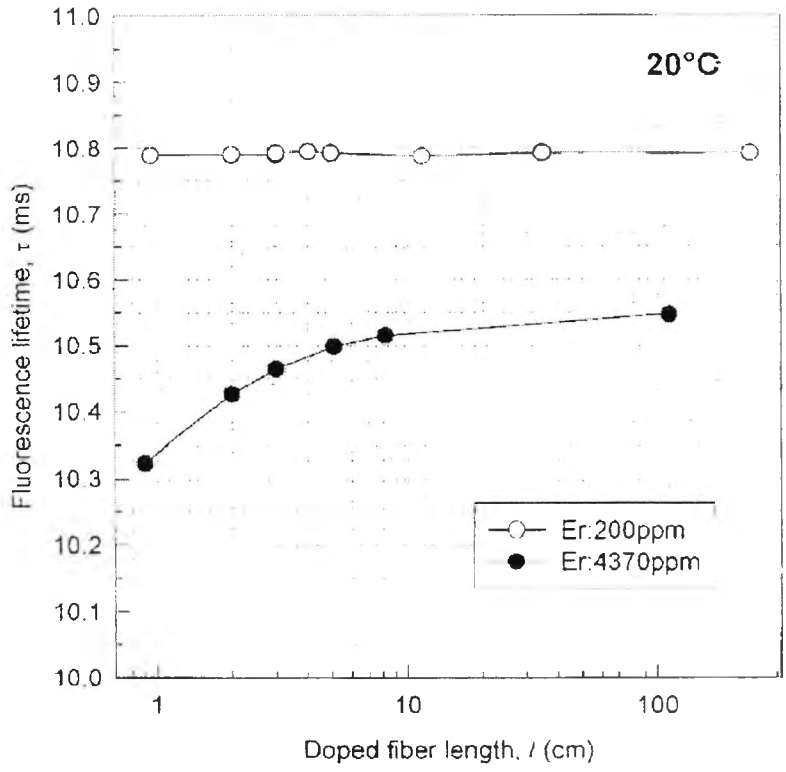

Figure 2.10 Fluorescence intensity of Er-doped fibre under constant excitation radiance as a function of fibre length and dopant concentration. (after Ref.22)

To compare the thermal characteristics of the fluorescence decay between Er-doped fibres

of different active dopant levels under similar conditions, a special probe was fabricated comprising three doped fibre samples (Er: 200, 960, and 4370 ppm) in a single quartz sheath. All the three doped samples were of the same length, this being 5 cm. A calibration of this probe from 0 to 950 °C was performed after it was annealed initially at 950 °C for ~24 h to ensure stable operating conditions, and the results are presented in Fig.2.11

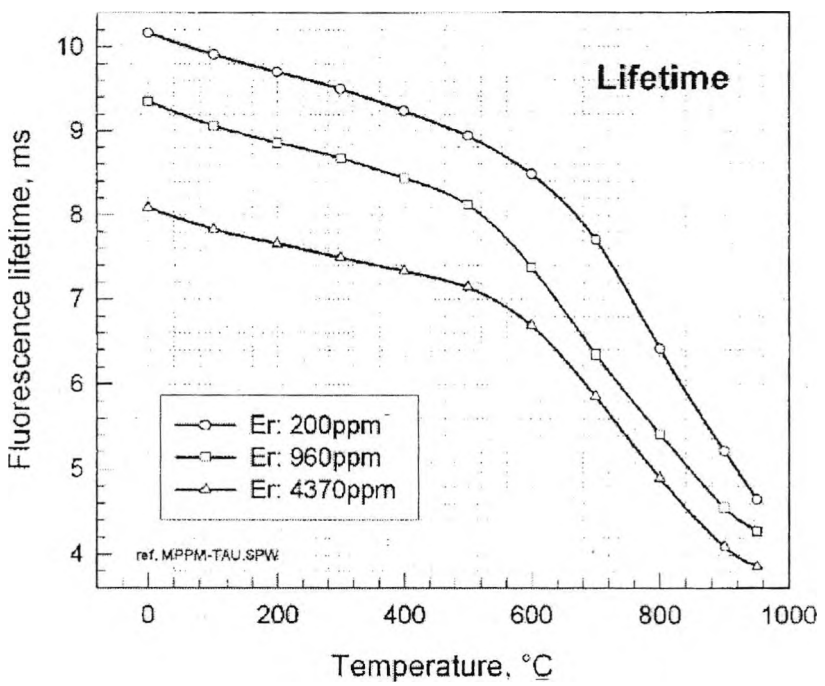

Figure 2.11 Thermal graph of Er-doped fibres which have been annealed at 950 °C for ~24 h. Lengths of these doped fibres are all ~5 cm (after Ref.22]).

Results of the tests on the fluorescence characteristics of the erbium doped fibres shown above indicate that the fibres are good candidates as a thermometer probe over the temperature region below 1000 ^{0}C. Unfortunately, due to difficulties in preventing the fibre material from crystallization at high temperatures, they are not suitable for long-term stable operation. Under these circumstances, fluorescence ion doped crystals may be better candidates if considering the performance stability at high temperatures.

2. 3 Crystal-based fluorescence lifetime thermometry

Though the silica fibres doped with fluorescence ions can be used as the temperature sensing probes at some high temperatures, they are generally not suitable for long-term operation in extreme environments mainly due to the fact that the silica fibre deteriorates or even becomes

opaque as a result of glass crystallization at very high temperatures.

To meet the requirement of long-term operation at high temperatures, probes fabricated from crystal materials are normally preferred. They are physically and chemically stable without any tendency of becoming opaque after long-term operation at those high temperatures as long as the melting points of these crystals are substantially higher above the working temperature concerned. These crystals can be the transition metal ion (for example, Cr^{3+}) doped crystals or rare earth ion (for example, Nd^{3+}) doped crystals. Among all these crystals, Cr^{3+} doped alumina oxide crystal (ruby) has been most widely investigated and the details of the work are introduced below.

2.3.1 Ruby

As is well-known, the energy levels of transition-metal ion doped crystals are strongly affected by the host materials. Cr^{3+} ions in ionic crystals interact strongly with the crystal field and the lattice vibrations. Thus, the Cr^{3+} activated materials are characterized by wide optical absorption spectra, and a significant variety of the temperature dependence of fluorescence lifetimes, which are suitable for a wide range of temperature measurement.

Compared with rare-earth activated materials, the Cr^{3+} activated materials show some significant advantages when used as sensors. Firstly, the wide optical absorption spectra of Cr^{3+} activated materials enable the excitation to be realized by a variety of light sources such as the relatively inexpensive LEDs and laser diodes (LDs). These diode light sources are normally convenient to be modulated by the driving current and thus make the system simple. Secondly, due to their wide absorption spectra, a small level of wavelength drift in an LED or LD would not cause a significant change in the intensity of the resulting fluorescence. This frees the excitation schemes from the strict control of the spectrum of the excitation light and gives a substantial tolerance to the excitation schemes.

A range of Cr^{3+} doped crystals has been investigated as the sensor materials in a fluorescence lifetime based fibre thermometry. These crystals include alexandrite [23], emerald [24], and Cr^{3+}:YAG [25], for example.. Though they are somewhat different in their fluorescence characteristics from ruby, the performances of fibre thermometers based on these crystals are similar to that of the ruby-based system to some extent. Thus, in the following section, the focus will be on the ruby-based fibre thermometer.

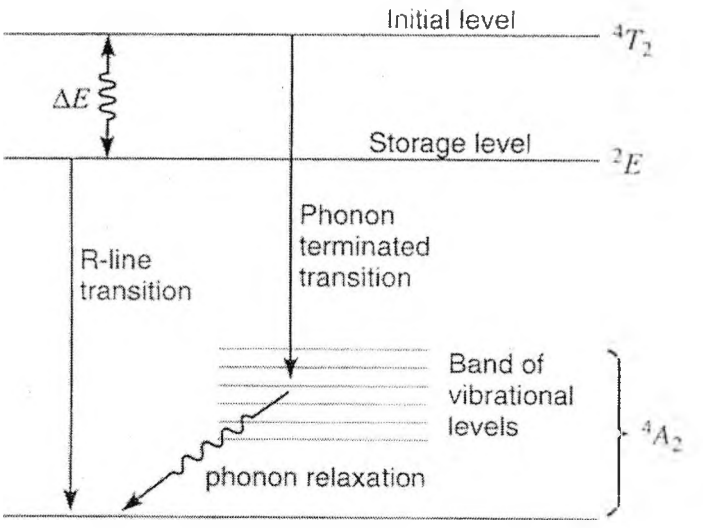

Figure 2.12 The two-level model for Cr^{3+} fluorescence in high field crystals (Ref.27)

The energy level bands of ruby can be simplified into a two-level model as was shown in published work [24,26]. As can be seen from Figure 2.12, the population in the upper level – ^2E may relax by the R-line transition. Due to the thermal equilibrium population distribution between the ^2E and the $^4T_2$, some population in the $^4T_2$ may relax by mean of a phonon terminated nonradiative transition and then make the lifetime of the upper level become shorter. In this way, a mathematical expression for the fluorescence lifetime as a function of temperature was deduced as follows [27]

$$\tau = \tau_s \cdot \frac{1+C_d \cdot e^{-\Delta E / kT}}{1+(\tau_s / \tau_t)e^{-\Delta E / kT}} = \tau_s \cdot \frac{1+3e^{-\Delta E / kT}}{1+\alpha \cdot e^{-\Delta E / kT}} \qquad (2\text{-}2)$$

where τ is the fluorescence lifetime; ΔE, the energy gap between the $^4T_2$ and ^2E states as shown in Figure 2.12; τ_t and τ_s, the lifetime of the $^4T_2$ and ^2E states respectively; and C_d, the ratio of the degeneracy of $^4T_2$ to that of ^2E with a value of 3.

The results of a calculation using such an equation were compared with the experimental data [28]. As shown in Figure 2.13, the data from Eq.(2-2) fits the fluorescence lifetime data quite well over the region from 200 K to 700 K.

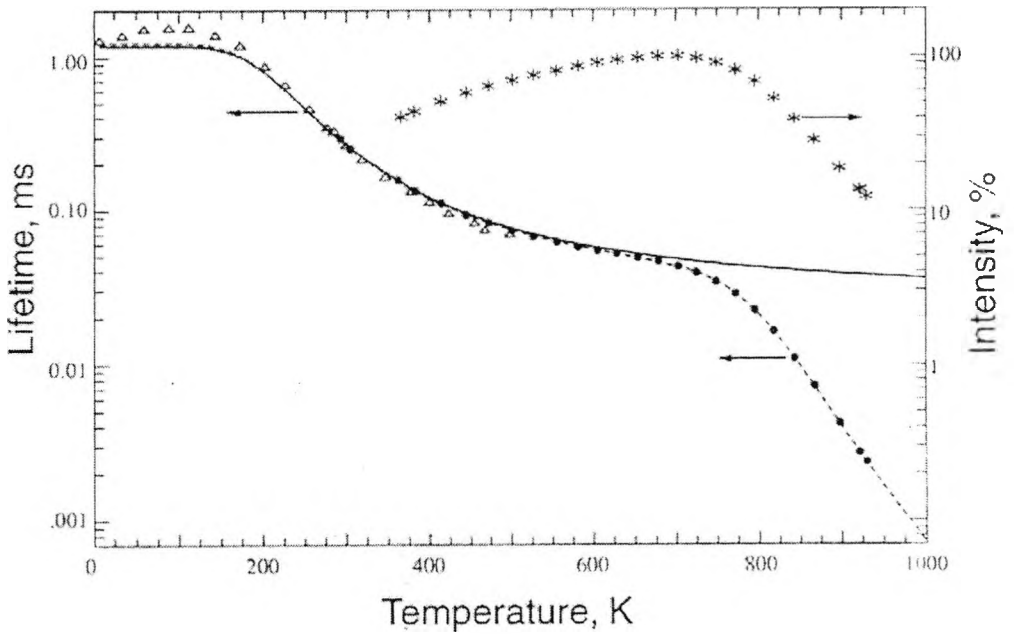

Figure 2.13 Temperature dependence of the alexandrite fluorescence (after Ref.23)

However, at high temperatures beyond 700 K, the lifetime measured decreases sharply and deviates significantly from the fitted value. It has been revealed that this discrepancy of the two-level model with the experimental data over this region is due to the nonradiative transitions which are becoming stronger with increasing temperature beyond 700 K. The nonradiative transitions accelerate the decrease in the fluorescence lifetime with increasing temperature, and make the fluorescence lifetime much more sensitive to temperature variance at high temperatures.

To include the effect of the nonradiative transitions, a single configuration coordinate model, as shown in Figure 2.14, has been used by Zhang et al [29]. According to this model, the fluorescence lifetime, τ, can be given by:

$$\tau = \tau_s \cdot \frac{1+3e^{-\Delta E/kT}}{1+\alpha \cdot e^{-\Delta E/kT}+\beta \cdot e^{-(\Delta Eq+\Delta E)/kT}} \qquad (2\text{-}3)$$

where $\alpha=\tau_s/\tau_i$; $\beta=\tau_s/\tau_q$; $1/\tau_q$, the thermal quenching rate; ΔEq, the thermal activation energy needed to elevate ions at the bottom of the excited state to the level crossing, **Q**. The other parameters are the same as defined in Eq.(2-2). It has been confirmed that the fitted curve using Eq(2-3) is in very good agreement with the experimental data [29].

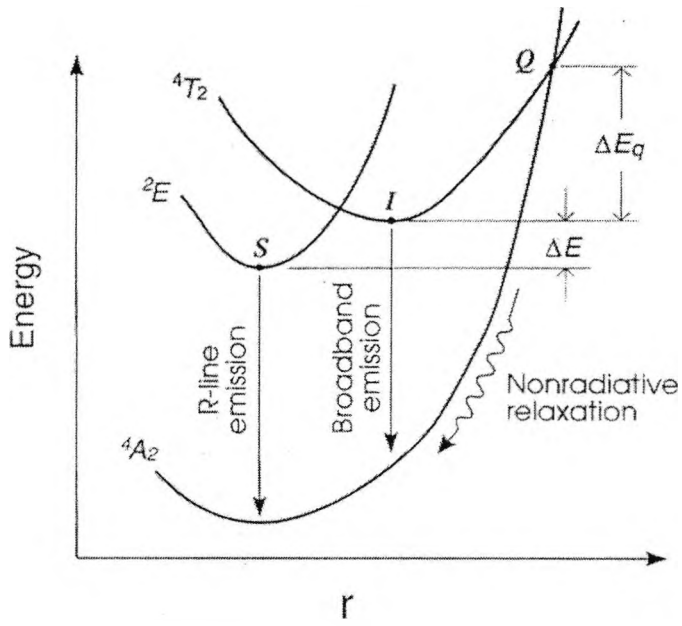

Figure 2.14 The single configurational coordinate model for Cr^{3+} fluorescence in high field crystals. r: the configurational coordinate similar to the wavenumber of the phonon in the lattice (after Ref.29])

A ruby based fluorescence thermometer developed by Zhang et al is schematically depicted in Figure 2.15 as introduced in reference [30]. A green LED was used as the excitation source, which can pump the ruby via the strong absorption band centreed at 550 nm. A short-pass optical filter, F1, with a cut-off wavelength of 630 nm is used to eliminate the red "tail" of the LED emission. A band-pass interference filter with the pass-band centreed at 694.3 nm and a bandwidth of 12 nm was employed as the filter F2, as shown in Figure 2.15.

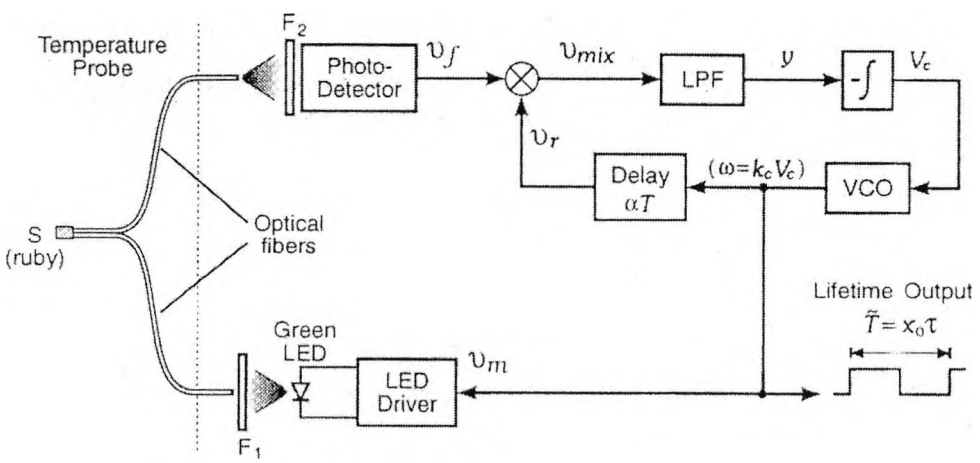

Figure 2.15 The ruby fluorescence lifetime based fibre optic thermometer system. F_1: short pass optical filter; F_2: R-line band-pass optical filter (after Ref.30)

In this system, gold-coated silica fibres were first used to fabricate the probe for temperature measurement up to ~600 ^{0}C. The core diameter of the fibre used was 400 μm. The probe was configured in the reflection-type configuration. A so-called phase locked detection with pulse modulation (PLD-PMSR) technique was devised by Zhang et al [30] and used for the signal processing in this system.

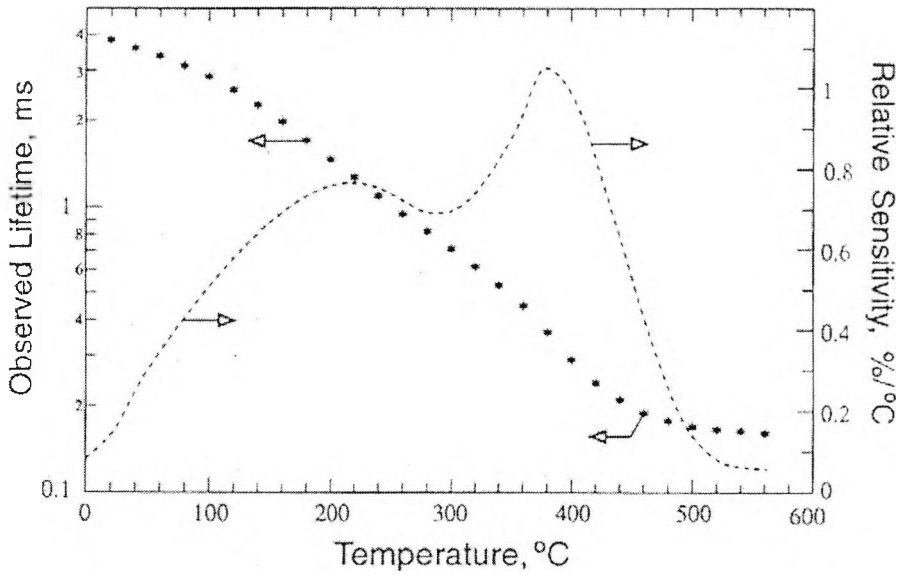

Figure 2.16 Characteristic calibration curve for the ruby fluorescence based thermometer in the region from room temperature to ~ 550 ^{0}C (after Ref.28)

The fluorescence lifetime output was monitored via the period of the modulation frequency as indicated in Figure 2.15, and a characteristic calibration curve is shown in Figure 2.16 on a logarithmic scale, over a range from 30 ^{0}C to 550 ^{0}C [28]. In the region between 150 ^{0}C and 450 ^{0}C, maximum sensitivity is seen. Beyond 500 ^{0}C, the calibration curve tends to 'flatten out' quite dramatically, and the sensitivity of measurement achievable in this region is limited, as shown by the dashed line in Figure 2.16, which represents the relative temperature sensitivity of the observed fluorescence lifetime.

The intensity of the fluorescence emission with temperature change, detected at the photodetector stage, is shown in Figure 2.17. It falls off rapidly with temperature increase over the whole temperature region.

The performance of this system in measurement was tested to determine the reproducibility of the system, based on the observation of the measurements at several fixed temperature points

carried out under laboratory conditions. The results indicate that this system can reach a reproducibility of about 2 ^{0}C at these temperature points.

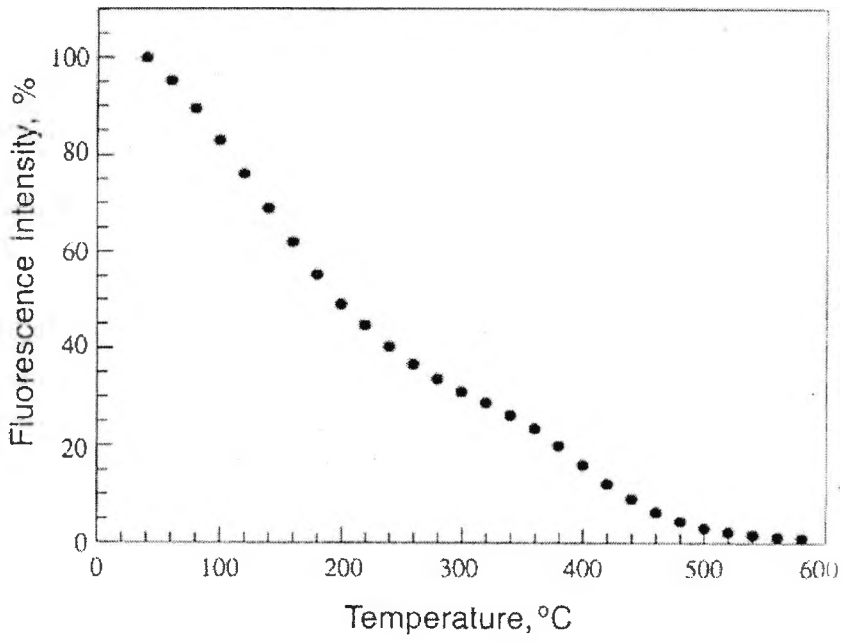

Figure 2.17 The ruby fluorescence intensity recorded in the experiment (after Ref.30)

2.3.2 Nd^{3+}:YAG and Er^{3+}:YAG

In addition to the transition-metal ion doped crystals, rare-earth ion doped oxides or crystals are also good candidates for the probing material in fluorescence lifetime thermometer. Several types of rare earth ion doped oxides or garnets have been extensively investigated. as the availability of these materials enables a fibre thermometer to be designed using the fluorescence lifetime technique and to cover a wide temperature range. Previous work has shown the potential of using rare earth ion doped crystals for high temperature sensing.

Grattan et al have investigated the fluorescence characteristics of Nd^{3+}: YAG at elevated temperatures up to 1100 K [31]. As shown in Figure 2.18, the sharp decrease in the decay lifetime of Nd^{3+}:YAG from 900 K to 1100 K makes it a sensitive candidate for a fluorescence based sensor element.

In addition to Nd^{3+}:YAG, Erbium (Er) doped Yttrium Aluminum Garnet (YAG) also shows a strong fluorescence even at temperatures up to 1100 K. In the work reported by Zhang et al [32], a monolithic crystalline fibre optic temperature sensor, with a tip doped by Er^{3+}, was used as the sensing probe, and the fluorescence lifetime via temperature was determined over the temperature

range from room temperature to 1100 K.

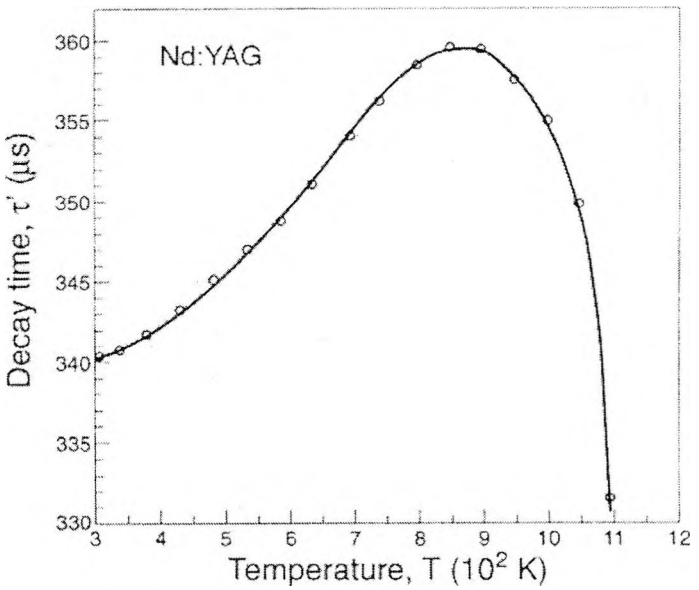

Figure 2.18 Observed fluorescence decay time, τ'(Nd:YAG) as a function of temperature (after Ref.31)

2. 4 Crystal fibre -based fluorescence thermometry

2.4.1 Introduction to crystal fibre

Known as functional fibres, optical crystal fibres offer a combination of material properties and waveguide geometry unavailable in either glass optical fibres or bulk crystals. Compared to glass fibres, they usually appear as single-crystal fibres with relatively large diameters and short length, and in most cases without claddings. They offer several special advantages such as broad transmission band, high melting point, favorable fluorescence characteristics, large nonlinear optical susceptibilities, and beam confinement of the waveguide structure, which can not be realized in glass fibres or bulk crystals.

The first research tide on single crystal fibres began in 1950s, when researchers found that crystals in this form demonstrated high crystalline perfection and near theoretical strength. However, it declined rapidly due to the difficulties of controlling the geometric parameters of these fibres and the impracticability of their device applications. It was not until 1966, when Kao and Hockham [33] pointed out the possibility of fabricating glass fibres with very low losses, did researchers pay attention to crystal fibres again. In 1967, LaBelle and Mlavsky [34] reported on the growth of sapphire filaments using a modified Czochralski pulling method with induction

heating system. In 1970, the laser heating technique was first applied to the growth of single-crystal fibres by Gasson et al [35] and later developed into the well-known laser heated pedestal growth (LHPG) method by Burrus and Coldren [36] in 1975. Since then, properties of single-crystal fibres have been significantly improved, various doped or un-doped single-crystal fibres were grown and studied, and a number of crystal-fibre devices have also been developed.

The applications of single-crystal fibres can be classified into three categories: passive, active, and nonlinear. The passive devices, including fibre-optic sensors and energy delivery systems in industrial and medical applications, are usually made of sapphire or YAG single-crystal fibres. The active devices, represented by fibre laser, typically employ doped YAG single-crystal fibres. The nonlinear devices usually use $LiNbO_3$ single-crystal fibres for both high laser intensities and long interaction length. These devices show special advantages that can not be achieved by traditional devices.

2.4.2 Laser-heated pedestal growth of single-crystal fibres

There are a number of single-crystal fibre growth techniques, among which the melt growth is considered the most important. The melt growth technique includes hot rolling [37], capillary-Bridgman growth [38], edge-defined film-fed growth (EFG) [39], laser-heated pedestal growth (LHPG) [36] and several other methods [40][41]. In these processes, LHPG has been developed into one of the most successful growth methods.

The basic two-beam LHPG system is shown in Figure 2.19. Two laser beams from symmetric directions are focused to melt the tip of a solid rod (termed the source rod) of the material to be grown. A seed crystal is dipped into the melt, then withdrawn at a faster rate than the source rod is fed in, resulting in the growth of a fibre of reduced diameter. The source rod can be easily manufactured in the form of either a round or square cross-section rod from polycrystalline material that has been fabricated from solidified melt, pressed and sintered powder, or hot-pressed sample. In order to grow fibre with low diameter fluctuation, the growth conditions such as laser powers and growth rates (pulling rate and feeding rate) must be very stable, and the source rod should have a round cross section with very uniform diameter along the symmetric axes. Doping can be achieved by using a powder mixture in the preparation of source rod, or more easily by coating source rods with dopant material providing the dopants are not volatile. In some cases

when oxidizable or volatile source materials are used, additional protection atmosphere is required. Although the two-beam LHPG systems are suitable for growing most of the fibres, some difficulty remains for the growth of some materials. This is mainly due to the molten zone around which the temperature distribution may not be homogeneous enough as it is heated from two opposite directions. As a result, some problems arise during fibre growth, especially for those materials with low thermal conductivities. For this reason, work has been done to improve the heating configuration. A typical successful design is the circular focusing, in which the laser beam was focused onto the fibre in a 360° axial symmetric distribution [42].

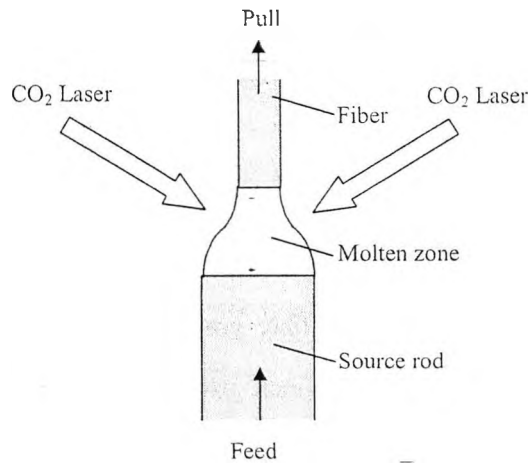

Figure 2.19 The laser-heated pedestal growth process

The LHPG method has advantages of no crucible contamination, no melting temperature limit, with short growth time, low cost, high versatility and excellent ability for growing crystals of solid solutions and crystals with a wide range of dopant concentrations. It is the most successful method for the growth of refractory oxide materials, and, for some types of crystal fibres, it is the only method that can achieve high optical qualitys. It is also a powerful technique for growing new compounds in single-crystal forms for physical, chemical, and crystallographic property evaluations. The weakness of the LHPG method appears in the difficulties in the stabilization of the fibre diameter, and for some materials, the large residual thermal stress in as-grown fibres due to its large temperature gradient and high growth rate in the growth process.

Typical fibre growth rates of LHPG method range between 0.5 and 10 mm/min, although growth rate as high as 20 mm/min has been reported under certain conditions [43]. While the

growth rates of crystal fibres are slow compared with glass fibre pulling rates, they are much faster than the growth rates in bulk crystal by the Czochralski method.

Diameters of crystal fibres grown by the LHPG method range from several microns to over one millimeter, and the initial source rod diameters are usually prepared from hundreds of microns to several millimeters. A diameter reduction of no more than 3 to 1 is normally used during the growth for maintaining equilibrium melting zones. Very small diameter fibres are grown by using as-grown fibres as source rods and usually grown for several times. Sometimes, repeated growth is also applied to improve the fibre quality especially when growing from powder-made source rods.

Another noteworthy technique is the edge-defined film-fed growth (EFG) method. It was first reported by LaBelle in 1971 [39], and was originally developed for growing continuous sapphire fibres for structural applications in ceramic and matrix composites. The main advantage of the EFG method is its mass-production capability, which allows for the continuous growth of multiple fibre strands from a single machine, but the optical quality of EFG fibres remains lower than that of LHPG fibres in the past years. Recently, low loss EFG sapphire fibres have been reported [44], showing potential for growing high quality crystal fibres for optical applications.

2.4.3 Crystalline fibre based fluorescence lifetime thermometry

Among a range of the crystalline optical fibres, the oxide crystal fibres are of the greatest importance in the fibre thermometry, mainly due to their high melting points and good high temperature stability. Among all the oxide crystal fibres, the sapphire fibre and the YAG fibre deserve most attention as they are all suitable for various fibre thermometry applications.

Sapphire fibres have been successfully used in blackbody radiance based fibre thermometry for accurate measurement of temperature with high sensitivity and fast dynamic response as presented by Dils [45]. The device, as illustrated in Figure 2.20, consists of a small blackbody cavity which is sputtered on the end of a thin (0.25-1.25 mm diameter, 0.05-0.30 m length) sapphire fibre, a connecting low-temperature glass fibre, and a conventional optical detector. The radiance from the cavity is used to measure its temperature. The thermometer is calibrated at a single temperature and uses the fundamental radiation laws to extrapolate to other temperatures.

This type of fibre thermometer has found commercial applications [46]. Accufibre Corporation has developed a series of sapphire fibre thermometers ranging from 100 ℃ to 1800

℃ with a highest temperature resolution of 0.01 ℃, and these have been marketed commercially. .

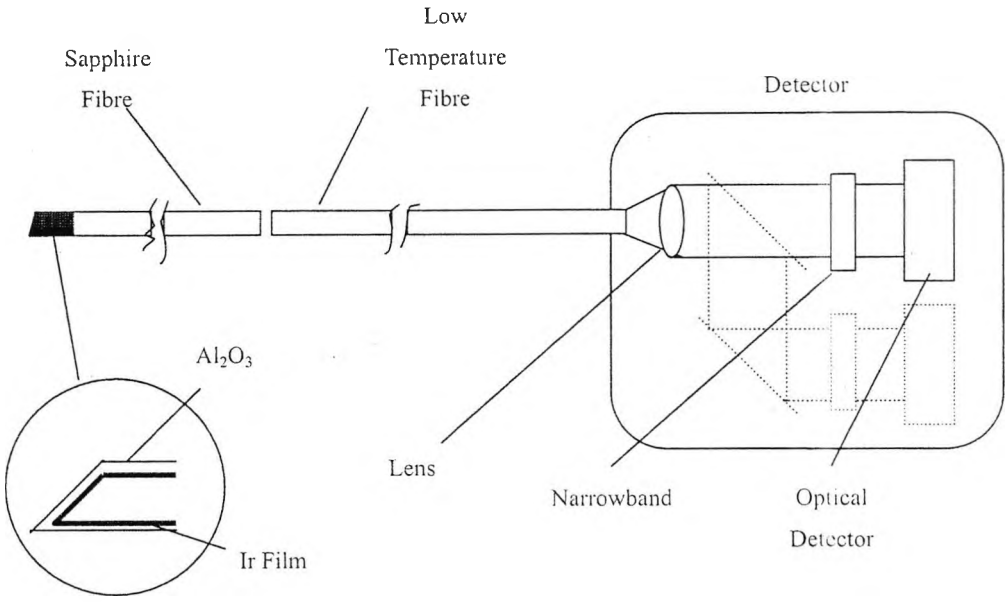

Figure 2.20 High temperature optical fibre thermometer using radiance detection (after Ref. 45)

Fibre thermometry based on the fluorescence properties of certain materials, such as the fluorescence intensity and fluorescence lifetime, is a major focus in this thesis. Generally, fibre thermometers based on fluorescence decay of certain crystals have similarities in their probe construction. As shown in Figure 2.21, the temperature sensing fluorescent material is directly coupled to the system through the guiding fibre bundle. Such coupling is made by attaching the fluorescent substance to the fibre bundle using a mechanical external cover sheath as a support for the strength. Usually gold-coated fibre is used in the fibre bundle for elevated ambient temperature applications. However, the covered probe, due to its large thermal mass, makes the probe construction complicated and the thermal response somewhat slow. The sustainable temperature of the guiding silica fibre bundle also limits the highest working temperature of the system.

Crystal optical fibres were first introduced as a promising fluorescent sensing candidate by Shen et al in 1996 [47]. The construction of the crystalline fibre probe, as illustrated in Figure 2.22, offers great advantage in performance. In such a probe, a certain length of sapphire and YAG crystal fibres is usually used with a millimetre long of temperature-sensing tip.

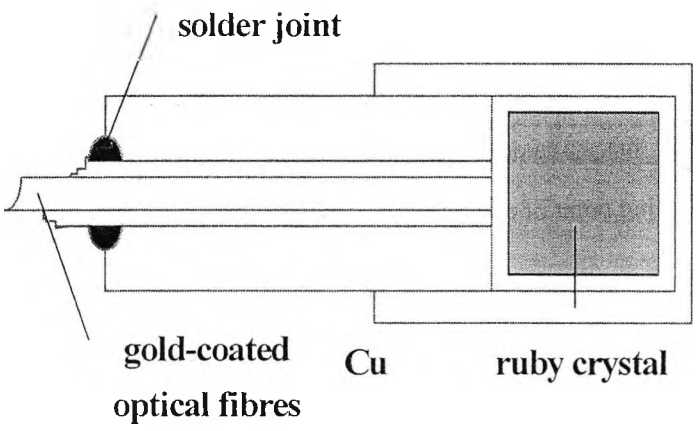

Figure 2.21 Normal probe construction of the fluorescence based fibre thermometer (after Ref. 30)

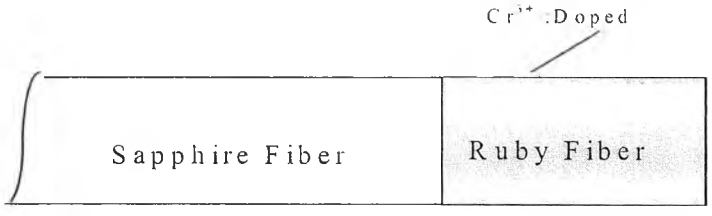

Figure 2.22 Construction of crystal fibre probe with active ions in its tip (after Ref.47)

Due to the specific feature of its probe construction, a fibre thermometer [48] using such a composite crystalline fibre probe, as shown in Figure 2.23, has many advantages. First, the thermometer probe is compact. Because of the excellent mechanical properties of sapphire or YAG fibres, additional mechanical external coverage is unnecessary outside the fibre probe. Thus, the pin-like thermometer probe makes its thermal response much faster. The space used for the fibre probe in the ambient environment can also be very small and the probe exerts less interference to the ambient environment during temperature measurement. Secondly, because the sapphire or YAG fibre is of sufficient length, all of the guiding fibre bundle and the coupling portion can be positioned far away from the severe hot environment. Thus, the fibre thermometer can be used in severe environment situations where the probe itself can sustain. Less expensive commercial silica fibre can be used as the guiding fibre bundle for signal transmission. The coupling between the fibre bundle and the crystal fibre probe would not easily deteriorate so that

the performance stability of the system can be improved. Thirdly, by combining the techniques of fluorescent lifetime detection and radiance detection, such a thermometer probe can be used for wide range temperature measurement. The range can be from the cryogenic to very high temperature near the melting point of crystal fibre (1900 or 2000 ℃) [49].

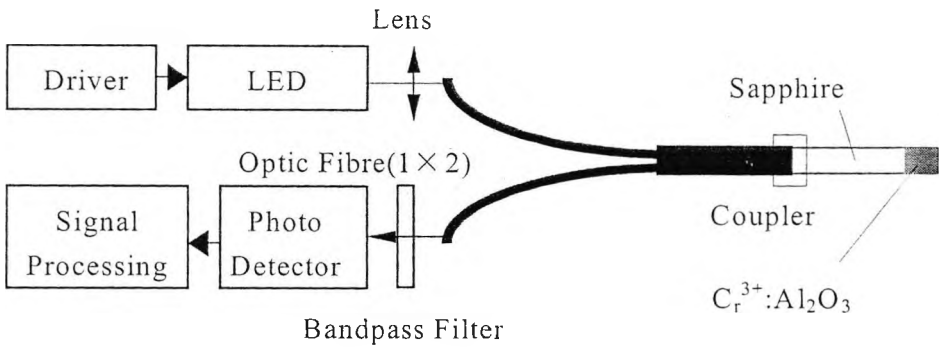

Figure 2.23 Crystalline fiber optic thermometry based on fluorescence decay (after ref. 48)

The sapphire fibre with a ruby tip was also grown by means of the LHPG method, as introduced in the early part of this section. A two step growth process must be used for the fibre with a fluorescence ion doped tip [47]. At first, a pure sapphire fibre with the required size and optical quality was grown, and then used as a seed. A short ruby rod or a sintered powder rod combined with Cr_2O_3 and Al_2O_3 powder is used as the source rod. By dipping the seed sapphire fibre into the melting zone of the source rod mentioned above, a tip of the Cr^{3+} ion doped sapphire fibre (ruby fibre) can be grown readily in the pure sapphire fibre end. A smooth combination between the doped and undoped part can be realized by carefully adjusting the speed of the seed fibre and the source rod. Such a growth procedure is illustrated in Figure 2.24.

The tip-doped fibre grown by this method can be of very good optical quality. The loss for the undoped sapphire fibre can be as low as 1~2 dB/m. There is no obvious edge loss zone between the doped and the undoped fibre. The mechanical strength of the fibre is also very good.

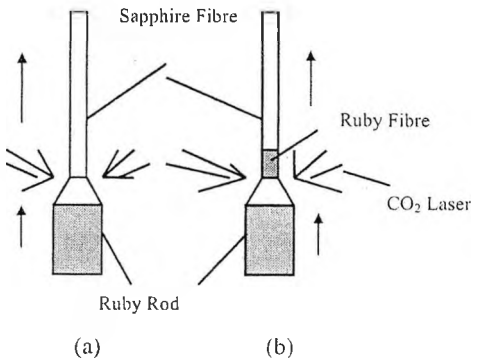

Figure 2.24 Growth of the crystal fibre with a fluorescence tip
(a) before growth (b) after growth (after ref.48)

2.5 Summary

As an important introduction to the technical background of this thesis, previous work on various aspects of the fluorescence based fibre thermometry, and the crystalline fibres, is reviewed in this chapter.

The operational principle of fluorescence based fibre thermometer has been discussed in detail together with several important signal processing techniques involved. It has been shown that the fluorescence based fibre thermometers using doped glass fibre, such as Nd^{3+} and Er^{3+} doped glass fibres, and crystals have demonstrated good performance over a comparatively low temperature region.

The use of crystalline fibre has been discussed, as this is a specialist fibre suitable for long-term applications at high temperatures. The techniques used for crystalline fibre growth, especially the LHPG method, are introduced. A composite crystalline fibre probe with a fluorescence ion doped tip at the end part of fibre is considered to be especially suitable for fluorescence based thermometry at high temperatures. This overview of previous research, including that by the author, sets the scene for the work discussed in subsequent chapters of the thesis which are based upon the techniques and methods discussed.

2.6 References

[1] J.H. Schulman and C.C. Klick, Fluorescence. In: McGraw-Hill Encyclopedia of Science & Technology. (New York, St. Louis, Sab Francisco: McGraw-Hill) (1987)

[2] K.A. Wickersheim, and R.V. Alves, Fluoroptic thermometry: a new RF-immune technology. Biomedical Thermology. Pub:Alan Liss, New York, pp547-554 (1982)

[3] C. Ovren, M. Adoleson, and B. Hok,. "Fibre optic systems for temperature and vibration measurements in industrial applications", In: Proc. Int. Conf. Optical Techniques in Progress Control, The Hague (Pub:BHRA – British Hydromechanical Research Association, Cranfield, Bedford, UK) (1983)

[4] K.A. Wickersheim and M.H. Sun, "Fibreoptic thermometry and its applications", Journal of Microwave Power 22, pp85-94 (1987)

[5] R.R. Sholes and J.G. Small, "Fluorescent decay thermometer with biological applications", Rev. Sci. Instrum. 51, pp882-884 (1980)

[6] Th. Bosselmann, A. Reule, and J. Schröder, "Fibre-optic temperature sensor using fluorescence decay time", In Proceedings of 2nd Conference on Optical Fibre Sensors (OFS'84). SPIE Proceedings 514, pp151-154 (1984)

[7] K.T.V. Grattan, A.W.Palmer, "A fibre-optic temperature sensor using fluorescence decay". SPIE Proceedings 492, pp535-542 (1984)

[8] S.A. Wade, S.F. Collins, K.T.V. Grattan and G.W. Baxter, "Strain-independent temperature measurement by use of a fluorescence intensity ratio technique in optical fibre", Applied Optics, 39, pp3050- 3052 (2000)

[9] S.A. Wade, S.F. Collins, and G.W. Baxter, "Fluorescence intensity ratio technique for optical fibre point temperature sensing", Journal of Applied Physics, 94, pp4743-4756 (2003)

[10] K.T.V. Grattan, A.W.Palmer, "Infrared fluorescence 'decay-time' temperature sensor", Rev. Sci. Instrum. 56, pp1784-1787(1985)

[11] K.A. James, W.H. Quick and V.H. Strahan, "Fibre Optics: the way to true digital sensors?" Control Engineering, 26, pp30-33 (1979)

[12] M. Sun, "Fibreoptic thermometry based on the photoluminescent decay times", In: Temperature- Its Measurement and Control in Science and Industry, Vol.6, Part 2(New York: American Institute of Physics), pp715-719 (1992)

[13] L.J. Dowell and G.T. Gillies, "Errors caused by baseline offset and noise in the estimation of exponential lifetimes", Review of Scientific Instruments, 62, pp242-243 (1990)

[14] K.T.V. Grattan, R.K.Selli and A.W. Palmer, "Ruby decay-time fluorescence thermometer in a fibre-optic configuration", Review of Scientific Instruments, 59, pp1328-1335 (1988)

[15] A.T. Augousti, K.T.V. Grattan and A.W. Palmer, "Visible LED pumped fibre-optic temperature sensor", IEEE Transactions on Instrumentation and Measurement, 37, pp470-472 (1988)

[16] Z.Y. Zhang, K.T.V. Grattan, and A..W. Palmer, "Phase-locked detection of fluorescence lifetime and its thermometric applications", SPIE Proceedings, 1885, pp228-239 (1993)

[17] C.J. Koester, and E. Snitzer, "Amplification in a fibre laser", Applied Optics 3, pp1182-1186 (1964)

[18] J.C. Stone, and C.A. Burrus, "Neodymium-doped silica lasers in end-pumped fibre geometry", Applied Physics Letters 23, pp388-389 (1973)

[19] S.B. Poole, D.N. Payne, and M.E. Fermann, "Fabrication of low-loss optical fibres containing rare-earth ions", Electron Letters 21, pp737-738 (1985).

[20] B.J. Ainslie, S.P. Craig-Ryan, S.T. Davey, and B. Wakefield "The fabrication assessment and optical-properties of high-concentration Nd^{3+}-doped and Er^{3+}-doped silica-based fibres". Materials Letters, 6, pp139-144 (1988).

[21] Z.Y. Zhang, K.T.V. Grattan, A.W. Palmer, and B.T. Meggitt. "Spectral characteristics and effects of heat treatment on intrinsic Nd-doped fibre thermometer probes", Review of Scientific Instruments 69, pp139-145 (1998)

[22] Z.Y. Zhang, K.T.V. Grattan, A.W. Palmer et al. "Characterization of erbium-doped intrinsic optical fibre sensor probes at high temperatures". Review of Scientific Instruments 69, pp2924-2929 (1998).

[23] Z.Y. Zhang, K.T.V. Grattan, A.W. Palmer, "Fibre-optic high-temperature sensor based on the fluorescence lifetime of alexandrite", Review of Scientific Instruments, 63, pp3869-3873 (1992)

[24] W.H. Fonger and C.W. Struck, "Temperature dependences of Cr^{3+} radiative and non-radiative transitions in ruby and emrald", Physical Review B, 11, pp3251-3260 (1975)

[25] Z.Y. Zhang, K.T.V. Grattan, "Temperature dependance of YAG:Cr^{3+} fluorescence lifetime up to 550 K", Journal of Luminescence, 62, pp263-269 (1994)

[26] J .C. Walling, O.G. Peterson, H.P. Jenssen, R.C. Morris and E.W. O'Dell. "Tunable

alexandrite lasers", IEEE J. Quantum Electronics, QE16(12), pp1302-1315 (1980)

[27] Z.Y. Zhang, K.T.V. Grattan, A.W. Palmer, "Temperature dependences of fluorescence lifetimes in Cr^{3+} -doped insulating crystals", Physical Review B, 48, pp7772-7778 (1993)

[28] Z.Y. Zhang, "Fibre optic fluorescence thermometry", Ph.D thesis (London: City University) (1993)

[29] Z.Y. Zhang, K.T.V. Grattan, A.W. Palmer, "Thermal characteristics of alexandrite fluorescence decay at high temperatures, induced by a visible laser diode emission", Journal of Applied Physics, 73, pp3493-3498 (1993)

[30] Z.Y. Zhang, K.T.V. Grattan and A.W. Palmer, "A novel signal processing scheme for a fluorescence based fibre-optic temperature sensor", Review of Scientific Instruments, 62, pp1735-1742 (1991)

[31] K.T.V. Grattan, J.D. Manwell, S.M.L. Sim et al, "Lifetime investigation of fluorescence from neodymium-yttrium-aluminum garnet at elevated temperature". Optics Communications, 62, pp104-107 (1987)

[32] Z. Zhang, J.H. Herringer and N. Djeu, "Monolithic crystalline fibre optic temperature sensor", Review of Scientific Instrument, 68, pp2068-2070 (1997)

[33] K.C. Kao and G.A. Hockham, "Dielectric-fibre surface waveguides for optical frequencies", IEEE Proc. 113, pp1151-1158(1966).

[34] H.E. LaBell, and A.I. Mlavsky, "Growth of sapphire filaments from the melt", Nature, 216, pp574-577(1967).

[35] D.B. Gasson, and B. Cockayne, "Oxide crystal growth using gas lasers", Journal of Materials Science, 5, pp100-104 (1970).

[36] C.A. Burrus and J. Stone, "Single-crystal fibre optical device: A Nd:YAG fibre laser", Appl. Phys. Lett. 26, pp318-321 (1975).

[37] R.R. Turk, "Rolling a KCl fibre: a feasibility study", SPIE Proceedings 320, pp93-101(1982).

[38] B.Nayar, in Technical Digest of the Topical Meeting on Integrated and Guided Wave Optics, (OSA Washington D.C., 1982), paper ThA2.

[39] H.E.LaBell, Jr., "Growth of controlled profile crystals from the melt: Part II - edge-defined film-fed growth (EFG)", Mat. Res. Bull. 6, pp581-590 (1971)

[40] Y. Mimura, Y. Okmura, Y. Komazawa, and C. Ota, "Growth of fibre crystals for infrared

optical waveguides", Jpn. J. Appl. Phys. 19, ppL269-L272(1980).

[41] T.J.Bridges, J.S. Hasiak, and A.R. Strand, "Single-Crystal AgBr infrared optical fibres", Opt. Lett. 5, pp85-87 (1980).

[42] M.M. Fejer, J.L. Nightingale, G.A. Magel and R.L. Byer, "Laser-heated miniature pedestal growth apparatus for single-crystal optical fibres", Review of Scientific Instruments, 55, pp1791-1796(1984).

[43] V. Phomsakha, R.S.F. Chang, and N. Djeu, "Novel implementation of laser heated pedestal growth for the rapid drawing of sapphire fibres", Review of Scientific Instruments 65, pp3860-3861(1994).

[44] J.J. Fitzgibbon and J.M. Collins, "High volume production of low loss sapphire optical fibres by Sapphikon EFG(Edge defined, Film-fed Growth) method", SPIE Proceedings, 3262, pp135-141(1998).

[45] R. R. Dils, "High-temperature optical fibre thermometer", J. Appl. Phys., 54, pp1198-1201 (1983)

[46] H. Amick, "Optical fibre sensors broaden temperature measurement limits", Research & Development, pp64-69 (1986)

[47]Y. Shen, R. Xu, "Development of a compact sapphire fibre thermometer probe using fluorescent decay", SPIE Proceedings, 2895, pp144-153(1996)

[48] Y. Shen, Y. Wang, L. Tong and L. Ye. "A novel sapphire fibre thermometer using fluorescent decay", Sensors & Actuators A71, pp70-73 (1998)

[49] Y. Shen, L. Tong, Y. Wang, L. Ye, "Sapphire fibre thermometer ranging from 20 to 1800 ℃", Applied Optics, 38, pp1139-1143 (1999)

Chapter 3: Technical Background for Fibre Bragg Gratings: Fabrication and Applications in Optical Thermometry

3.1 Fibre Bragg gratings: Introduction

A fibre Bragg grating (FBG) comprises, in principle, a piece of optical fibre, the core refractive index of which is periodically modulated in the longitudinal direction. For a conventional FBG, the periodicity of the index modulation has a physical spacing that is one half of the wavelength of light propagation in the waveguide. It is the phase matching between the grating planes and incident light that results in coherent back reflection [1]. In this way, as shown in Figure 3.1, the Bragg wavelength of a fibre Bragg grating, λ_B, can be represented by

$$\lambda_B = 2n_{eff}\Lambda \tag{3-1}$$

where n_{eff} is the effective refractivity index of the core of the fibre, and Λ is the grating period of refractive index modulation. Normally, FBGs are fabricated by exposing so-called photosensitive fibres to an interference pattern of certain UV laser emission.

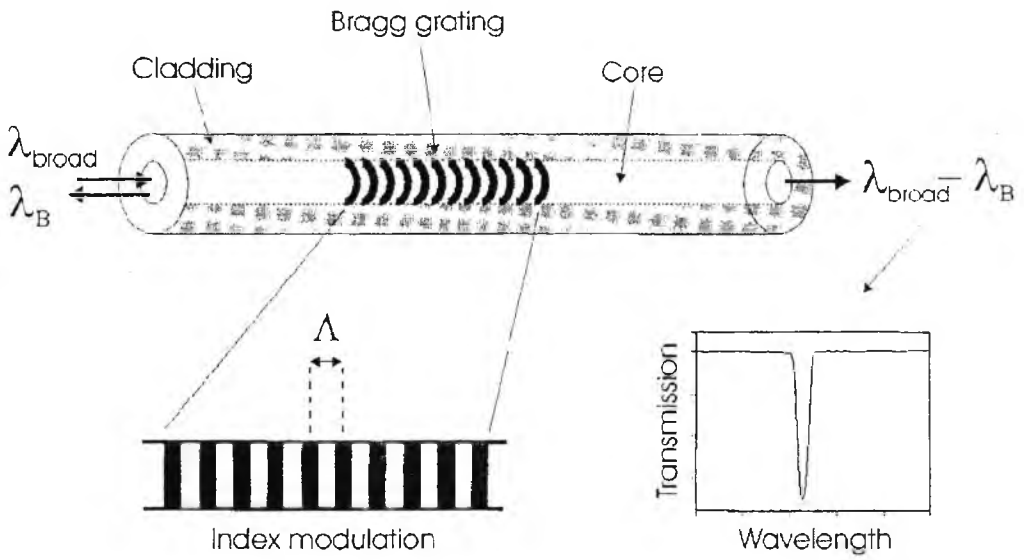

Figure 3.1 Illustration of a uniform Bragg grating with a constant index modulation amplitude and period. Also shown are the incident, diffracted, and grating wave vectors that match momentum conservation (after Ref. 1)

Fibre photosensitivity was first observed in germanium-doped silica fibre in experiments performed by Hill and coworkers [2,3] at the Communication Research Centre in Canada in 1978. During an experiment carried out to study nonlinear effects in a specially designed optical fibre, intense visible light from an argon ion laser was launched into the core of the fibre. Under prolonged exposure, an increase in the fibre attenuation was observed. It was determined that during exposure the intensity of the light back-reflected from the fibre increased significantly with time, with almost all of the incident radiation back-reflected out of the fibre. Spectral measurements confirmed that the increase in reflectivity was the result of a permanent refractive index grating being photoinduced over the 1-m fibre length, which was subsequently called a "Hill grating". This result spawned a new interest in a previously unknown photorefractive phenomenon of optical fibres called fibre photosensitivity.

Although the discovery of photosensitivity in the form of photoinduced index changes played a key role in the advancement of optical fibre technology, devices such as self-induced gratings were not practical. This was largely because the Bragg resonant wavelength was limited to the argon ion writing wavelength (488 nm), with only a very little wavelength change being induced by straining the fibre. The key development that turned the phenomenon from a scientific curiosity to a mainstream tool was the side-writing technique first demonstrated at the United Technologies Research Centre (this is sometimes called the transverse holographic technique). In 1989 Meltz et al [4], following the work by Lam and Garside [5], showed that a strong change of refractive index occurred when a germanium-doped fibre was exposed to direct UV light close to the range of 240 – 250 nm. Irradiating the side of the optical fibre with a periodic pattern derived from the intersection of two coherent 244-nm beams in an interferometer resulted in a modulation of the core index of refraction, inducing a periodic grating. Changing the angle between the intersecting beams alters the spacing between the interference maxima; this sets the periodicity of the gratings, thus making possible reflectance at any wavelength. Even though the writing wavelength was at 244 nm, gratings could be fabricated to reflect at any wavelength thus permitting their use in modern telecommunication and sensor systems.

A number of reviews of such gratings have been written, giving further details of characterization and performance, e.g. Othonos [1], from which further information is available.

3.2 Photosensitive optical fibres

3.2.1 Photosensitivity of optical fibre

Photosensitivity in optical fibre refers to a permanent change in the refractive index of the fibre core when exposed to light with characteristic wavelength and intensity that depends on the core material. Initially, photosensitivity was thought to be a phenomenon only associated with optical fibres having a large concentration of germanium in the core and photoexcited with 240 – 250 nm ultraviolet (UV) light. Following many years research, however, photosensitivity has been observed through photoexcitation at different UV wavelengths in a wide variety of different fibres, many of which do not have germanium as the only dopant and some of which contain no germanium at all. Nevertheless, germanium-doped optical fibre remains one of the most important materials for the fabrication of devices utilizing photosensitivity.

As mentioned above, photosensitivity was first observed in an optical fibre, that was exposed to laser light at 488 nm launched into its core [2,3]; this phenomenon was subsequently associated with a two-photon absorption process [5]. After a transverse writing method was later used to photo-imprint Bragg gratings at a direct excitation wavelength of 240 nm [4], the absorption band centreed on this excitation (240 nm) has been related to defect centres in germanosilicate glass [6,7]. Irradiation with a wavelength coincident with this band was shown to result in bleaching and the creation of other absorption bands, leading to a refractive index change that was described through the Kramers-Kronig relation. It was then discovered that photosensitivity could be improved by orders of magnitude through hydrogenation of the optical fibre core before grating inscription [8].

In addition to the use of hydrogen loading to create photosensitivity in fibre, many types of photosensitive fibres have been developed, these mainly including boron/germanium (B/Ge) codoped silica fibres [9], the rare-earth ion (such as Ce^{3+} and/or Er^{3+}) doped silica fibres [10][11] and the high germanium (Ge) doped silica fibres [12]. Enhanced photosensitivity was also reported in tin-doped phosphosilicate optical fibres [13].

3.2.2 Mechanism of photosensitivity

A. Types of photoinduced gratings

During the early stages of research in the field, when photosensitivity was thought to occur only in germanium-doped fibres, it was believed that the germanium oxygen vacancy defects, known as germanium oxygen-deficient centres (GODCs) were responsible for the photoinduced index changes. Clearly, germanium-doping is a very important factor in acquiring a significant degree of photosensitivity in silica fibres. However, with the demonstration of photosensitivity in different types of fibre, it is apparent that photosensitivity is a function of various mechanisms (photochemical, photomechanical, thermochemical) and its relative contribution will be fibre dependent, as well as intensity and wavelength dependent.

The growth dynamics of Bragg gratings as they are exposed to UV radiation have been carefully investigated by a number of authors [1]. The gratings fabricated are generally classified into three types. The first type, known as a Type I grating, experienced in most writing experiments, corresponds to a monotonic increase in the amplitude of the refractive index modulation. More specifically, this classification refers to a grating produced with less than 100 mJ/cm^2/pulse and a cumulative fluence that is typically less than 500 J/cm^2. This strongly depends on how photosensitive the fibre is and results in a positive refractive index change ($\Delta n>0$). Type IIA gratings are normally observed in high GeO_2 doped fibres (>25 mol%, high numerical aperture (NA) fibres). Protracted UV exposure of gratings in this type of fibre often results in complete or partial grating erasure, followed by a new spectral formation associated with a highly negative Δn (for a cumulative fluence exceeding 500 J/cm^2), and an accompanying increase in the reflecting wavelength. It is almost certain that the mechanisms responsible for Type I and Type IIA gratings are different. Phenomenological models that account for these observations usually assume that the refractive index evolution with exposure time results from two local reactions, the first of which erases and produces some defects or chemical species that lead to a positive change in the refractive index, whereas the second reaction, which is slower than the first, produces a negative change through structural reorganization. A typical fabricating process of Type IIA grating is illustrated in Figure 3.2 to show the growth of the reflectivity with time [14].

In addition to the two types of gratings introduced above, there is also a third type of grating classified as Type II. This type of grating corresponds to irradiation at energy levels greater than 1000 mJ/cm^2, resulting in a process that allows for a single excimer light pulse to photoinduce large refractive index changes in small localized regions at the core/cladding

boundary. It is considered to be a result of physical damage that is limited to the fibre core, producing very large refractive index modulations estimated to be close to 10^{-2} [15].

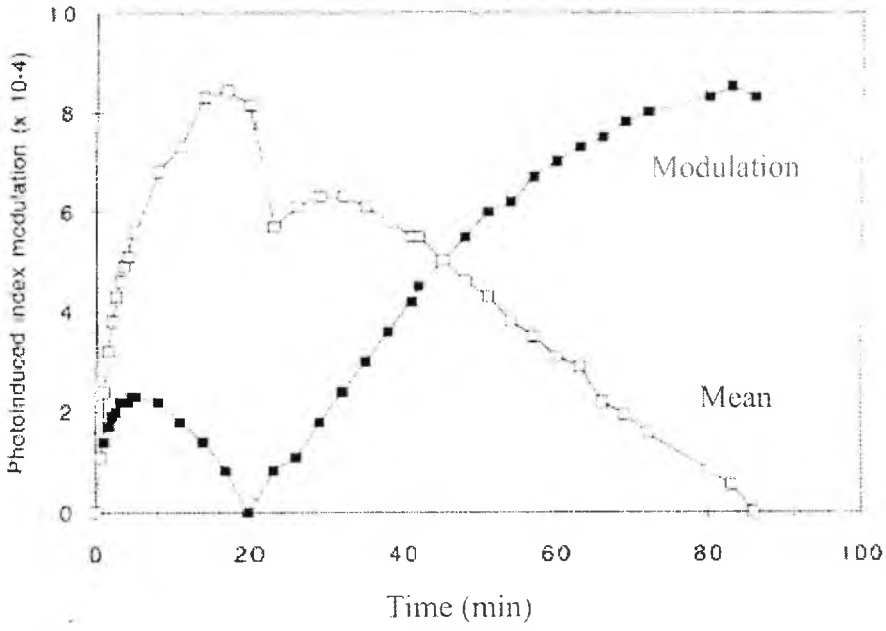

Figure 3.2 Formation of a Type IIa grating in an unloaded highly germanium doped fibre. Grating length was 2 mm, fluence 110 mJ/cm2 with a repetition rate of 10 Hz, fibre tension 20 g. "Modulation" represents the modulation index difference calculated from the reflectivity and "Mean," the mean index difference deduced from the Bragg wavelength shift (after Ref 13).

B. Mechanism of photosensitivity in fibres

Extensive research on photosensitivity mechanisms has been carried out to acquire a better understanding of the underpinning science behind the phenomenon of photosensitivity and since it was found, many theoretical models have been presented in an effort to explain the experimental phenomena. So far, there is limited knowledge about the origins of photosensitivity and its corresponding refractive index change. It is clear that no single model can explain all the experimental results reported, as there are several possible microscopic mechanisms at work.

Among all the models presented to account for the photosensitivity phenomenon, initially the color-centre model, and later the compaction and densification model seem to be accepted by the majority of researchers. There is substantial experimental evidence supporting the mechanism put forward by Hand and Russel [12]. The resultant color-centres are responsible for changes in the UV absorption spectrum of the glass, and the refractive index change following the Kramers-Kronig relationship. Many experiments [16,17,18,19,20] support the GeE' centre model

for photosensitivity, which is certainly the mechanism responsible for the original self-organized gratings [2]. The color-centre model, however, does not completely explain all the experimental observations [14,21], and later, an alternative model based on the glass densification induced by photoionization of the Ge defects [22] also has experimental support [23].

In addition to the color centre model and the compaction and densification model, as mentioned above, there are several other models dedicated to account for the phenomenon of photosensitivity. These include the Electron Charge Migration Model [24], Permanent Electric Dipole Model [12], Ionic Migration Model [25] and Stress-Relief Model [26]. As will be seen in chapter 6 of this thesis, a so-called cation-hopping model is being proposed by the author to account for the experimental phenomena associated with the FBG stability during annealing at high temperatures [27]. The work confirms that the model can explain many experimental results reasonably and are especially important in the research work of high-temperature sustainable gratings. The detailed work on the cation-hopping model will thus be presented in Chapter 6 of this thesis.

3.3 Thermal decay of fibre Bragg gratings ? the high temperature sustainability of FBGs

As mentioned in the previous sections, fibre Bragg gratings (FBGs) have been widely used in the optical communications and fibre-optic sensing fields now [1]. For stable applications of FBGs in industry and the laboratory, their thermal properties, such as their wavelength stability or the decay characteristics of the peak reflectance have long been an important factor to be taken into consideration in a range of applications. It has been confirmed that the thermal decay characteristics of those UV induced FBGs behave very differently by one from another.

Among the three types of gratings, Type II gratings, fabricated under very large UV light intensity, normally have very good thermal stability. However, the bandwidth of Type II gratings is generally large and thus the gratings are not suitable for wavelength-determined sensing applications. Compared with this, the bandwidth of Type IIA grating is comparatively narrow and can be applied in some specific sensing field. As mentioned earlier, Type IIA gratings are normally fabricated into high germanium doped silica fibres with prolonged exposure to UV laser emission. The temperature stability of these gratings is satisfactory at temperatures below 650 ^{0}C. Almost no decay in reflectivity or refractive index modulation can be observed during the annealing process

below 650 ^{0}C. However, the gratings decay very rapidly at temperatures of 700 ^{0}C and above. They will disappear or be erased completely by the annealing temperature above 750 ^{0}C within several hours.

The Type I grating is the most widely fabricated and used in various applications and thus most attention will be paid to this type of gratings in this thesis. For this type of grating, the composition of the fibre for grating fabrication has a very important effect on the photosensitivity of the fibre and the temperature stability of the gratings written into it. Some gratings of this type, for example, those written into boron and germanium codoped silicate fibre, can survive only at comparatively low temperatures of about 300 ^{0}C and normally disappear after being annealed for hours at temperatures over 350 ^{0}C [28]. Compared with these, FBGs written into germanium doped silicate fibres can survive some higher temperatures of about 700 ^{0}C [29]. Moreover, the FBGs written into the Sn doped photosensitive fibre can even survive at a annealing temperature of 800 ^{0}C for hours [30]. Clearly, the thermal stability of these gratings is strongly dependent on the glass fibre composition, into which the gratings are embedded, as well as the conditions in which the gratings are fabricated.

Recent work by the author and co-workers have revealed that the FBGs written into several Sb or In codoped germano-silicate fibres can all survive much higher temperatures, of up to 800 ^{0}C [31] and 900 ^{0}C [27][32]. Detailed work on the fabrication, testing and evaluation of these strong gratings will be presented in Chapters 5 and 6 of this thesis.

In addition to the work mentioned above, there have also been several reports on the specially fabricated gratings which can be operated up to high temperature. Among these, the gratings fabricated into a germanium free silicon oxynitride fibres using an excimer laser working at 193 nm[33], the chemical composition gratings (CCG) using fluorine diffusion during laser exposure [34][35] and the gratings fabricated by using high power femtosecond laser [36] are considered to be sustainable at high temperatures up to even 900 ^{0}C or 1000 ^{0}C. Clearly, these gartings are important for applications at high temperatures. However, as the fabrications of these gratings are related to special laser system [33][36] or special fabricating procedure[34][35], the applications of these methods are limited. In this thesis, the work on the gratings will thus focus on that fabricated into normal photosensitive fibres by exposuring them to excimer laser emissions.

3.4 Summary

Fibre Bragg gratings have now been shown to be very important components in the optical communications and the fibre optic sensing fields. FBGs can be fabricated by exposing so-called photosensitive fibres to an UV laser interference pattern. There are generally three types of FBGs, named Type I, Type IIA and Type II respectively, depending on the writing condition of the gratings.

For high temperature sensing applications, the thermal stability of the gratings is essential. There are several important factors affecting the temperature sustainability of the gratings. A number of investigations have been carried out on the mechanism of FBG formation, as well as the characteristics of FBGs at high temperatures. This brief overview of the field, coupled with the extensive reports on the properties and fabrications of FBGs, e.g. [1], forms a background for the work reported in subsequent chapters of this thesis.

3.5 References

[1] A. Othonos, "Fibre Bragg Gratings", Review of Scientific Instruments, 68, pp4309-4341 (1997)

[2] K.O. Hill, Y. Fujii, D. C. Johnson, and B. S. Kawasaki, "Photosensitivity in optical fibre waveguides: Application to reflection filter fabrication," Applied Physics Letters, 32, pp647-649 (1978)

[3] B.S. Kawasaki, K. O. Hill, D. C. Johnson, and Y. Fujii, "Narrow-band Bragg reflectors in optical fibres," Optics Letters, 3, pp66-68 (1978)

[4] G. Meltz, W.W. Morey and W.H. Glenn, "Formation of Bragg gratings in optical fibres by a transverse holographic method," Optics Letters, 14, pp823-825 (1989)

[5] D.K.W. Lam and B.K. Garside, "Characterization of single-mode optical fibre filters," Applied Optics, 20, pp440-445 (1981)

[6] H. Hosono and Y. Abe "Nature and origin of the 5-eV band in SiO2:GeO2 glasses," Physical Review B, 46, pp11445-11451 (1992)

[7] J. Nishii, K. Fukumi, and H. Yamanaka, "Photochemical reactions in Ge-SiO2 glasses induced

by ultraviolet irradiation: comparison between Hg lamp and and excimer laser," Physical Review B, 52, pp1661-1665(1995)

[8] P.J. Lemaire, R.M. Atkins, V. Mizrahi, W.A. Reed, "High-pressure H_2 loading as a technique for achieving ultrahigh UV photosensitivity and thermal sensitivity in GeO_2 doped optical fibres," Electronics Letters, 29, pp1191-1193 (1993)

[9] D.L. Williams, B.J. Ainslie, J.R Armitage, J.R. Kashyap and R. Campbell, "Enhanced UV photosensitivity in boron codoped germanosilicate fibres," Electronics Letters, 29, pp45-47(1993)

[10] M.M. Broer, R.L. Cone, and J.R. Simpson. "Ultraviolet-induced distributed-feedback gratings in Ce^{3+} -doped silica optical fibres," Optics Letters, 16, pp1391-1393(1991)

[11] F. Bilodeau, D.C. Johnson, B. Malo, K.A. Vineberg, K.O. Hill, T.F. Morse, A. Kilian, and L. Reinhart, "Ultraviolet-light photosensitivity in Er^{3+}-Ge-doped optical fibre," Optics Letters, 15, pp1138-1140 (1990)

[12] D.P. Hand and P.St.J. Russel, "photoinduced refractive-index changes in germanosilicate fibres," Optics Letters, 15, pp102-104 (1990)

[13] L. Dong, J.L. Cruz, J.A. Tucknott, L. Reekie, D.N. Payne, "Strong photosensitivity gratings in tin-doped phosphosilicate optical fibres," Optics Letters, 20, pp1982-1984 (1995)

[14] I. Riant and F. Haller, "Study of the photosensitivity at 193 nm and comparison with photosensitivity at 240 nm influence of fibre tension: type IIa aging," IEEE J. Lightwave Technology, 15, pp1464-1469 (1997)

[15] J.L. Archambault, L. Reekie and P.St.J. Russell, "100% reflectivity Bragg reflectors produced in optical fibres by single excimer laser pulses," Electron Letters, 29, pp453-455 (1993)

[16] R.M Atkins, V. Mizrahi and T. Erdogan, "248- nm induced vacuum UV spectral changes in optical fibre perform cores: Support for a color centre model of photosensitivity," Electronics Letters, 29, pp385-387 (1993)

[17] K.D. Simmons, S. LaRochelle, V. Mizrahi, G. I. Stegeman, D. L. Griscom, "Correlation of defect centres with wavelength-dependent photosensitive response in germania-doped silica optical fibres," Optics Letters, 16, pp141-143 (1991)

[18] R.M Atkins and V. Mizrahi, "Observations of changes in UV absorption bands of single mode germanosilicate core optical fibres on writing and thermally erasing refractive index gratings," Electron Letters, 28, pp1743-1744 (1992)

[19] D.L. Williams, et al. "Direct observation of UV induced bleaching of 240 nm absorption band in photosensitive germanosilicate glass fibres," Electron Letters, 28, pp369-371 (1992)

[20 T.E. Tsai, E.J. Friebele, and D.L. Griscom. "Thermal stability of photoinduced gratings and paramagnetic centres in Ge- and Ge/P-doped silica optical fibres," Optical Letters, 18, pp935-937 (1993)

[21] P. Niay, P. Bernage, S. Legoubin, M. Douay, W.X. Xie, J.F. Bayon, T. Georges, M. Monerie, and B. Poumellec, "Behavior of spectral transmissions of Bragg gratings written in germania-doped fibres: Writing and erasing experiments using pulsed or CW UV exposure," Optics Communications, 113, pp176-192 (1994)

[22] J.P. Bernadin and N.M Lawandy, "Dynamics of the formation of Bragg gratings in germanosilicate optical fibres," Optics Communications, 79, pp194-199 (1990)

[23] K.S. Chiang, M.G. Sceats and D. Wong. "Ultraviolet photolytic-induced changes in optical fibre :The thermal expansion coefficient," Optics Letters, 18, pp965-967 (1993)

[24] F.P. Payne, "Photorefractive gratings in single-mode optical fibres". Electronics Letters, 25, pp498-499 (1989)

[25] N.M. Lawandy, "Light induced transport and delocalization in transparent amorphous systems," Optics Communications, 74, pp180-184 (1989)

[26] M.G. Sceats, G.R. Atkins and S.B. Poole. "Photo-induced index changes in optical fibres," Annual Reviews in Material Science, 23, pp381-410 (1993)

[27] Y. Shen, J. He, T. Sun and K.T.V. Grattan, "High temperature sustainability of strong FBGs written into Sb/Ge co-doped photosensitive fibre — decay mechanisms involved during annealing", Optics Letters, 29, pp554-556 (2004)

[28] S. R. Baker, H. N. Rourke, V. Baker and D. Goodchild, "Thermal decay of fibre Bragg gratings written in boron and germanium codoped silica fibre," IEEE J. Lightwave Technol., 15, pp1470-1477 (1997)

[29] Y. Shen, S. Pal, J. Mandal, T. Sun, K.T.V. Grattan, S.A. Wade, S.F. Collins, G.W. Baxter, B. Dussardier, and G. Monnom, "Investigation on the photosensitivity, temperature sustainability and fluorescence characteristics of several Er-doped photosensitive fibres", Optics Communications, 237, pp301-308 (2004)

[30] G. Brambilla, V. Pruneri and L. Reekie, "Photorefractive index gratings in SnO_2:SiO_2 optical

fibres", Appl. Phys. Lett., 76, pp807-809 (2000)

[31] Y. Shen, T. Sun, K.T.V. Grattan and M. Sun, "Highly photosensitive Sb/ Er/Ge codoped silica fibre for fibre Bragg grating (FBG) writing with strong high-temperature sustainability," Optics Letters, 28, pp2025-2027 (2003)

[32] Y. Shen, J. Xia, T. Sun and K.T.V. Grattan, "Photosensitive Indium doped germano-silica fibre for strong FBGs with high temperature sustainability", IEEE Photonic Tech. Lett., 16, pp1319-1321(2004)

[33] E.M. Dianov, K.M. Golant, R.R. Khrapko, A.S. Kurkov, B. Leconte, M.Douay, P. Bernage and P. Niay, "Grating formation in a germanium free silicon oxynitride fibre", Electronics Letters, 33, pp236-238 (1997)

[34] M. Fokine, "Formation of thermally stable chemical composition gratings in optical fibers", J.O.S.A. B, 19, pp1759-1765 (2002)

[35] M. Fokine, "Thermal stability of chemical composition gratings in fluorine– germanium-doped silica fibers", Optics Letters, 27, pp1016-1018 (2002)

[36] S.J. Mihailov, C.W. Smelser, D. Grobnic, R. B.Walker, P. Lu, H. Ding, and J. Unruh, "Bragg gratings written in wll-SiO2 and Ge-doped core fibers with 800-nm femtosecond radiation and a phase mask", J. of Lightwave Technology, 22, pp94-100 (2004)

Chapter 4: Fibre Thermometer Based on the Fluorescence Decay Lifetime Detection for High Temperature Measurement

4.1 Introduction to fluorescence based fibre thermometry

High temperature measurement is important in industry – in chemical plant, in furnaces and kilns, and in a range of situations where the use of higher temperatures enhances a reaction or process. For most applications, the thermocouple approach will be adequate – for some, especially where there are issues of intrinsic safety or when thermocouples offer a poor lifetime due to the excessive temperature, a fibre optic probe may be preferred. Such sensors are immune to the interfering effects of electro-magnetic radiation (often not the case with thermocouples) and may be lighter in weight and durable in use. Thus there is a clear application domain for fibre optic temperature sensors and this includes those devices operating at the very high temperatures discussed in this work.

Over the past ten years, many fluorescent materials have been tested for performance evaluation when used in a fluorescence based fibre thermometer. The doped silica fibres, laser crystals and even fluorescent powders were found applicable to the sensing purpose over some specific temperature region. Normally, the silica fibres can be used as the probing material at a comparatively moderate temperature range [1], while some crystals and powders can be applied for fluorescence measurement at higher temperatures of close to 1000 ^{0}C [2][3]. However, it is still difficult to find a fluorescence material which can serve as the sensing probe to cover a wide temperature range from room temperature to above 1000 ^{0}C with reasonably high resolution. Though a ruby tip based sapphire crystal fibre was successfully assembled into a fibre thermometer to cover the wide temperature range from room temperature to a very high temperature (approaching 1800 ^{0}C) [4], the system needs a cross-referencing scheme between the fluorescence lifetime measurement and the blackbody radiation measurement, and is thus comparatively complicated in its system construction.

It is desirable for several industrial applications to find a novel fluorescence sensing material by which the fluorescence detecting scheme can cover the whole temperature range from room temperature to above 1000 ^{0}C and with a reasonably high temperature resolution. It is valuable with such a sensing material to simplify the sensor system and enhance the system

reliability when the sensor is used for the actual applications, such as heat flux measurement, brick performance monitoring of a steel furnace etc.

4.1.1 Fluorescent thermometry: lifetime and intensity -based methods

As has been presented in detail in Chapter 2, there are several important methods suitable for fluorescence –based thermometry. They can be lifetime-based or intensity-based. Among the intensity-based fluorescence thermometry, the temperature measuring method based on the fluorescence intensity ratio of specific materials [5][6] is important as it offers the advantage of strain independence so that the value of fluorescence intensity ratio can be directly used to determine the temperature.

As known by us, many materials emit fluorescence in such a way that the fluorescence lifetime is monotonically dependent on their ambient temperature. Thus, by the measurement of fluorescence lifetime, the corresponding temperature can be deduced, based on the known relationship between the fluorescence lifetime and temperature providing a calibration for the device. As the work involved in this thesis is concerned mainly with temperature, and is fundamentally strain free, the fluorescent lifetime –based method was chosen in this work.

From Figure 2.1, it can be seen that the fluorescence intensity decays in an exponential way in most situations when the fluorescent ion concentration doped into the host is not high. Based on this, several lifetime detecting schemes have been presented, these including the schemes involving the pulse measurement, the phase and modulation measurement and the phase-locked detection method. Among these schemes, the phase-locked detection scheme proposed [7] and developed by Zhang et al [8] possesses the advantage of high accuracy and only moderate system complexity, and is the preferred approach for accurate measurement of the fluorescent lifetime for most fluorescent sensing materials.

As the fluorescence performance of most transition metal ion doped crystals deteriorates at a temperature of 700 ^{0}C or below (for example, the Alexandrite with Cr^{3+} dopant [9]), the rare earth ion doped crystals are considered as the main candidates to meet such a requirement to cover the wide temperature range. In this thesis, a Tm^{3+} doped YAG crystal was chosen from many candidate materials to act as the sensing probe. It has been found that its fluorescence generally cover the wide temperature range from room temperature to above 1200 ^{0}C. The performance of

the fluorescence intensity and the lifetime with temperature was tested. The results showed that the crystal is suitable to be used as a promising sensing material for the fluorescence lifetime based sensor system.

4.2 Fluorescence decay characteristics of Tm^{3+} doped YAG crystal

4.2.1 Selection of the Tm doped YAG crystal as the sensing material

As has been mentioned above, fibre optic temperature sensors based on the fluorescence characteristics of a wide range of materials have been extensively investigated over the past ten years [8][10]. These studies have usually focused on the characteristics of signal intensity independence on the measurand and thus on how best to design a system to achieve a stable performance. In general, the fluorescence technique is well suited to lower temperature applications (<500 ^{0}C), as the fluorescence intensity observed often deteriorates at high temperatures due to the poor quantum efficiency of the material. This is seen especially with ruby, which has been reported to be stable at temperatures up to 1400 ^{0}C, but due to its poor fluorescence intensity, can only yield measurable results in a fibre optic fluorescence based sensor operating at up to 600 ^{0}C [11]. It is important to search for and use materials whose high temperature performance matches better their high temperature stability to enable higher temperature to be measured reliably. Fortunately, materials do exist where their fluorescence signal can still be strong enough at temperatures >1000 ^{0}C, and to incorporate these in sensor probes. Several kinds of rare earth ion doped oxides or garnets have been extensively investigated, as the availability of these materials can enable a fibre thermometer to be designed using the fluorescence lifetime principle and also cover a wide temperature range. Previous work has shown the potential of using rare earth ion doped crystals for high temperature sensing. For example, erbium (Er) doped Yttrium Aluminum Garnet (YAG) shows a strong fluorescence even at temperatures up to 830 ^{0}C [3] and thulium doped Y_2O_3 powder also has a detectable fluorescence lifetime change with temperature of up to 1000 ^{0}C [12].

For many practical applications, a number of factors should be considered when selecting the material for the probe including high sensitivity, good stability, high signal to noise ratio for detection and a wide coverage of the temperature range needed. Although Er-doped YAG has a strong fluorescence at up to 830 ^{0}C, it is not well suited as the material for this type of sensors as it

shows a severe hysteresis effect with lifetime at high temperatures [3]. Moreover, its fluorescence lifetime sensitivity from room temperature to 400 ^{0}C is very low and this will result in comparatively poor temperature resolution over this temperature region. For Tm doped Y_2O_3 powder, the fluorescence signal is weak and thus it is difficult to detect reliably and as a result to achieve good resolution in a temperature sensing application. In addition, a stable coupling between the transmission silica fibre used and the powder forming the probe is difficult to achieve accurately and reproducibly. These reasons make powders of this type not practical probe materials for high temperature use.

From the work of Tm doped Y_2O_3 powder [12], the potentiality of Tm doping into some hosts when they are used as the fluorescence based sensing materials has been seen. The stable performance at high temperature makes such kind of materials possible candidates for the practical sensing application. For proper signal coupling and better efficiency, a Tm doped crystal material was used in this thesis. Its fluorescence performance was investigated comprehensively.

Due to the difficulty in the coupling between a fluorescence crystal and the guiding optical system (normally the silica optical fibre) when the crystal works at high temperature above 1000 ^{0}C, it is almost impossible to carry out a systematic test on the performance of the fluorescence from room temperature to above 1200 ^{0}C. To solve this problem, a YAG crystal fibre with a Tm doped end tip was designed for a sensor application and grown by means of the laser heated pedestal growth (LHPG) method [13], then incorporated in a fluorescence lifetime based fibre thermometer. Its fluorescence decay characteristics, including the lifetime and intensity, were comprehensively investigated over the temperature range from room temperature to a very high temperature of 1200 ^{0}C. Experimental results obtained have shown that the fibre is an excellent candidate material for this type of fibre thermometer probe.

4.2.2 Growth, preparation and spectroscopy of the Tm doped YAG crystal fibre

As discussed above, YAG crystal fibre was chosen for use in the work. A Tm doped YAG end tip in the crystal fibre was designed and was grown by means of the LHPG method. The growth process was similar to that of a sapphire crystal fibre with a Cr^{3+} doped (ruby) end tip previously reported by some of the authors [13,14]. An undoped YAG crystal fibre (with a length of 300 mm and a diameter of 0.7 mm) was first grown from a source rod, which was cut from a

bulk YAG crystal. The fibre was then used as a seed for the growth of the Tm doped tip (5 mm in length) while a Tm doped YAG crystal fibre (rod), which was directly grown from a sintered powder rod also by LHPG, was then used as the source rod. The Tm doping concentration resulting in the tip region was about 10%. The aluminum-oxide (Al_2O_3) powder and the rare-earth powders (Y_2O_3 and Tm_2O_3) used for the sintered powder rods were all of high purity (>99.99%). In this way, the fibre grown showed little scattering loss at the junction region between the doped and undoped parts, and this was about 2 mm in length. The growth process is illustrated schematically in Figure 4.1.

The crystal fibre was finely polished on its end surface and directly coupled to a transmission silica fibre (core diameter 300 μm) by being fixed in a short stainless tube and placed in an alumina ceramic tube for protection. The probe design is illustrated schematically in Figure 4.2.

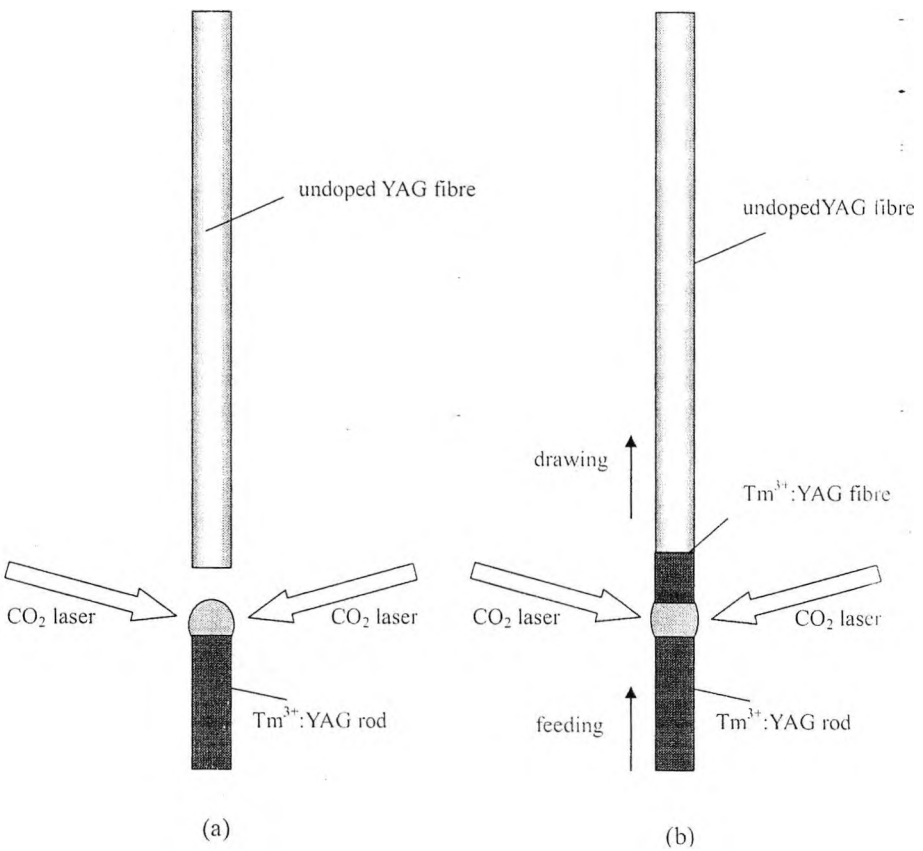

Figure 4.1 Schematic of the growth of the YAG crystal fibre with a Tm ion doped end tip

(a) the YAG fibre before connection (b) the YAG fibre after connection

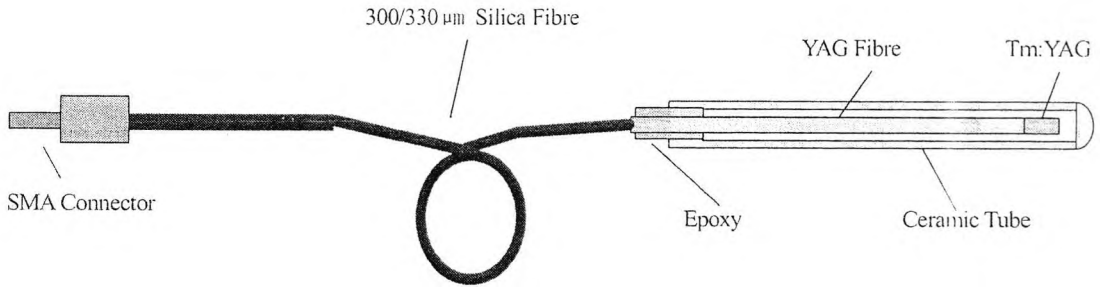

Figure 4.2 Schematic of the probe construction of the Tm doped YAG crystal fibre sensor

There is no reason to believe that the spectra and energy levels of Tm doped YAG crystal fibre should be other than the same as for the bulk material, which has been investigated in detail by Gruber et al in 1989 [15]. The fluorescence involved in this experiment comprises the $^3F_4$ to $^3H_6$ transition centreed at 1.88 μm and the $^3H_4$ to $^3F_4$ centreed at 1.47 μm (see Figure 4.3 for the corresponding energy levels).

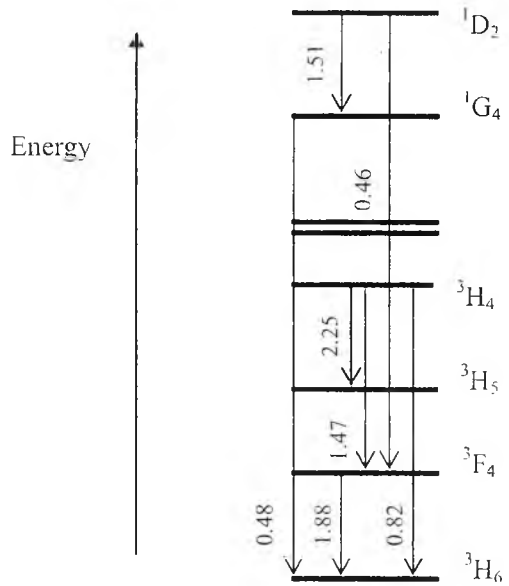

Figure 4.3 Electronic energy levels for Tm^{3+}:YAG crystal showing the important transitions for the probe developed (after Ref [15])

4.2.3 Fluorescence decay characteristics of the Tm doped YAG crystal

A. Experimental setup

An experimental system for the fluorescence lifetime monitoring and the intensity measurement was set up, as illustrated in Figure 4.4. A modulated laser diode (LD) centreed at 785 nm with a fibre pigtailed output power of 20 mW emitted the light to excite the Tm doped YAG crystal fibre probe via a Y-shaped fibre coupler and a piece of silica fibre (core diameter 300 μm)

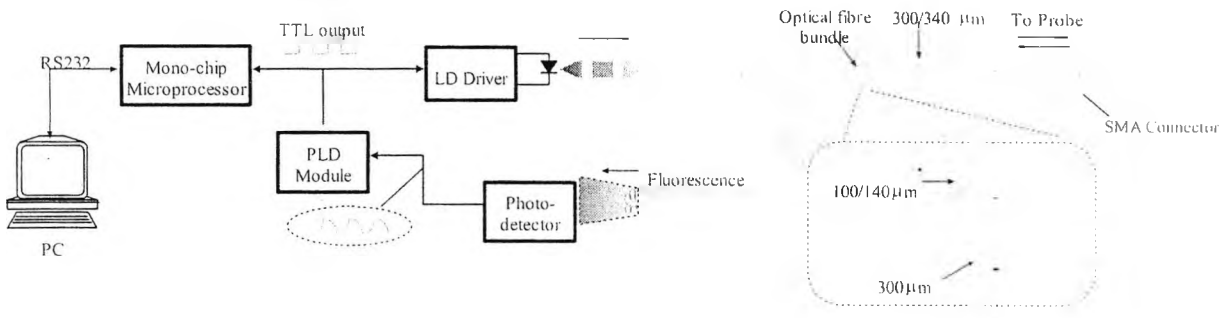

Figure 4.4 Schematic diagram of the sensor system

shown in Figure 4.2. The Y-shaped fibre coupler was composed of 7 multimode silica fibres with the centre fibre being used for the excitation laser light transmission and the others being used to receive the fluorescence signal. The crystal fibre and the silica fibre collected and transmitted the fluorescence signal, as well as the background radiation, passing it to the InGaAs photodiode through the Y-shaped coupler where the light signal was converted into an electrical signal and then amplified in a three-stage amplifier. To cover the wide fluorescence spectrum, an extended range InGaAs photodiode, which could respond to the radiation from 0.9 μm to 2.1 μm, was used in the experimental setup, shown in Figure 4.4. A spectral filter was placed in front of the photodiode to filter out the excitation laser light at 785 nm. An oscilloscope was employed to monitor the amplified signal, which was simultaneously sent to a phase-locked-detection (PLD) [7] circuit to generate a square-wave modulation signal. The modulation signal was then fed back to control the modulation of the LD. In this way, its modulation period, T, was made proportional to

the fluorescence lifetime, τ , of the sensing material, i.e. $T = 9.75\ \tau$, as detailed previously by Grattan and Zhang [8]. In this system, a 89C51 mono-chip microprocessor was used in the circuit to measure the modulation period and transfer the data to a computer via a RS232 serial port. The fluorescence intensity was directly recorded from the oscilloscope. Calibration was then carried out to analyze the characteristics of the fluorescence lifetime versus temperature and thus determine the performance of the sensor probe.

B. Background radiation compensation in the PLD

The principle of the PLD scheme has been presented previously by Zhang et al [7] and was improved in this work to compensate for the effect of the background radiation observed at these very high temperatures. Such compensation was necessary, as the amplifier would easily saturate at the high temperature due to the strong background signal from the blackbody radiation which was superimposed on the fluorescence signal. That means, if a large amplification coefficient was used to amplify the fluorescence signal to a value suitable for the processing of PLD, the background radiation would also be amplified by the same coefficient and that would exceed the maximum voltage value the amplifier could provide, which was closely below the power supply voltage of the amplifier. As a result, the amplifier would only give a flat signal output and lose the fluorescence decay signal if no compensation were made. The principle of the compensation circuit is illustrated schematically in Figure 4.5. Two sample/hold amplifiers were used to separate

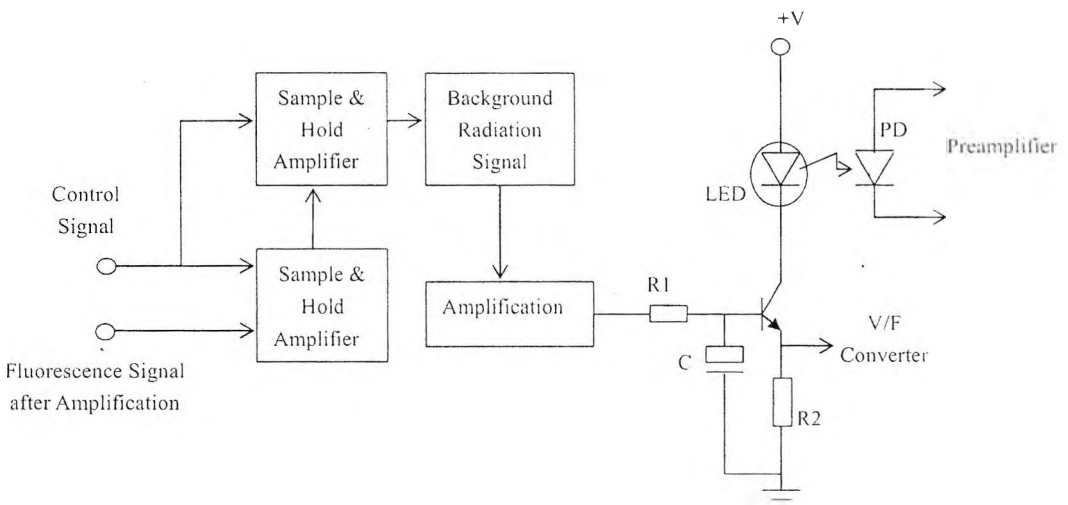

Figure 4.5 Circuit diagram for the background radiation compensation

the background signal from the fluorescence, which was then amplified to drive a LED. The light emitted from the LED was detected by a silicon photodiode and inversely amplified by the preamplifier (the same as was used for the amplification of the fluorescence signal). The stronger the background signal, the more intense the LED emission. As a result, due to the opposite sign of the compensating signal in the preamplifier, the background signal could be compensated very effectively so that it could always remain at an acceptable value (around 1 V), without deteriorating the signal to noise ratio (SNR) of the fluorescence signal which carried the measurement information.

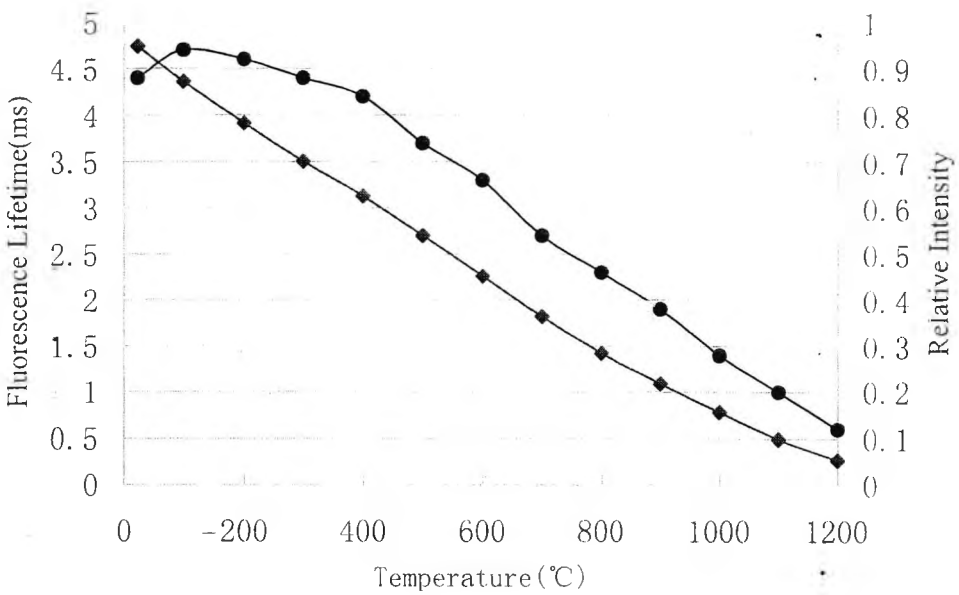

Figure 4.6 Fluorescence characteristics of Tm doped YAG crystal fibre probe with temperature, showing both the change of lifetime (♦) and fluorescence intensity (•) over the range from room temperature to 1200 ^{0}C

C. Performance characteristics of the Tm:YAG crystal fibre probe

The temperature dependence of the fluorescence lifetime and its corresponding intensity, over the range from room temperature to 1200 ^{0}C, was measured and is illustrated in Figure 4.6. It can be seen from Figure 4.6 that at 1200 ^{0}C, the Tm:YAG crystal fibre probe still had a strong fluorescence signal (about 15% of the initial intensity at room temperature) and a long fluorescence lifetime (greater than 0.2 ms), both of which could be accurately measured. The standard deviation of the lifetime measurement was determined to be within 2 μs. An important feature of the crystal fibre produced in this way, when compared to silica fibre for example, is that

the cycling of temperature from room temperature to 1200 ^{0}C seemed to show no effect on the fluorescence lifetime observed. This contrasts sharply with work reported previously on the use of doped silica fibre at these high temperatures [16] where these so-called "annealing effects" were seen much more severely. The stability and repeatability were all very satisfactory within this temperature range and there was no hysteresis observed in the output characteristic of the fibre.

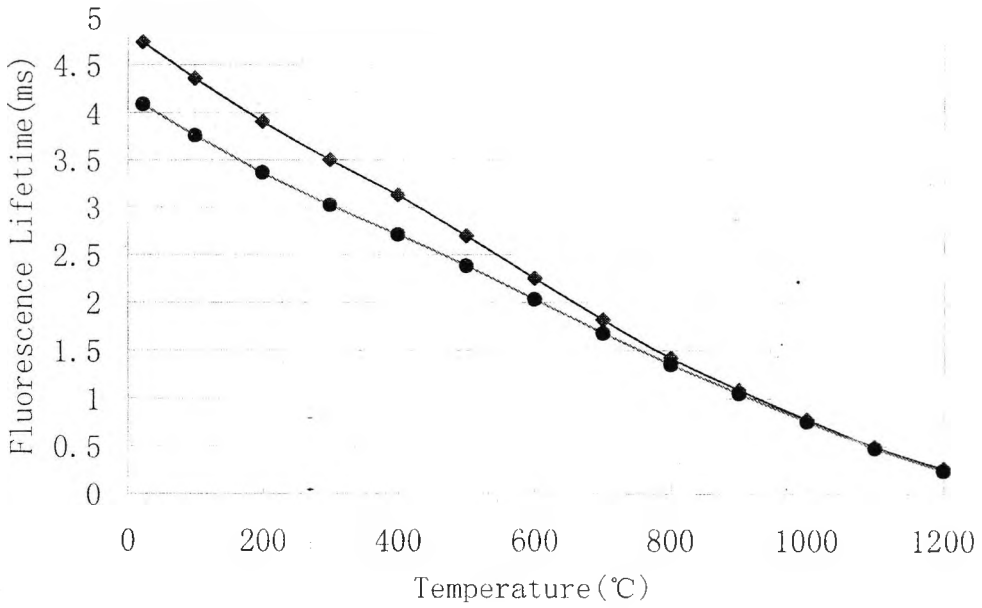

Figure 4.7 Dependence of fluorescence lifetime on temperature after the probe being annealed at 1400 ^{0}C for 24 hours ♦ before annealing •after annealing

In order to create a probe offering a stable performance, the crystal fibre was annealed before use. There has been some discussion as to the physical nature of the annealing process, especially in silica [17] and it is believed that similar processes may occur in the crystal but perhaps to a lesser extent than in the viscous heated silica glass. The major difference (and indeed the *raison d'être* for the use of the crystal material) is its ability to sustain the high temperature and the higher melting/softening point of the material compared to that of silica. In this work the annealing is limited by the upper temperature of the oven used (~1400 ^{0}C) – it may be interesting to anneal at higher temperatures but the scope for this is also limited by the melting point of the YAG crystal.

The crystal fibre probe was thus annealed at a very high temperature, of 1400 ^{0}C for 24 hours, to test the sustainability of the performance at such a high temperature. The fluorescence

lifetime and the associated signal intensity were measured again after this annealing process had been carried out. Some differences were found, as illustrated in Figure 4.7. However, further annealing at 1400 ^{0}C did not result in any further change in the temperature dependence of the fluorescence lifetime and it was concluded that the performance had stabilized at this very high temperature. This work suggested that probes of this type should be annealed to temperatures in this region (the upper limit being set here by the maximum oven temperature available) before use in a sensor probe over the derived measurement range discussed in this paper. After the annealing process discussed, the probe performance was seen to be much improved – the drift (such as occurred) was within the measurement precision of the system as a whole. With the equipment used, it is not possible to be more indicative than that.

The average sensitivity of the lifetime was 3 μs/^{0}C within the temperature range from room temperature to 1200 ^{0}C. Thus, a minimum temperature resolution of ±0.3 ^{0}C is associated purely with the measurement system, given the time resolution of the detection scheme of 1μs. The data above suggested that the Tm doped YAG crystal fibre material could be an excellent candidate as the fluorescence material to be used in the fibre thermometer to cover a wide temperature range from room temperature to 1200 ^{0}C, offering superior performance to that of silica fibre.

4.3 Fibre thermometer using Tm^{3+} doped YAG as the fluorescence sensing material

A fibre thermometer based on the fluorescence lifetime detection of the Tm doped YAG crystal has been developed. The systematic construction of the thermometer, including the laser used for excitation, the photo-detector, the Y-shaped fibre bundle construction of the light signal transmission system, and the PLD signal processing scheme, is similar to that used in the characterization evaluation of the Tm:YAG crystal fibre probe, as presented in Section 4.2. The performance of the thermometer system was comprehensively investigated from room temperature to temperatures in excess of 800 ^{0}C.

4.3.1 Probe construction

It was important in this work to construct a stable and reliable probe, as it was planned for use for high temperature measurements in furnace refractory linings. Within the probe, a piece of Tm doped YAG crystal (with a Tm concentration of 10%) was the essential sensing material. A

silica fibre was used to transmit the excitation laser emission to the crystal and, also the fluorescence signal back to the photodiode by means of a Y-shaped fibre bundle.

It is important to ensure that there is a good optical contact between the crystal and the silica fibre for a stable fluorescence signal to be detected. As the probe would be used in situations where the temperature would rise to as high as 800 ^{0}C, any method which involved using a glue to fix the optical components seemed unsuitable. It was partly due to the unavailability of suitable epoxy glue that could sustain such high temperatures, and concerns that any such glue may affect the fluorescence signal detected. Further, any reaction of the crystal with the glue material may deteriorate its fluorescence performance and could also degrade its mechanical strength.

A mechanical fixing method was finally adopted as the best solution. To avoid the adverse effect of different expansion coefficients of the material used and to make the probe compact, a metal holder was not used. Instead, a silica tube, with an inner diameter of 530 μm, an outer diameter of 700 μm and a length of 450-500 mm, was used to hold the crystal and the silica fibre together. The crystal was ground into a thin rod with a diameter of less than 500 μm and a length of around 1 mm and was inserted into the tube. The end part of the tube was then fused with the help of a micro-torch. To fabricate the probe, the silica fibre was then placed in the tube and aligned until the fluorescence signal in the thermometer was optimized. Following that, the silica fibre was fixed to the tube by fusing it at several positions along its length, also using the micro-torch. In this way, the silica tube holding the crystal and the silica fibre were formed into a stable probe.

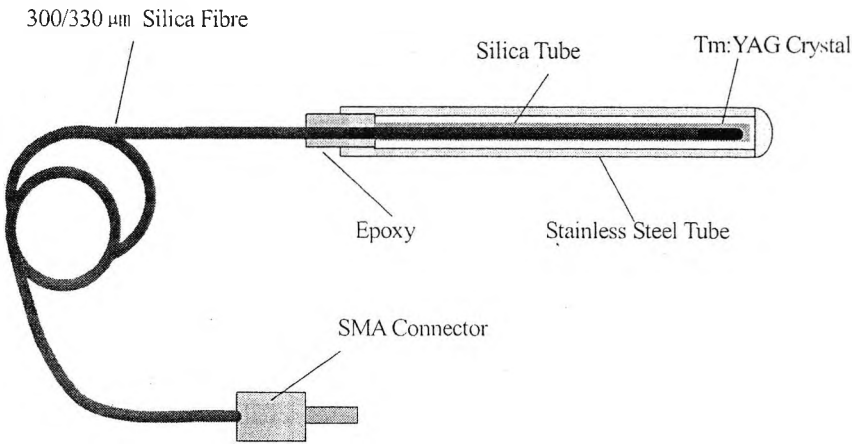

Figure 4.8 Schematic of the probe construction of the fibre thermometer with a Tm doped YAG crystal

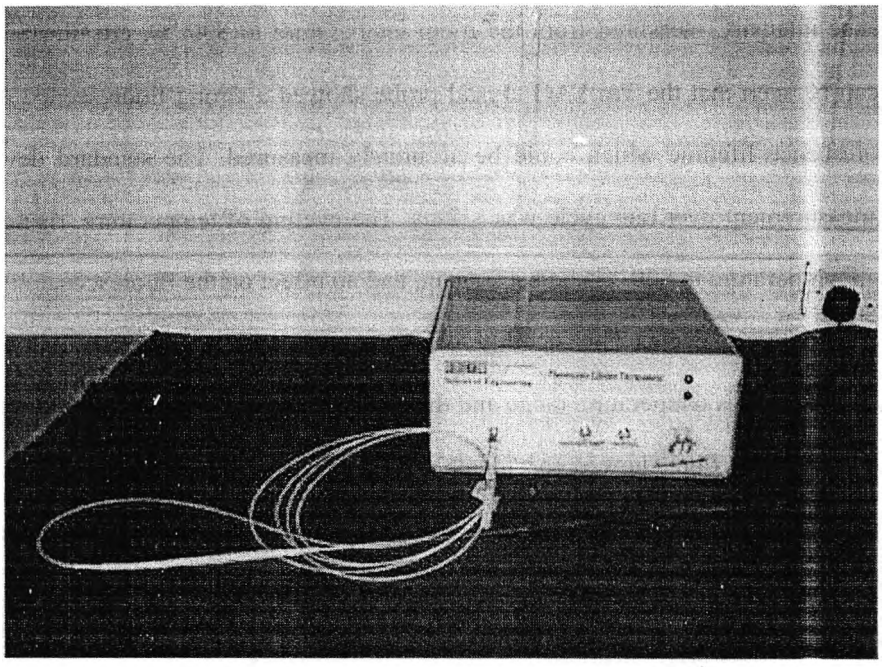

Figure 4.9 Photo of the fibre thermometer using Tm:YAG as the sensing material, showing the compact nature of the sensor system

For further protection of the probe, the silica tube was inserted into a stainless steel tube with an inner diameter of 1.5 mm. Some alumina refractory fibres were used to fill the space between the stainless tube and the silica tube to reduce the effects of any mechanical oscillation and thus minimize the potential for fibre damage. The construction of the probe is illustrated schematically in Figure 4.8. A photo of the fibre thermometer system developed is shown in Figure 4.9, demonstrating the compact nature of the device overall.

4.3.2 Results and analysis

A calibration of the probe was carried out to determine its fluorescence characteristics versus temperature, i.e. to calibrate it over the range from room temperature to 800 ^{0}C. During the calibration process, the fibre thermometer probe was placed in the centre of a Carbolite tube oven, with a K-type thermocouple attached to the probe to provide a temperature reference. The temperature of the oven was increased in increments of 50 ^{0}C. Data were recorded after the oven temperature had been fully stabilized. The fluorescence lifetimes were calculated from the data obtained over a wide range of temperatures and, for reference, the fluorescence intensities were directly determined from the oscilloscope.

The temperature dependence of the fluorescence lifetime and the corresponding

fluorescence intensity, measured from the room temperature to 800 ^{0}C, are illustrated in Figure 4.10. It can be seen that the Tm:YAG crystal probe showed a strong fluorescence signal, with a long fluorescence lifetime which could be accurately measured. The standard deviation of the lifetime measurement over one cycle was ≤ 2 μs. The cycling of temperature, rising and cooling from room temperature to 800 ^{0}C and back again, had no effect on the fluorescence lifetime during the next temperature cycle. The stability of the system and its repeatability were all very satisfactory within this temperature range and there was no hysteresis observed. Previous work [16] with Tm-doped silica fibre showed considerable annealing effects at these temperatures, resulting in a less stable performance than was achieved in this work with the Tm doped crystal as the sensing material.

Due to the limitations of the silica fibre used to carry the light to and from the Tm:YAG crystal, the probe was designed for use at temperatures below 800 ^{0}C. Tests carried out at higher temperatures (for example, 900 ^{0}C) always resulted in the fluorescence signal being attenuated with time, an indication that the transmission of the silica fibre deteriorated with exposure to such high temperatures, due likely to fibre crystallization. Moreover, the temperature dependence of the fluorescence lifetime indicated that there were some permanent changes after the probe was exposed to temperatures in that region, due to the annealing effect that was occurring.

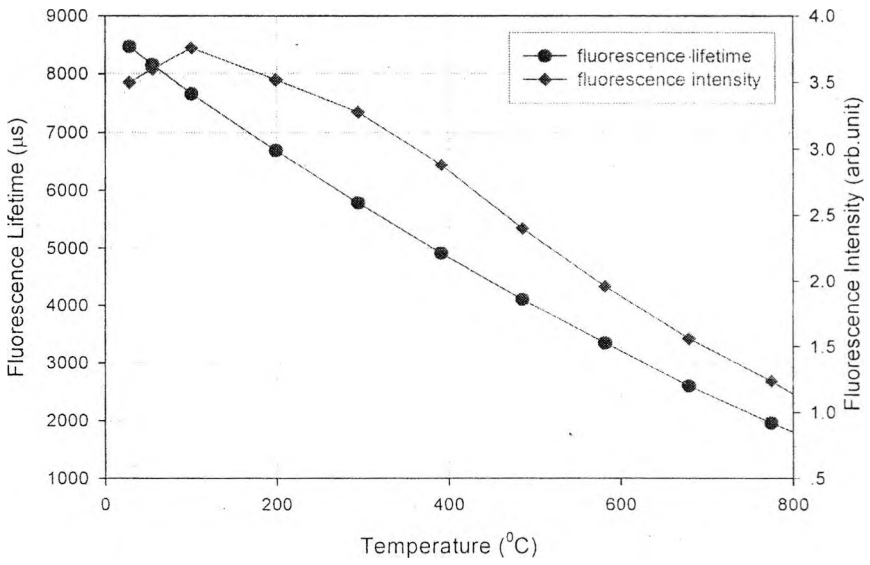

Figure 4.10 Fluorescence decay characteristics of Tm doped YAG crystal probe with temperature, showing the change of both the lifetime (•) and fluorescence intensity (♦) over the temperature range from room temperature to 800 ^{0}C

From Figure 4.10, it could be deduced that the average sensitivity of the lifetime was greater than 7 μs/^{0}C within the temperature range from room temperature to 800 ^{0}C, which is quite satisfactory compared with 3 μs/^{0}C for a crystal fibre constructed from Tm:YAG as presented in Section 4.2. This higher sensitivity, compared with that of the Tm:YAG crystal fibre, was possibly due to the better crystal quality of the crystal used. (As for the Tm:YAG crystal fibre, grown by means of the laser heated pedestal growth (LHPG) method [13], a sintered powder mixture rod was used as the source rod and the growing speed was faster (1~3 mm/minute), and this could result in a comparatively poor crystal quality with large inner stress and some coalescence of the fluorescent ions, which results in a shorter fluorescence lifetime at room temperature). As mentioned above, the lifetime measurement alone gave a ~ 2μs time resolution by using the mono-chip microprocessor. The results showed that, from the PLD, the period stability was within 20 μs, which corresponded to a lifetime resolution of ≤ 2μs. Thus, a corresponding optimum temperature resolution of ±0.3 ^{0}C could be inferred.

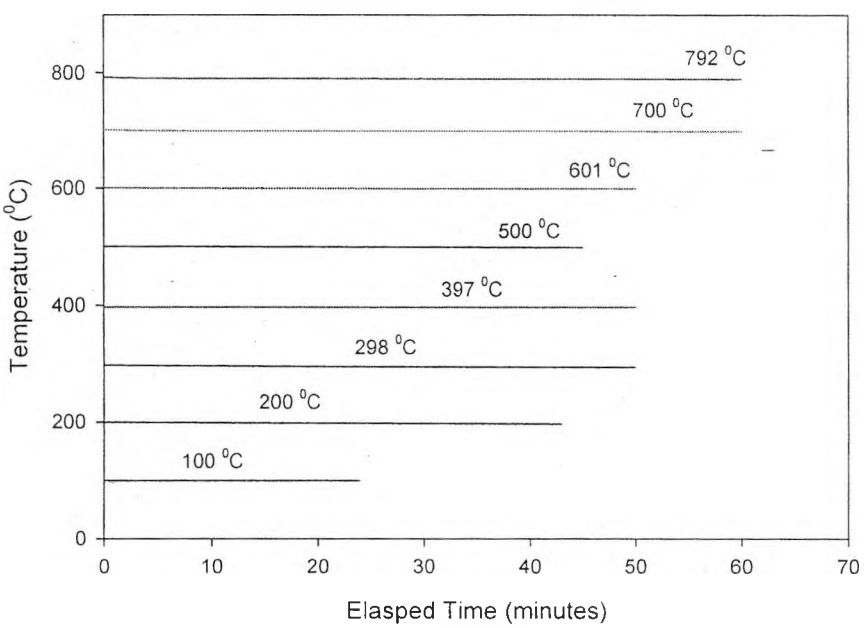

Figure 4.11 Thermometer performance with time at several discrete temperatures, from 100 ^{0}C to 792 ^{0}C, showing stability over the range studied

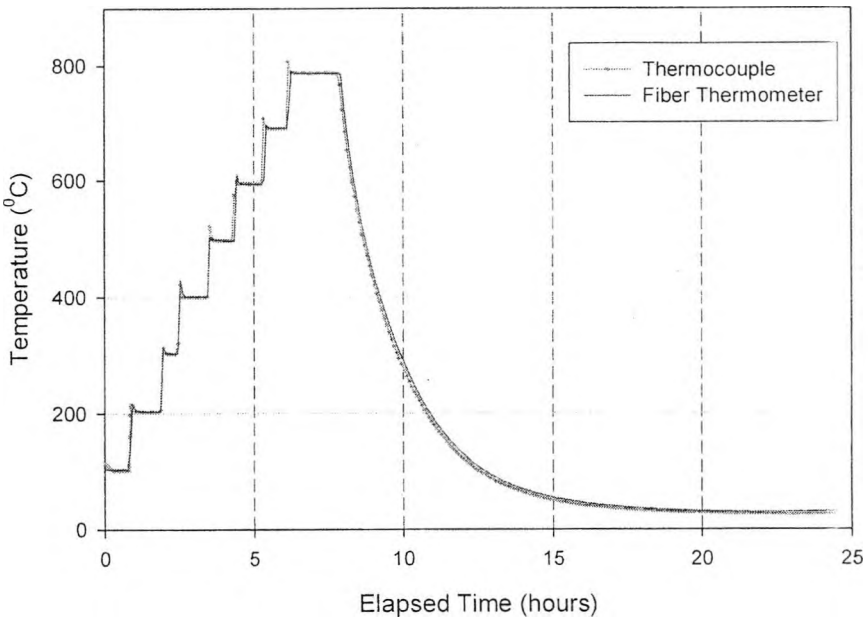

Figure 4.12 Temperature cycling experiments from room temperature to ~ 800 ^{0}C over a 24 hour cycle. Probe (using K-type thermocouple for comparison) was heated in steps, stabilized and then slowly cooled

The performance of the fibre thermometer at several discrete temperatures was tested and the results are presented in Figure 4.11. It could be seen that the deviations at these fixed temperatures were very small, over the test period. By using the data obtained during the measurement at these temperatures, standard deviations of less than 1 ^{0}C were realized over all the temperature range from room temperature to 800 ^{0}C. Cycling of the temperature was also carried out to show the dynamic performance of the fibre thermometer by comparing it with a K-type thermocouple and agreement was good. In Figure 4.12, a complete temperature rising and cooling cycle is presented, again by comparison to the response of a K-type thermocouple. It can be seen that very good agreement over the whole range studied was achieved in this test.

4.4 Cross-comparison of the fluorescence characteristics of Tm doped YAG crystal and the crystal fibre

The fluorescence decay data measured in the experiment indicated that the lifetime of Tm doped YAG crystal fibre at room temperature was near 4 ms. It was much shorter than that of the bulk crystal (it is normally from 6 ms to 10 ms, depending on the Tm dopant concentration). The

difference may result from a higher doping concentration of the Tm ion due to the inhomogeneity resulting from pressing the sintered powder rod. However, it was most likely due to the imperfect crystal lattice formed during the fibre growth process, in which a large temperature gradient existed and a fast growth speed was involved. Some degree of clustering of the doped ion within the crystal fibre may explain the relatively short lifetime. Similar phenomena could also be found with the bulk Tm^{3+}:YAG crystal when it experienced an annealing process at temperatures > 900 ^{0}C, though the change in fluorescence lifetime was not so great. For a fuller understanding of the phenomena involved, further experimental effort needs to be made by examining the deviation of the exponential decays through analyzing the fluorescence decay waveform from the sample.

Experimental results obtained in this work have shown that the fluorescence lifetime of the fibre decreased smoothly and monotonically from near 4 ms at room temperature to 0.26 ms at 1200 ^{0}C. The average sensitivity of the lifetime was 3 μs/^{0}C. With the thermometer system set up in this experiment, an average lifetime resolution (corresponding to one standard deviation, σ) of 2 μs was achieved, which corresponded an average temperature resolution that could be as low as ±0.7 ^{0}C. For a thermometer probe to have such a good potential temperature resolution over the wide temperature range would be very useful. However, it should be noted that to achieve such a high level of accuracy, a specific voltage-period conversion circuit in the PLD should be designed to cover the wide range of fluorescence lifetimes experienced. An analogue switch connected to a RC circuit would be useful in extending the lifetime measurement range and improving the resolution. Several cycles of temperature, both rising and cooling, were also carried out to check the long-term stability of the sensor system. Results from the monitoring of the relationship between the lifetime and temperature indicated that the repeatability was satisfactory and the drift was within the range of the equipment (including the oven and the thermocouple) accuracy. Thus, it was concluded that the sensor could reach a high temperature resolution of less than ±2.5 ^{0}C (3σ) and achieve an accuracy of better than ±5 ^{0}C.

In addition to the crystal fibre probe, an effective Tm:YAG crystal based, fibre coupled probe was also constructed. The fluorescence lifetime measured in the laboratory for the Tm doped YAG crystal showed a change from 8 ms at room temperature, decreasing smoothly and monotonically to 1.8 ms at 800 ^{0}C. The average sensitivity of the lifetime was > 7 μs/^{0}C. The results obtained confirmed the importance of this optoelectronic approach, thus to create an

effective, stable temperature monitoring system over this temperature range. This sensitivity was comparable with that of the scheme using the fluorescence lifetime detection of ruby (about 8 μs/^{0}C) as reported in several papers [11][14][18] over a temperature range from room temperature to 400 ^{0}C. However, the temperature range covered in this work was larger, as discussed.

As the temperature dependence of fluorescence lifetime was related to the dopant concentration, each probe used should be separately calibrated to ensure an accurate reference. This is especially true for a crystal with a Tm concentration as high as the 10% used in this work, as the fluorescence lifetime is relatively sensitive to the concentration. Even with different thin crystal rods cut from the same bulk crystal, there was still a small difference observed in tests carried out for the evaluation of their fluorescence characterization. However, the advantage of using a very high dopant crystal is clear — a greater sensitivity of the lifetime to the temperature change and a higher fluorescence signal-to-noise ratio due to the high concentration of the emissive species. In previous work with silica fibre, a similar effect with concentration was seen [16]. This concentration is greater than is typically achieved from rare-earth doped-silica fibres, and made it well suited to the application here. In comparison to ruby [11], for example, the work shows that in typical samples the fluorescence intensity falls off at temperatures approaching 600 ^{0}C, and this sets an effective limit on the probe performance with this material.

In this work, the absorbed power in the crystal was limited by the geometry of the system but at higher pumping power issues such as up-conversion may occur at a significant rate [19]. This may be having an effect, even at the power level used, at temperatures > 800 ^{0}C on the transmittance of the fibre. Equally, at high levels of pump power, radiation-self-heating may become appreciable, but this is not seen as significant under the experimental conditions discussed.

The fibre thermometer probe developed in this work has the potential for an average temperature resolution of < 1 ^{0}C over the temperature range from room temperature to 800 ^{0}C. The standard deviation of fluorescence lifetime measured was 2 μs over one measurement cycle, corresponding to a standard temperature deviation of ±0.3 ^{0}C in the results obtained.

4.5 Cross-referencing of the fibre thermometer using the fluorescence lifetime

decay and the thermal background radiation

4.5.1 Introduction

Fibre optic temperature sensors based on the fluorescence characteristics of the materials have been extensively investigated over the past ten years, mainly due to their independence of signal intensity and thus the ease of system construction with stable performance. Intrinsically, the technique is more suitable for relatively low temperature applications as the fluorescence generally deteriorates at high temperatures due to the poor quantum efficiency. Compared with this, the fibre thermometer based on the Plank blackbody radiation approach would be more advantageous for high temperature measurement (above 500 ^{0}C). In general, the combination of these two techniques should enable a fibre thermometer to cover a much wider temperature range from the cryogenic to high temperatures. Such an effort was made by the author and his colleagues in 1999 by using a sapphire-ruby crystal fibre as a thermometer probe and a sandwiched InGaAs-Si photodiode as the photodetector to detect the background radiation and the fluorescence signal [4]. The experimental results obtained have shown good fluorescence stability when the probe experienced high temperatures up to 1400 ^{0}C [11]. However, a drift in the fluorescence lifetime occurred when the probe was exposed to and maintained at a temperature above 1500 ^{0}C for an extended period and the long-term performance of the thermometer was affected. Besides, as the fluorescence lifetime detection scheme only worked below 450 ^{0}C, the cross-referencing temperature region was limited to about only 70 degrees (from 380 ^{0}C to 450 ^{0}C).

In this thesis, the approach using the fluorescence detection scheme, as presented in Section 4.2, was combined with a blackbody radiation detection scheme. It was attempted to create a sensor system that could cover a wider temperature range from room temperature to over 1400 ^{0}C. As can be sees, with Tm:YAG crystal fibre as the sensing probe, a wide cross referencing temperature (from 600 ^{0}C to about 1200 ^{0}C) is potentially available. This will enable the system to be self-calibrating using the radiation detection scheme and thus maintain the long-term stability of the system.

4.5.2 System configuration using cross-referencing detection

A. Fluorescence characteristics of the Tm:YAG crystal fibre probe

As presented in Section 4.2, a Yttrium Aluminum Garnet (YAG) crystal fibre with a Tm^{3+}

doped YAG tip was grown by means of the laser heated pedestal growth (LHPG) technique and used as the fibre thermometer probe. A signal processing scheme using phase-locked-detection (PLD) [7] was employed to detect the fluorescence lifetime. A background compensation circuit was designed to measure the fluorescence signal at high temperatures as it could avoid the saturation of the amplifier arising from the strong background radiation that accompanied the fluorescence signal. The compensation current, which was directly related to the background radiation, was also used for the temperature measurement from 600 ^{0}C to 1400 ^{0}C. The cross-referencing of these two sensing schemes was made within the temperature range from 600 ^{0}C to 1200 ^{0}C. Experimental results have shown that such a scheme was effective to cover a wide temperature range, with a good long-term stability.

The temperature dependence of fluorescence lifetime and the intensity of the Tm:YAG crystal fibre probe, from room temperature to 1200 ^{0}C, are illustrated in Figure 4.6. It can be seen in Figure 4.6 that at 1200 ^{0}C, the Tm:YAG crystal fibre probe still had a strong fluorescence signal (about 15% of that at room temperature) and a long fluorescence lifetime (greater than 0.2 ms) and could be measured accurately. The stability and repeatability were all very good, within this temperature range and no hysteresis was observed. The average sensitivity of the lifetime within this temperature range was 3 μs/^{0}C. Thus an average temperature resolution of 0.3 ^{0}C could be expected for the system when the time resolution of detecting scheme was 1 μs. The above data suggested that the Tm doped YAG crystal fibre material could be an excellent fluorescence material to be used in the fibre thermometer, to cover a wide temperature range.

The fibre probe was also annealed at 1400 ^{0}C for 24 hours, as a result of which the fluorescence lifetime and intensity can be seen to be different from the values before annealing, as shown in Figure 4.7. However, further cycling of heating up to 1400 ^{0}C and subsequent cooling has shown no further annealing effect. The temperature dependence of the lifetime with temperature after annealing was quite stable.

It was noted that under 1200 ^{0}C, the Tm doped crystal fibre did not show any annealing effects in terms of the lifetime change. When it was heated to near 1300 ^{0}C, the relationship between the lifetime and the temperature showed a non-monotonic change. That is, when the temperature exceeded 1280 ^{0}C, the lifetime did not decrease monotonically and the fluorescence intensity became continuously weaker. This might be attributed to the annealing effect of the

probe, but the source of the mechanism yielding this phenomenon is still unknown.

B. Background radiation detection

In the system, the fibre probe was placed in an alumina ceramic tube with an inner-diameter of 2 mm. No specific fibre blackbody cavity [4] was fabricated around the tip of the crystal fibre and thus the probe only collected the radiation emitted from the inner surface of the alumina tube that was stable, under certain temperatures. This signal was also transmitted to the photodetector via a silica fibre in the same way to the transmitted fluorescence signal and added to it. Thus the signal after amplification would include the fluorescence and background radiation. A simple circuit was designed and used to separate them. As illustrated in Figure 4.5, two sample/hold integrated-circuit (IC) chips were used to separate the background signal from the fluorescence, which was then amplified to drive a LED. The light emitted from the LED was detected by a silicon photodiode and inversely amplified by the preamplifier. Thus, the background signal could be compensated in the preamplifier without causing a deterioration of the signal to noise ratio (SNR) of the fluorescence signal. The LED driving current was used to measure the background radiation intensity and then the temperature. To do so, an integrated voltage/frequency converter was used to convert the voltage signal to a periodic signal whose period was measured by the mono-chip processor and the data obtained were sent to the computer. The relationship of output period (frequency) with temperature was used for the calibration. As illustrated in Figure 4.13, the effective temperature range of the sensor was from 600 ^{0}C to 1400 ^{0}C.

C. Cross-referencing of fluorescence lifetime and background radiation

As discussed above, both the fluorescence lifetime and background radiation signal could be used to measure the temperature. The fluorescence lifetime was intensity independent, and the sensing probe had long-term stability even when the fibre connectors of the probes were realigned. However, the background radiation signal might change under these circumstances. Thus, the fluorescence lifetime-based temperature measurement could be used to recalibrate the system based on the background radiation detection. Whenever the connectors were realigned, the process of recalibration should be performed as long as the temperature was within the range within which both the fluorescence lifetime and background radiation schemes worked.

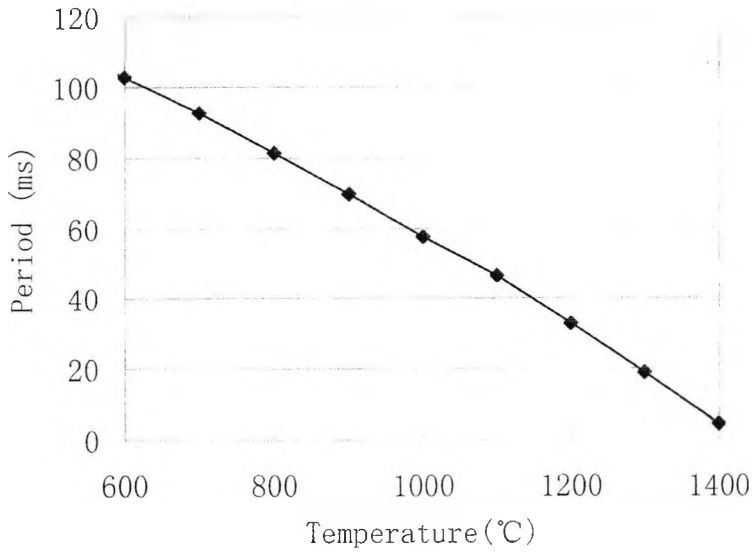

Figure 4.13 Temperature dependence of the oscillation period corresponding to the background radiation

The experimental data from both the temperature measurement schemes have shown that 600 ^{0}C to 1200 ^{0}C was the region over which both the schemes could work. The scheme based on background radiation could then be recalibrated through the fluorescence lifetime detection scheme at any time when the temperature was within this range. If there is any difference between them, a proportional factor could be calculated, stored, and used to adjust the corresponding voltage and then the period value (the relationship between the voltage and period was known for the voltage/period conversion circuit).

Based on the data shown in Figures 4.7 and 4.13, a complete calibration was carried out to cover a wide temperature range from room temperature to 1400 ^{0}C and the results are shown in Figure 4.14. Experimental results showed that a good resolution of better than 1 ^{0}C over the whole region could be obtained.

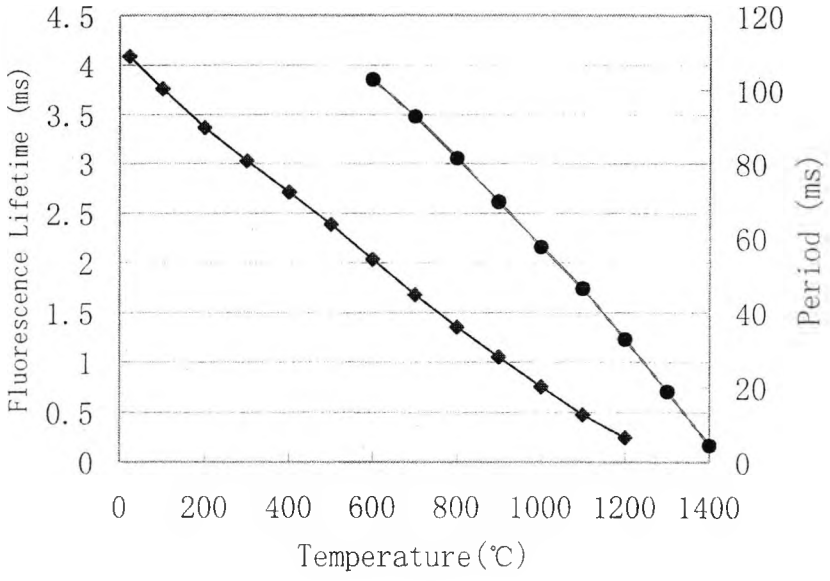

Figure 4.14 Calibration curves for the cross referencing scheme

◆ fluorescence lifetime •signal period corresponding to background radiation

4.6 Summary

A fibre thermometer based on the fluorescence characteristics of Tm:YAG crystal has been developed. An undoped YAG crystal fibre with a Tm:YAG tip was grown by means of the LHPG method and used as the sensing probe to cover a wide temperature range from room temperature to 1200 ^{0}C. Detailed fluorescence characteristics, such as the fluorescence lifetime and the intensity of the signal received at the probe were investigated systematically. Silica tube-supported compact Tm:YAG crystal probes were also fabricated and demonstrated to have a stable performance over the temperature range from room temperature to 800 ^{0}C. An attempt at cross-referencing between blackbody radiation detection and the fluorescence lifetime measurement was also made.

The work presented in this chapter reports some improved performances of the fibre thermometer based on the fluorescence characteristics, which cover a wider temperature range than those using Cr^{3+} doped crystal as the sensing element. However, for both systems, the temperature sensitivity and the system resolution achieved are similar.

4.7 References

[1] Z.Y. Zhang, K.T.V. Grattan, A.W. Palmer, and B.T. Meggitt. Spectral characteristics and effects of heat treatment on intrinsic Nd-doped fibre thermometer probes. Review of Scientific Instruments 69, pp139-145 (1998)

[2] K.T.V. Grattan, J.D. Manwell, S.M.L. Sim et al, "Lifetime investigation of fluorescence from neodymium-yttrium-aluminum garnet at elevated temperature". Optics Communications, 62, pp104-107 (1987)

[3] Z. Zhang, J.H. Herringer and N. Djeu, "Monolithic crystalline fibre optic temperature sensor", Review of Scientific Instrument, 68, pp2068-2070 (1997)

[4] Y. Shen, L. Tong, Y. Wang, L. Ye, "Sapphire fibre thermometer ranging from 20 to 1800 ℃", Applied Optics, 38, pp1139-1143 (1999)

[5] S.A. Wade, S.F. Collins, K.T.V. Grattan and G.W. Baxter, "Strain-independent temperature measurement by use of a fluorescence intensity ratio technique in optical fibre", Applied Optics, 39, pp3050- 3052 (2000)

[6] S.A. Wade, S.F. Collins, and G.W. Baxter, "Fluorescence intensity ratio technique for optical fibre point temperature sensing", Journal of Applied Physics, 94, pp4743-4756 (2003)

[7] Z.Y. Zhang, K.T.V. Grattan, and A.W. Palmer, "Phase-locked detection of fluorescence lifetime and its thermometric applications", SPIE Proceedings, 1885, pp228-239 (1993)

[8] K.T.V. Grattan, Z. Y. Zhang, Fibre Optic Fluorescence Thermometry, Chapman & Hall (1995)

[9] Z.Y. Zhang, K.T.V. Grattan, A.W. Palmer, "Thermal characteristics of alexandrite fluorescence decay at high temperatures, induced by a visible laser diode emission", Journal of Applied Physics, 73, pp3493-3498 (1993)

[10] S.W. Allison and G.T. Gillies "Remote thermometry with thermographic phosphors: Instrumentation and applications", Rev. Sci. Instrum. 68, pp2615-2650 (1997)

[11] K.T.V. Grattan, Z.Y. Zhang, T. Sun, Y. Shen, L.Tong and Z. Ding, "Sapphire-ruby single-crystal fibre for application in high temperature optical fibre thermometers: studies at temperatures up to 1500 degrees" Measurement Science & Technology, 12, pp981-986 (2001)

[12] Z.Y. Zhang, T. Sun, K.T.V. Grattan and A.W. Palmer, "Optical fibre temperature sensor scheme using Tm: doped yttrium oxide powder-based probe", SPIE Proceedings 3746, pp422-425 (1999)

[13] Y. Shen, R. Xu, "Development of a compact sapphire fibre thermometer probe using fluorescent decay", SPIE Proceedings 2895, pp144-150 (1996)

[14] Y. Shen, Y. Wang, L. Tong and L. Ye "Novel sapphire fibre thermometer using fluorescent decay", Sensors & Actuators A71, pp70-73 (1998)

[15] J. B. Gruber, M.E. Hills, R.M. Macfarlane, "Spectra and energy levels of Tm^{3+}:$Y_3Al_5O_{12}$", Physical Review B, 40, pp9464-9478 (1989)

[16] Z.Y. Zhang, K.T.V. Grattan, A.W. Palmer and B.T. Meggitt, "Thulium-doped intrinsic fibre optic sensor for high temperature measurements (>1100 ^{0}C)", Rev. Sci. Instrum., 69, pp3210-3214 (1998)

[17] Z. Zhang, K.T.V. Grattan, A.W. Palmer, "A novel signal processing scheme for a fluorescence based fibre-optic temperature sensor", Rev. Sci. Instrum., 62, pp1735-1742 (1991)

[18] H.C. Seat, J.H. Sharp, Z.Y. Zhang et al, "Single-crystal ruby fibre temperature sensor", Sens. Actuators A: Phys. 101, pp24–29 (2002)

[19] L.B. Shaw, R.S.F. Chang, N. Djeu, "Measurement of up-conversion energy-transfer probabilities in Ho:$Y_3Al_5O_{12}$ and Tm:$Y_3Al_5O_{12}$", Phys. Rev. B, 50, pp6609–6619 (1994)

Chapter 5: Development of Specialist Photosensitive Fibres for High Temperature Sensing

5.1 Commercial photosensitive fibres

5.1.1 Introduction

The rapid development in the field of fibre Bragg gratings (FBG) has permitted the initiation of many novel devices and systems. These gratings are now widely used in fibre-optic communications and in the fibre-optic sensing field. Since 1990s, there has been a major development of FBG devices, such as the grating-based Dense Wavelength Division Multiplexing (DWDM) networks, and the grating-based fibre lasers, for example.

As has been introduced in Chapter 3, the gratings written into silica fibres are normally fabricated by exposing the silica fibre to an interference pattern created by using UV laser emission, such as from a KrF excimer laser working at 248 nm or a frequency doubled argon ion laser working at 244 nm. The fibres exposed to such an UV emission normally experience a photo-induced refractive index changes. With some fibres, this refractive index change is negligible, while with some other specific fibres, such a change is obviously observable and may result in several important phenomena, such as a strong peak wavelength reflection. The fibres with a large refractive index change when exposed to UV laser emission are normally termed photosensitive fibres.

Research work on the photosensitive fibres has revealed that heavily germanium doped silica fibres are generally highly photosensitive, and the common telecommunications oriented silica fibres, which are doped with lower Ge concentration (normally less than 4 mol%), are generally not photosensitive.

5.1.2 H_2 loading of the standard silica fibre for enhanced photosensitivity

Since the discovery of the photosensitive phenomenon in silica fibre in 1978 [1] and especially the invention of the side-writing FBG fabrication technique in 1989 [2], research work on photosensitive fibres has progressed rapidly. Many methods of creating photosensitivity in silica fibres have been presented (see references [3] and [4]) over the past ten years. Among these, the so-called hydrogen loading approach [5] and the photosensitive element doping technique are the most important.

As has been mentioned above, normal silica fibre developed for telecommunication purposes is almost non-photosensitive due to its low germanium doping concentration. By using a special processing, so-called H_2 loading, before being exposed to UV laser emission, the fibre can be made very photosensitive. In this approach, the fibres are normally treated in hydrogen gas at temperatures ranging from 20 – 75 ^{0}C and pressures from ~ 20 atm to more than 750 atm (typically 150 atm), which results in the diffusion of hydrogen molecules into the fibre core. In excess of 95% equilibrium solubility at the fibre core can be achieved with room temperature treatment. A permanent refractive index change of 0.01 is made possible, depending on the nature of the H_2 loading and the intensity of the laser emission.

The effectiveness of H_2 loading to create photosensitivity in fibres has been confirmed with many kinds of low germanium doped standard silica fibres. As a result, this approach of H_2 loading is indeed a very important and effective technique for creating photosensitivity in normal low-germanium silica fibre and has been widely used in practical applications.

The approach of H_2 loading needs special apparatus to allow H_2 to diffuse into the core of the silica fibre. The H_2 pressure used within the cavity for 'soaking' the fibre normally exceeds 100 atm. The fibres thus processed should be used immediately for FBG fabrication when they are taken out from the H_2 loading apparatus, or the H_2 may diffuse out and this may affect the photosensitivity of the fibre processed. To deter the diffusing out of H_2, storage of the H_2 loaded fibres at low temperature is necessary.

Clearly, the factors outlined above make the H_2 loading approach not readily acceptable in many laboratories for FBG fabrication and sensor performance investigation. The process of H_2 loading needs a special apparatus and the high pressure involved requires important safety considerations. The time schedule requirement and the limitation on the processed fibre for the use in FBG fabrication also are inconvenient to the average user. Moreover, as will be detailed in this thesis later, the stability of FBGs written into the H_2 loaded fibres is not good enough and is generally not suitable for sensing applications at high temperatures.

5.1.3 Commercial photosensitive fibres

In addition to H_2 loading, the addition of various co-dopants in germanosilicate fibres has resulted in a photosensitivity enhancement. It is clear that high germanium doped silica fibres are

quite photosensitive. In particular, boron (B) co-doping can lead to a saturated index change which is ~ 4 times larger than that obtained in pure germanosilicate fibres [6]. Such fibres were generally fabricated by means of the modified chemical vapor deposition (MCVD) technique and they are currently the most widely accepted commercial photosensitive fibres.

The high germanium doped silicate fibre is the first fibre in which the phenomenon of photosensitivity was observed [1]. The commercial high Ge doped fibre available today (such as that fabricated by Fibrecore Limited, USA) has a germanium concentration of about 20 mol%. It is very photosensitive when exposed to UV laser emission such as at 244 nm, 248 nm and 193 nm from available laser systems. A value of 2.5 $x10^{-4}$ in the refractive index change can easily be obtained when the fibre is exposed to such strong UV laser emission.

As the refractive index of silica fibre increases with the concentration of Ge doping, the core diameter of the fibre has to be small enough (normally 3~4 μm) to retain its single mode characteristics. This generally results in a larger transmission loss and additional splicing loss.

Compared with high germanosilicate fibre, B doped germanosilicate fibre has shown a higher photosensitivity and a comparatively lower value of numerical aperture (which means a large core diameter is possible to keep its single mode characteristics). With a modest power intensity of 1 W/cm^2 from a frequency-doubled CW argon ion laser, a large refractive index change of about 7.5 $x10^{-4}$ can be easily obtained after the fibre has been exposed to the laser emission for several minutes [6]. Today, the B codoped germanosilicate fibre is the "standard" photosensitive fibre. Fibres for different purpose working at different wavelength bands, such as those named PS1500, PS1250 or PS 980 from Fibrecore Limited, are commercially available and widely used.

5.2 Tin doped photosensitive fibres for the fabrication of FBGs with high temperature sustainability

5.2.1 Introduction to performance stability of the gratings at high temperatures

As has been presented above, the B codoped germanosilicate fibres are highly photosensitive and have been widely used in the fibre-optic communications and the fibre-optic sensing fields. Unfortunately, the temperature sustainability of these gratings written into B codoped fibres is usually not good enough for many sensor applications. The gratings decay quickly at elevated temperatures and can be completely "washed out" at a temperature above 350

^{0}C in a few hours [7]. Due to this problem, the gratings written into B codoped fibres through UV emission are not suitable for sensing applications at high temperatures.

Compared with this, the performance of FBGs written into high germanium doped silicate fibres is much more stable. Normally, the gratings can survive at temperatures below 650 ^{0}C for many hours. For type IIA gratings written into high Ge doped silicate fibre, the temperature sustainability is even better. Almost no decay phenomena are observed when the gratings are annealed at temperatures below 650 ^{0}C. Thus they are generally suitable for sensing applications over the moderate temperature region.

However, further annealing tests on gratings written into high Ge doped silica fibres have revealed that the gratings (including type I and type IIA gratings) decay very quickly at temperatures above 700 ^{0}C and will finally vanish after being annealed at 750 ^{0}C for hours [8]. In order to further explore the high temperature applications of FBGs, novel fibres with higher temperature sustainabilities are required.

5.2.2 Tin doped photosensitive fibre for FBGs with high temperature sustainability

In 1995, Dong et al at Southampton [9] developed a novel photosensitive fibre by co-doping tin (Sn) into the fibre core to increase the photosensitivity of the phosphosilicate fibre. It was found that through the inclusion of a small amount of tin into the phosphosilicate fibre or germanosilicate fibre, an enhanced photosensitivity in the fibre can be realized and strong gratings can be written into these fibres [10].

The tin doped fibres were fabricated by using the modified chemical vapor deposition (MCVD) technique. The tin component could easily be incorporated into the fibre core by using a volatile liquid, $SnCl_4$ with a vapor pressure of 40 torr at 35.2 ^{0}C, during the vapour deposition process [9]. It could also be added into the fibre by using the solution-doping technique. [11]

The work on tin doped fibres has continued over recent years toward the performance evaluation of the gratings written into this kind of fibre. It was found that the gratings can survive an extremely high temperature (of 800 ^{0}C) for several hours [12].

5.3 Highly photosensitive Sb/ Er/Ge codoped silica fibre for fibre Bragg grating writing with strong high-temperature sustainability

The gratings written into the tin doped germanosilicate fibre can sustain a high temperature up to 800 ^{0}C and still retain a considerable amount of reflectivity after annealing at that temperature for several hours [12]. However, the photosensitivity of tin doped silica fibre is still not as high as that of B/Ge codoped fibre. To fabricate a FBG with a reflectivity greater than 95% in tin doped fibre normally takes around half an hour, while creating FBGs in B/Ge fibre with a reflectivity greater than 99% only takes less than one minute under the same experimental conditions with 12 mJ pulses from a KrF excimer laser at 100Hz. This problem makes it difficult to create a significant volume of FBGs using tin doped fibres.

To meet the requirements set by sensing applications at higher temperatures, the development of several novel fibres with higher photosensitivity and higher temperature sustainability is desired. These fibres are especially valuable in the sensing field for high temperature use.

In this thesis, several doping techniques have been investigated by the author and his colleague to enhance the photosensitivity of the fibres and their associated temperature sustainability of the gratings written into them. Several types of novel photosensitive fibres, such as the antimony/erbium/germanium codoped silica fibre, the antimony/germanium codoped silica fibre, the indium/germanium codoped silica fibre, and the bismuth/germanium codoped silica fibre, have been designed and fabricated. A performance evaluation of these fibres in terms of the photosensitivity and temperature sustainability of the gratings written into them has been carried out. Results of experiments have shown that these fibres are highly photosensitive for grating fabrication, and the gratings written into them can sustain high temperatures up to 800 ^{0}C and even 900 ^{0}C for over 24 hours.

5.3.1 Development of antimony/erbium/germanium codoped silica fibre

In an initial attempt to investigate this fibre, a novel highly photosensitive fibre, antimony/ erbium/germanium (Sb/Er/Ge) co-doped photosensitive fibre was developed [13]. The choice of the element antimony has mainly been on the basis of the electron charge effect of the outer shell electrons in the atom, similar to the situation in P-doped fibre, with the large Sb^{3+} ion size (76 pm, greater than the 70 pm of Sn^{4+}) in its atomic construction. It is believed that this larger size of the

doping ion may effectively stabilize the performance of the material concerned, as in the situation of the fluorescence performance of Tm-doped Yttrium Aluminum Garnet (YAG), where the doping of the Tm ion composition has created a garnet with a very stable fluorescence intensity and decay lifetime when experiencing annealing temperatures as high as 1200 ^{0}C [14]. The choice of Er is mainly due to its well-known fluorescence properties, as well as the photosensitivity of the fibre itself. It is expected that the fibre can be used for sensing purposes by the utilization of its fluorescence characteristics, such as the fluorescence lifetime [15] or the fluorescence intensity ratio, for temperature determination [16]. Several schemes using fluorescence lifetime detection combined with a method of wavelength interrogation of the FBGs created in these fibres may enable a sensing system to be created to allow the monitoring of both temperature and strain parameters, as was previously illustrated [17]. Finally, the doping of the third element, Ge, is included mainly to enhance the photosensitivity and increase the refractive index of the fibre core.

The method of modified chemical vapor deposition (MCVD) was used for the fabrication of the fibre preform. Initially, the highly purified Er_2O_3 and Sb_2O_3 powders used were dissolved in hydrochloric acid and then diluted with de-ionized water. The two solvents were then mixed in a specific ratio (such as 10 for Sb and and 1 for Er respectively) to form an Er^{3+}/Sb^{3+} solvent. A silica tube was used for the deposition of a SiO_2 inner cladding layer, at a temperature of 1750 ^{0}C. A loose opaque layer of SiO_2—GeO_2 was deposited on the SiO_2 layer at a comparatively low temperature of 1200 ^{0}C, following the deposition of the SiO_2 layer. The silica tube was then soaked in the Er^{3+}/Sb^{3+} solvent for one hour so that the ions of Er and Sb were absorbed in the loose layer of SiO_2—GeO_2. The silica tube was placed again into the MCVD lathe and heated up to 600 ^{0}C for dehydration. After that, it was sintered at 2000 ^{0}C to transform the loose SiO_2—GeO_2 layer into a transparent glassy core layer. To deter the evaporation of GeO_2, a small amount of $GeCl_4$ and O_2 gases were allowed into the tube during the process. The silica tube was finally heated to 2100 ^{0}C and became a solid fibre perform after the collapse of the silica tube, as a result of the effect of the surface tension of glass. A fibre with a core diameter of about 4.5 μm and a cladding diameter of 125 μm was then drawn from the preform at 2100 ^{0}C, by using the normal fibre drawing approach. The composition of the fibre thus created was: GeO_2 ~15 wt%, Er^{3+}: 500 ppm, Sb^{3+}:5000 ppm.

The fibre was fabricated at the China Building Materials Academy, Beijing, China as a

joint research venture. In Figure 5.1, the photos of the MCVD system used for the fibre preform fabrication are shown, where Figure 5.1a is the MCVD chamber for vapor deposition and Figure 5.1b is the MCVD lathe.

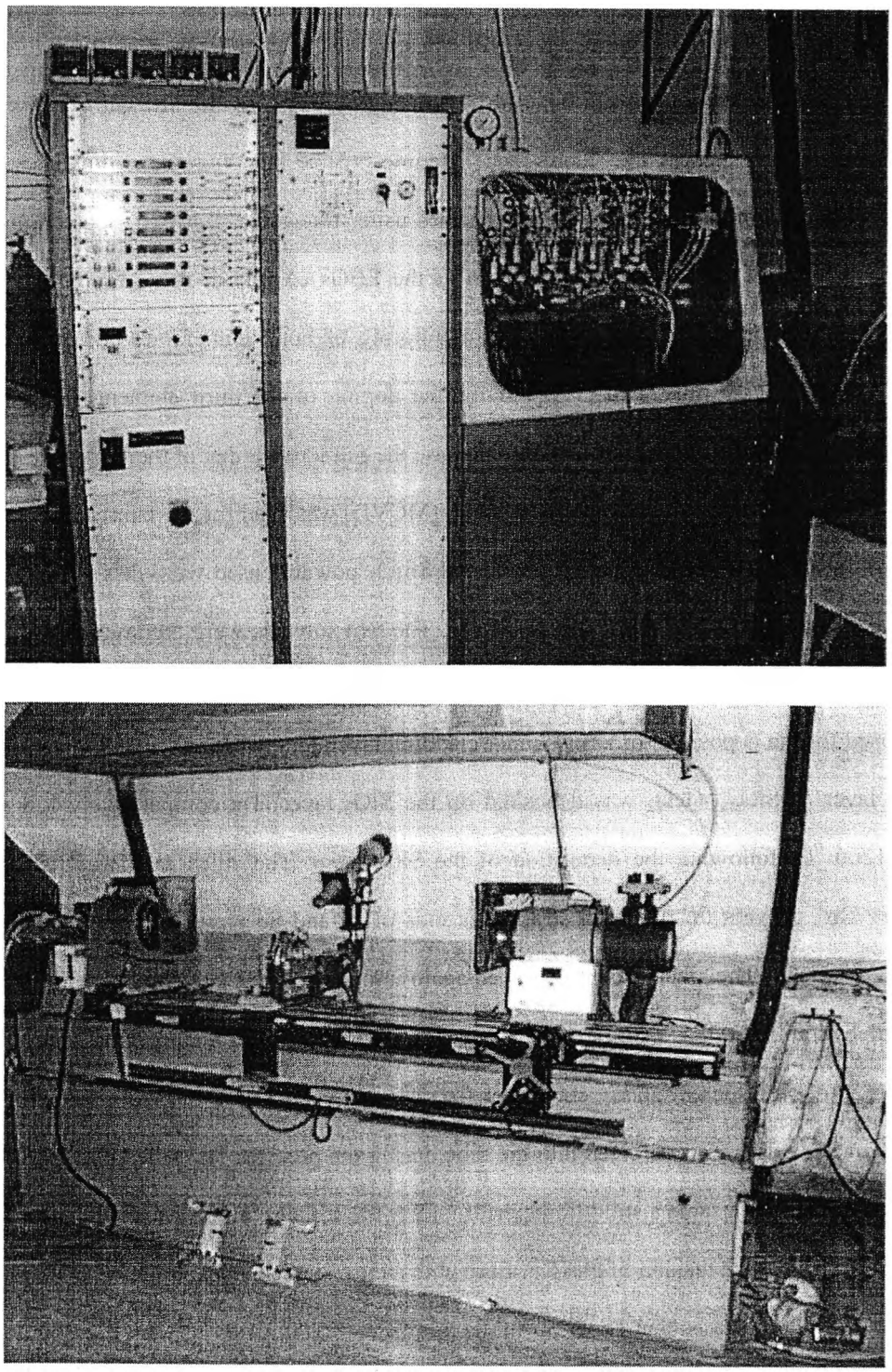

(a)

(b)

Figure 5.1 Photos of MCVD apparatus for fibre preform fabrication
(a) MCVD Chamber (b) MCVD lathe

5.3.2 Performance tests on the photosensitivity of the fibres and the temperature sustainability of the gratings

The performance of the Sb/Er/Ge co-doped photosensitive fibre thus developed was tested through a series of experiments on FBG fabrication and on the temperature annealing process for the gratings. The properties of photosensitivity and the high temperature sustainability of FBGs created in this fibre were examined and compared with that produced in a Sn doped silica fibre. The results showed that the Sb/Er/Ge fibre had a much higher level of photosensitivity than the Sn doped silica fibre and a similar very high temperature sustainability, up to 800 ^{0}C. for the FBGs written in the fibre.

Two pieces of the fibre were used in the experiments to fabricate FBGs, by exposing them to the UV emission from a KrF excimer laser (Braggstar-500 by Tuilaser AG) at 248 nm through a phase-mask (pitch period:1060 nm, supplied by OE-Land Inc., Canada). The parameters of the excimer laser used for FBGs writing were: repetition rate 100 Hz, energy per shot 12 mJ (corresponding to a power density of 200 mJ/cm^2). For comparison, a Sn co-doped high germanium fibre sample was also used (also made in China, with a composition of GeO_2 ~15 wt% and SnO_2 of ~ 0.5 wt%) for the grating fabrication. The writing time of the FBGs was controlled individually for each sample until the FBG achieved a high level of reflectivity and this was monitored by using an optical spectrum analyzer (Agilent 86142). The FBG writing system used in this experiment is illustrated in Figure 5.2.

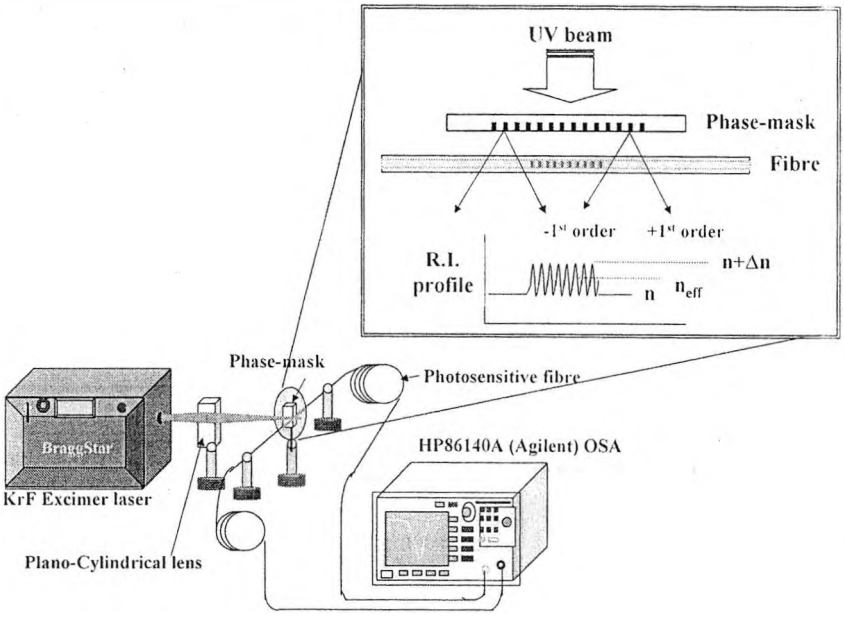

Figure 5.2 Experimental configuration diagram for FBG fabrication

From the experiments, it was observed that the reflectivity of the FBGs written into the Sb/Er/Ge fibres increased quickly during the initial stage. By the time the UV exposure exceeded 5 minutes, the grating reached a high reflectivity of greater than 96%. By using the following equation, the refractive index modulation dn could be calculated [3].

$$dn = [\lambda / \pi L n(V)] \bullet \tanh^{-1}(R^{1/2}) \qquad (5.1)$$

where λ is the operating wavelength for a grating length, L, of reflectivity, R, with an overlap function of the fibre, $n(V) = \{1 - [1/2.405 \bullet (\lambda_{cutoff} / \lambda)]^2\}$.

By considering the FBG length (of 6.5 mm), it could be deduced that there was a refractive index modulation of 1.9×10^{-4}. Following that, the reflectivity of the FBGs continued to increase at a slower rate and finally, after a UV exposure of 12 minutes for the 1st sample and 14 minutes for the 2nd sample, the gratings reached their highest reflectivity of 99.6% and 99.3% respectively, which corresponded to refractive index modulations of 2.8×10^{-4} and 2.5×10^{-4}. Using the same experimental configuration, the FBG writing in the Sn fibre achieved a highest value of reflectivity of 97.8%, in 30 minutes, which corresponds to a refractive index change of 1.97×10^{-4}.

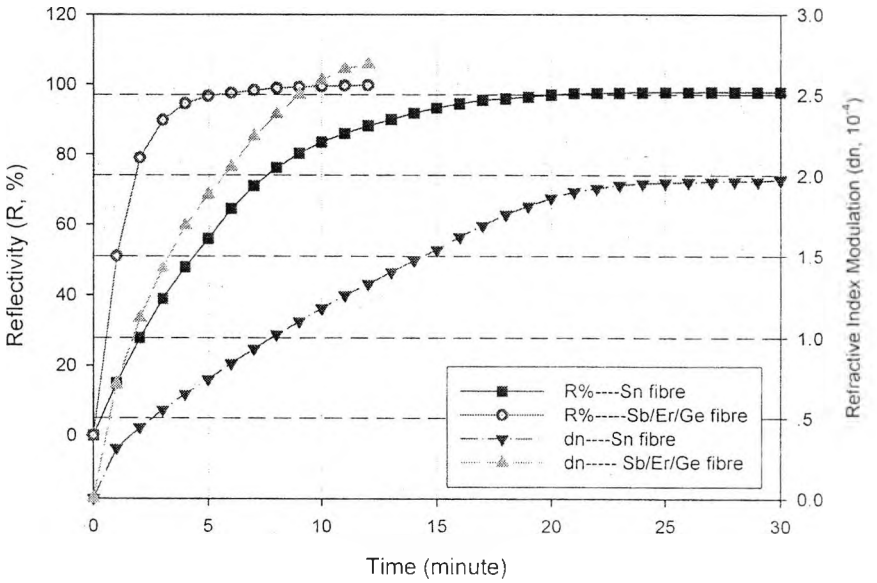

Figure 5.3 Reflectivity and refractive index modulation increase for an FBG written in Sb/Er/Ge fibre, with time, compared to the performance of an FBG written into an Sn doped silica fibre under the same experimental conditions

The increase of the reflectivity of the FBGs, as well as the modulation of the refractive index, with time, for one of the Sb/Er/Ge fibre samples and the Sn doped silica fibre is illustrated in Figure 5.3. It is obvious that the Sb/Er/Ge co-doped fibre has a much higher photosensitivity than the Sn doped fibre.

The FBGs fabricated in this way were then placed loosely in a silica tube and put into a Carbolite tube oven to observe their thermal decay characteristics over a period of time, taking results in a series of isothermal steps, starting from 100 ^{0}C, with increments in temperature of initially 100 ^{0}C, and then 50 ^{0}C, with an annealing time of 24 hours at each step. At each temperature, a fast decay of the grating characteristic was seen, followed by a more substantial slow decay being observed. The decay of the reflectivity of the FBGs studied, after annealing at those temperatures, is illustrated in Figure 5.4.

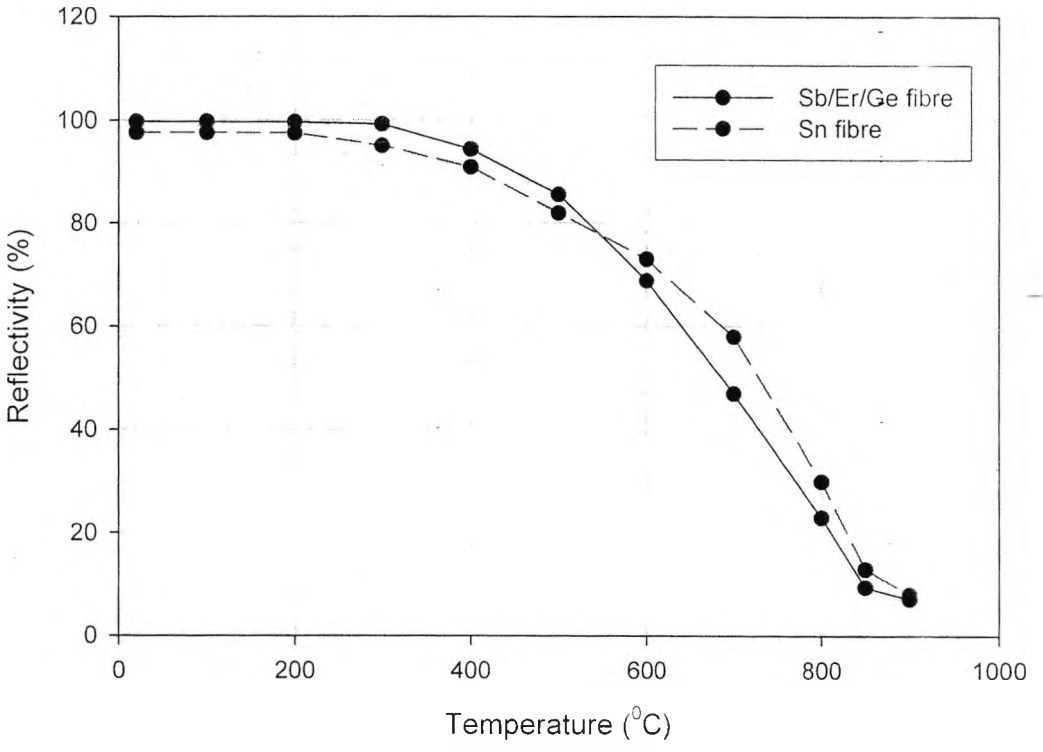

Figure 5.4 Annealing results for FBGs written into the Sb/Er/Ge fibre with temperature, in an oven operating from room temperature to 900 ^{0}C, compared with a FBG written into an Sn doped silica fibre under the same experimental conditions. For each dot in the curve, the annealing period is 24 hours, at temperatures below 850 ^{0}C and 4 hours at 900 ^{0}C.

The experimental results of the annealing tests on the FBGs shown above have clearly indicated that the gratings fabricated into the Sb/Er/Ge fibre had a high temperature sustainability, similar to those in the Sn doped fibre. They could still retain a particular value of reflectivity after annealing at 850 ^{0}C for 24 hours and 900 ^{0}C for 4 hours (no further annealing test was performed at 900 ^{0}C), while similar tests on the FBGs from high germanium doped silica fibre (Ge:SiO_2 fibre) showed a highest sustainable temperature of only 700 ^{0}C. The reflection spectrum of the FBG written into the Sb/Er/Ge fibre after annealing at 900 ^{0}C is illustrated in Figure 5.5. It is clear from the figure that the peak wavelength of this spectrum can be readily determined and used as measurand-sensitive feature for sensor applications.

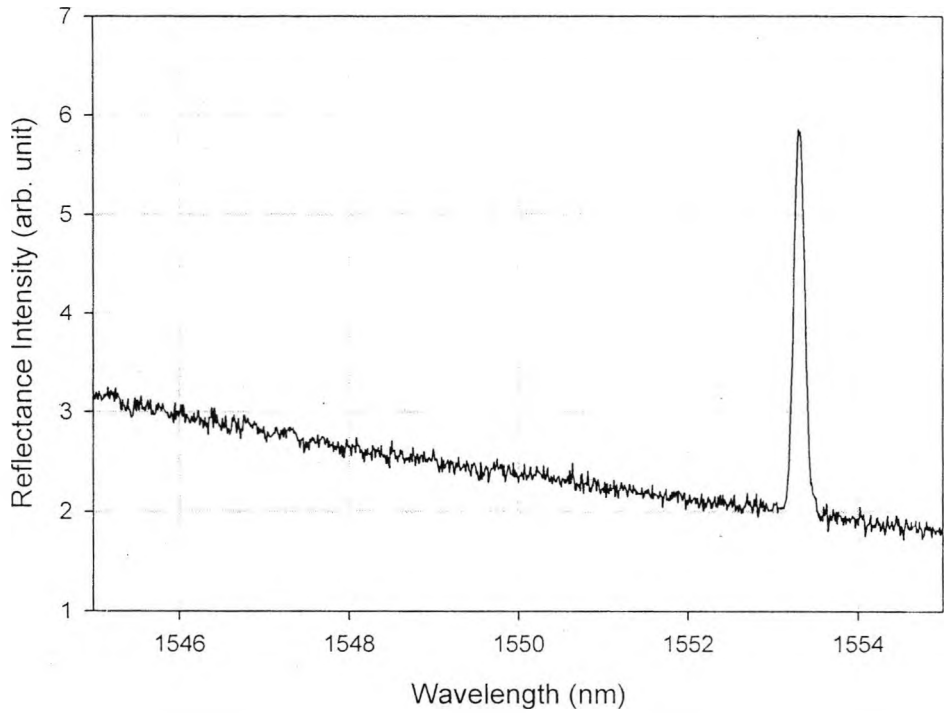

Figure 5.5 The reflectance spectra of an FBG written into the Sb/Er/Ge fibre at 900 ^{0}C after long term annealing from room temperature to 850 ^{0}C. The time period of the annealing is 24 hours at each hundred degree Celsius point below 850 ^{0}C.

The FBG samples, after annealing at 900 ^{0}C for 4 hours, were cooled to room temperature and then heated step by step, until a temperature of 850 ^{0}C was reached. The peak wavelengths of the reflective spectra were recorded after the temperature was stabilized at each multiple of one hundred degrees Celsius point. This process was repeated several times to test the reproducibility of the peak wavelength determined. The results show an excellent repeatability of the peak

wavelength in the reflection spectra with a deviation of less than 0.02 nm, which was equivalent to less than 2 ^{0}C of temperature change. This deviation might be attributed to the temperature fluctuations in the oven and the limited resolution of the OSA (with the highest resolution of 0.01 nm being used). The data for the peak wavelength shift with temperature are presented in Figure 5.6 for both the FBGs written into Sb/Er/Ge and tin fibres. It may be computed that the temperature sensitivity of the peak wavelengths for the FBGs of Sb/Er/Ge fibre is about 12 pm/^{0}C at room temperature and 18 pm/^{0}C at around 800 ^{0}C.

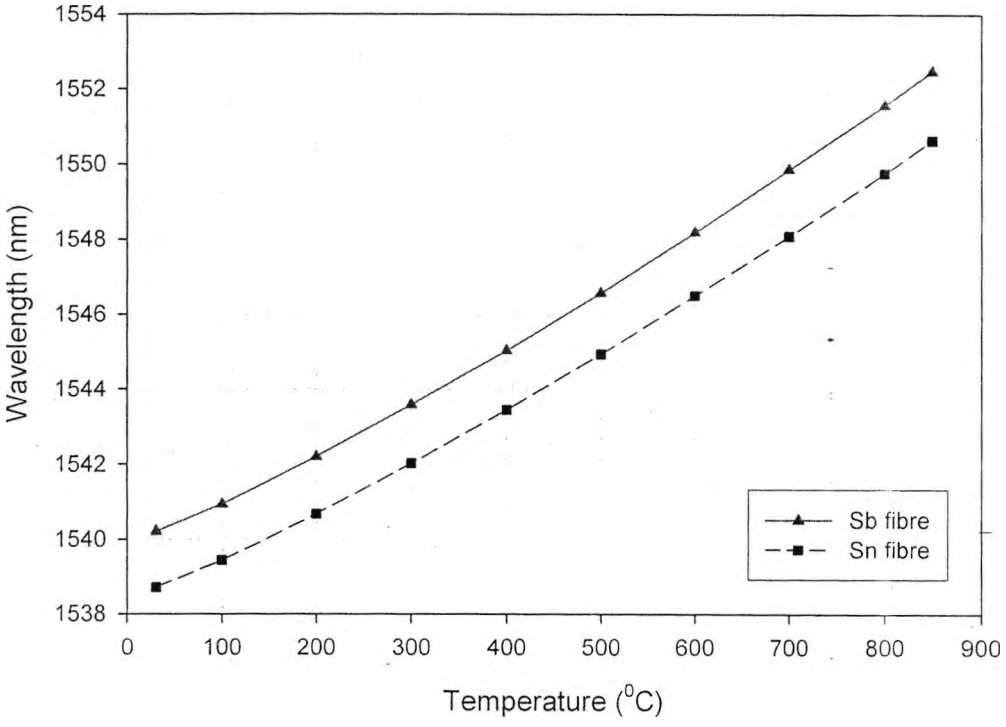

Figure 5.6 Dependence of the peak wavelength in the reflection spectrum of the FBG written into the Sb/Er/Ge fibre with temperature

5.3.3 Performance evaluation of the fluorescence characteristics

The fluorescence characteristics of the Sb/Er/Ge fibres were investigated to determine their suitability as either high temperature fluorescence-based or laser-based sensors. These include studying the excitation of the fluorescence on the band around 1550 nm, and investigating fibre laser performance [8].

The familiar fluorescence spectrum in the 1550 nm band was clearly seen for the Sb/Er/Ge

fibre when excited by light from a fibre pigtailed laser diode (LD) with an output power of 20 mW at 980 nm. A typical fluorescence emission spectrum is presented in Figure 5.7. Compared with the Sn/Er fibre, however, the situation is a little different when the fibres were excited by emission from a fibre pigtailed LD working at 1480 nm. The fluorescence peaks could still be seen for the Sb/Er fibre, as illustrated in Figure 5.8, but not in the case of Sn/Er and Ge/Er fibres where the fluorescence was almost wholly hidden by the emission tail of the LD. These experiments showed that the fluorescence conversion efficiency and thus the fluorescence intensity achieved under the same pump conditions are much higher for the Sb/Er fibre sample tested than for the Sn/Er and Ge/Er fibre samples used.

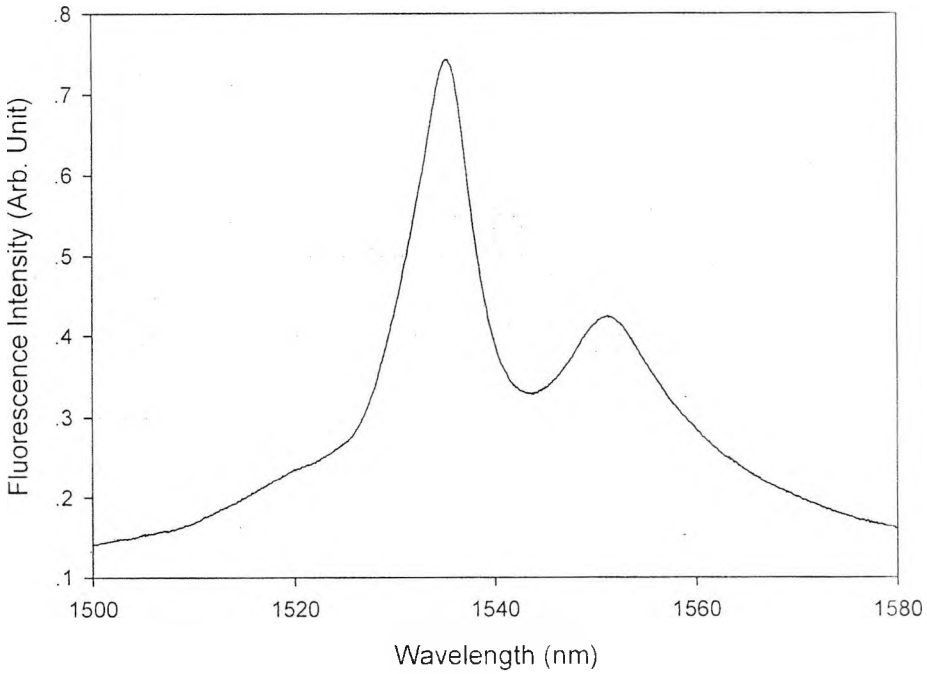

Figure 5.7 Fluorescence emission of Sb/Er fibre in the wavelength region of 1500 nm – 1580 nm band when excited by a LD operating at 980 nm

A similar conclusion was also obtained when using Er doped fibres to demonstrate laser operation. Recent work on FBG-based laser sensors has shown their value for high temperature measurement [18]. Laser operation could be readily realized with the Sb/Er fibre but failed with Sn/Er fibre when a similar configuration was employed. It is interesting to note that there was no aluminium in the composition of the Sb/Er fibre, while its inclusion is generally regarded as a key element in deterring the clustering of the rare-earth fluorescent ions and thus enhancing the

fluorescence efficiency [19][20]. It is possible that the doping of the Sb ion in the fibre may have played a similar role to that of aluminium, as a similar effect was also reported with the co-doping of phosphorus in glass [21].

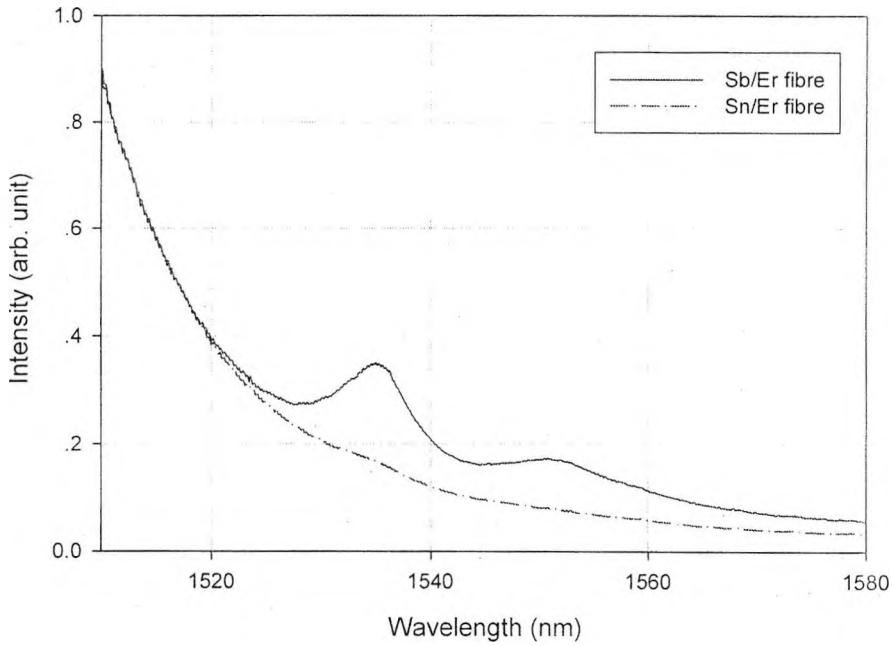

Figure 5.8 Fluorescence emission of Sb/Er fibre and Sn/Er fibre observed in transmission mode when excited by a LD operating at 1480 nm. The fluorescence peaks from the Sn/Er fibre could not be seen due to the strong tail of the emission from the LD on the 1530 nm band

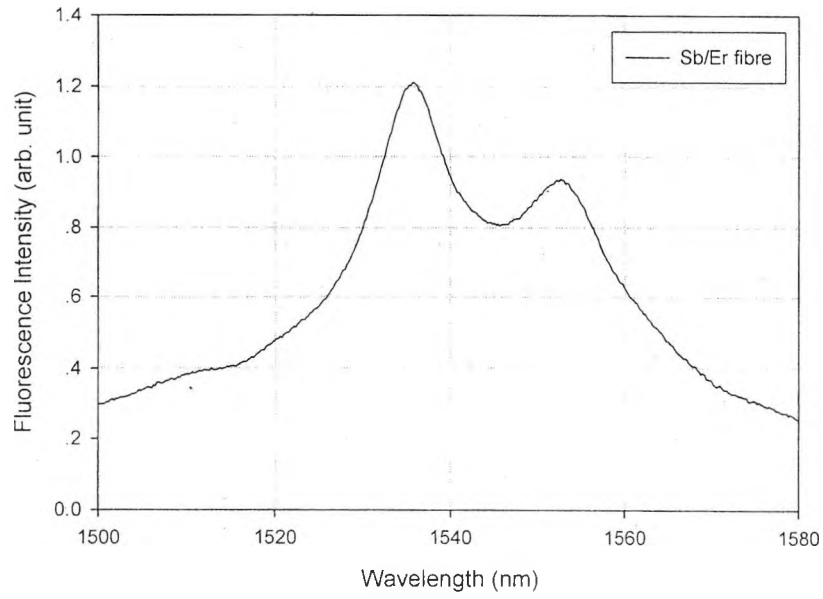

Figure 5.9 Fluorescence spectrum of Sb/Er fibre at 800 °C when excited by a LD working at 980 nm

The fluorescence emission at high temperatures was also investigated. It is clear that, for the Sn/Er and Sb/Er fibres, there was still an observable fluorescence signal even at a temperature as high as 800 °C, when excited by the 980 nm LD, which is illustrated in Figure 5.9. When a high resolution measurement is required, however, the working temperature of the fibre should be below 700 °C for a strong signal and a high signal to noise ratio. For reference, in Figure 5.10, the fluorescence spectrum taken at a temperature of 600 °C from a sample of Er-doped Sb/Er fibre, of length 10 cm, with an FBG written into the fibre, is shown.

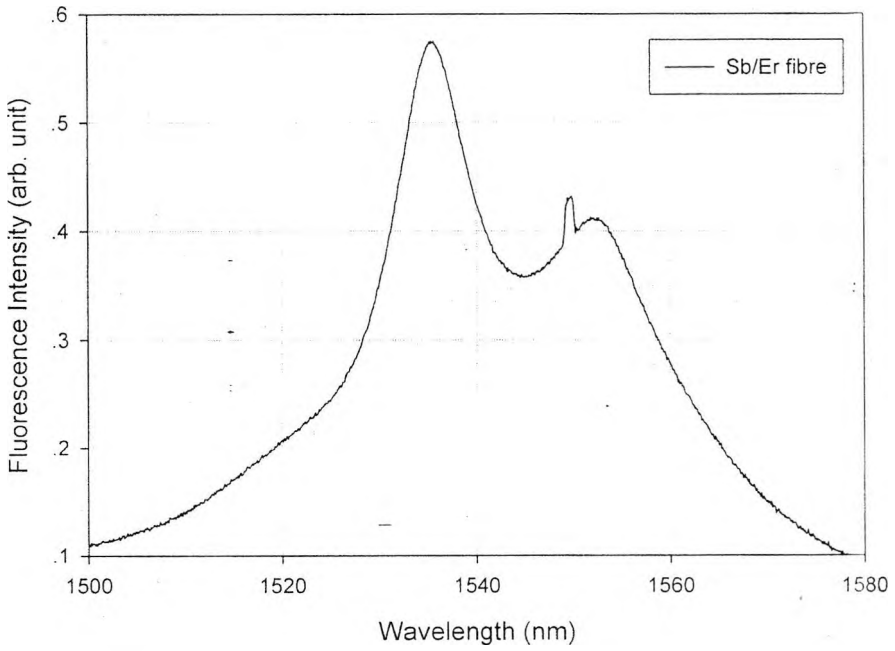

Figure 5.10 Fluorescence spectrum of a piece of Sb/Er fibre, with an FBG written into the fibre, at 600 °C

5.4 Photosensitive Sb/Ge codoped fibre and In/Ge codoped fibre for strong FBG fabrication with high temperature sustainability

The work on the development of novel photosensitive fibres with better performance in terms of photosensitivity and grating sustainability has continued with the success seen in Sb/Er/Ge fibres. As presented in section 5.3, the Sb/Er/Ge fibre has a much better photosensitivity than tin doped germanosilicate fibre. The temperature sustainability of the gratings written into this fibre is similar to that written into tin doped fibre.

It is noted from Figure 5.6 that the germanium concentration in the Sb/Er/Ge fibre may be

higher than that in the tin doped fibre as the peak wavelength of the FBG in Sb/Er/Ge fibre is larger (normally, the refractive index of the fibre core increases with Ge concentration). Such a difference in germanium concentration may greatly affect both the performance of photosensitivity and grating sustainability. Besides, the codoping of erbium into the fibre may possibly play some role in photosensitivity. To develop novel fibres with better performance, more efforts were made by the author and colleagues. An antimony-germanium codoped fibre and an indium-germanium codoped fibre have been fabricated. Performance of these two fibres has been tested and evaluated. The results obtained have shown great potential of these fibres for high temperature sensing applications and these are presented as follows.

5.4.1 Antimony co-doped photosensitive fibre for FBGs with strong temperature sustainability

As has been presented in Section 4.3, the antimony/erbium/germanium co-doped photosensitive fibre (Sb/Er/Ge fibre) has not only a high photosensitivity, but also a very good temperature sustainability at temperatures up to and in excess of 800 ^{0}C [13]. To meet the requirements of sensing applications at even higher temperatures, a novel Sb/Ge co-doped photosensitive fibre was developed, this having been specially designed and developed for the fabrication of "strong" FBGs with higher temperature sustainability. Results obtained from tests on the photosensitivity of the fibre and the high temperature sustainability of the FBGs written into it are very encouraging, in that the FBG written into the Sb/Ge fibre could reach a high refractive index modulation of greater than 2.7×10^{-4} and sustain a high temperature of 900 ^{0}C over a period of 24 hours and yet still retain a quite large reflectivity of greater than 18% [22]. This is much better than the results previously reported for Sn doped fibres [12] and Sb/Er/Ge fibres [13], and the grating reflectivity is high enough for the peak wavelength interrogation of the FBG created in this way.

The Sb/Ge fibre used in this work was fabricated by means of the modified chemical vapor deposition (MCVD) method, which was similar to that for the fabrication of Sb/Er/Ge fibre, as reported in [13]. The Ge and Sb concentrations doped into the fibre were controlled to about 12 wt% and 5000 ppm respectively, and no erbium was included in the fibre as it was not designed for fibre fluorescence studies.

Several pieces of Sb/Ge fibres were used in the experiments to fabricate the FBGs tested, by

exposing the fibre samples to the UV emission from a KrF excimer laser at 248 nm through a phase-mask. A cylindrical plano-convex lens was used to focus the laser beam onto the photosensitive fibre. The parameters of the excimer laser beam used for FBG writing were: repetition rate of 100 Hz, 200 Hz and 300 Hz respectively with an energy per shot of 12 mJ. For comparison, another fibre sample, this being Sn co-doped high germanium fibre (made in China, with a composition of GeO_2 ~15 wt% and SnO_2 of ~ 0.5 wt%) was also used with similar laser parameters of 300 Hz and 12 mJ. The time for the FBG writing was controlled individually for each sample until the FBG achieved the highest level of reflectivity, this having been monitored using an Optical Spectrum Analyzer (OSA).

The reflectivity of the FBGs written into the Sb/Ge fibres was recorded with time during the fabrication process. The results, as illustrated in Figure 5.11, showed that the highest reflectivity (and the corresponding refractive index modulation, dn) achieved for the gratings were quite different with the three different repetition rates of the excimer laser used. The higher the repetition rates of the laser emission, the greater the achievable reflectivity of the FBG. Under the condition of same energy (12 mJ) per pulse, a highest reflectivity of 99.5% (which corresponded to $dn=2.7x10^{-4}$ when considering the grating length of 6.5 mm) was obtained with a laser repetition rate of 300 Hz, which differed significantly from the situation using a 100 Hz repetition rate when a highest reflectivity of only 90.2% (corresponding to $dn=1.5x10^{-4}$) was achieved.

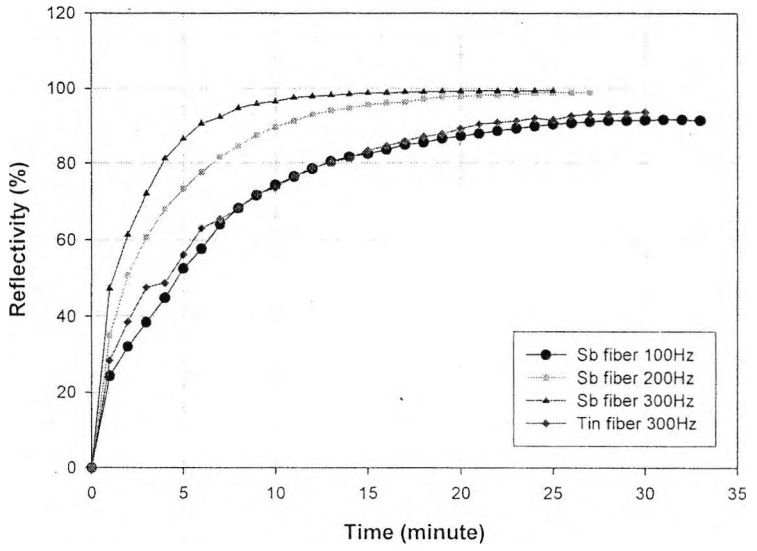

Figure 5.11 Reflectivity increase for FBGs written into Sb/ Ge fibre, with time, compared to the performance of an FBG written into a Sn doped silica fibre under the same experimental conditions.

The temperature sustainability of the gratings fabricated in this way was then tested by putting the FBGs into a silica tube and placing this in a tube oven, to calibrate their thermal decay characteristics over a period of time. Results were taken in a series of isothermal steps, starting from 100 ^{0}C, with increments in temperature of initially 100 ^{0}C, and then 50 ^{0}C, with an annealing time of 24 hours at each step. The decay of the reflectivity of the FBGs with time was studied, and the values of reflectivity after annealing at those temperatures for 24 hours each are illustrated in Figure 5.12.

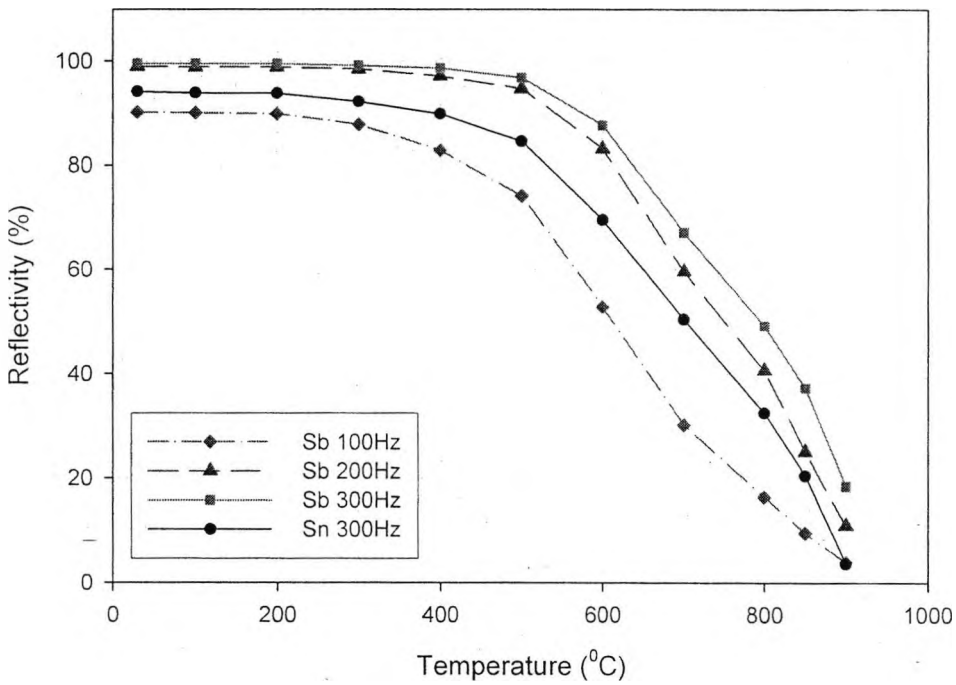

Figure 5.12 Annealing results for FBGs written into Sb/Ge fibre with temperature, in an oven operating from room temperature to 950 ^{0}C, compared with a FBG written into a Sn doped silica fibre under the same experimental conditions. For each data point in each curve, the annealing period is 24 hours

It is very encouraging to find that the temperature sustainability of these gratings written into the Sb/Ge fibre was especially good, compared to those written into other fibres, including the tin doped fibre and the Sb/Er/Ge co-doped fibre previously measured. Even after annealing at 900 ^{0}C for 24 hours, a large value of reflectivity (18.5%) still remained for the grating written at a 300 Hz repetition rate, compared to 11.0% and 3.9% for the FBGs written at 200 Hz and 100 Hz repetition rate respectively.

The gratings were then further annealed at an even higher temperature of 950 ^{0}C to test the performance. The reflectivity of the grating written at 300 Hz repetition rate was recorded at intervals of one hour over a period of 8 hours, showing a reflectivity of 3.4% still remained, after this extreme temperature exposure. The result showing the reflectivity decaying during this period of annealing at 950 ^{0}C is demonstrated in Figure 5.13. After annealing at 950 ^{0}C for 20 hours, the reflection peak could still be readily interrogated.

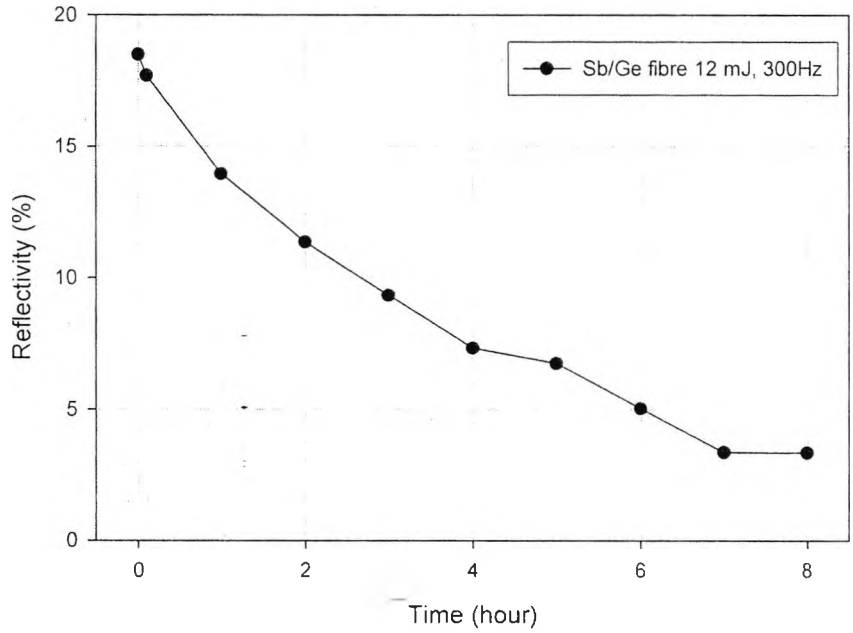

Figure 5.13 Reflectivity decay of an FBG written into the Sb/Ge fibre with time, in an oven operating at 950 ^{0}C, where the data were recorded continually for 8 hours until the reflectivity decreased to a value of 3.4%.

The gratings were then cooled down to lower temperatures for a peak wavelength and temperature calibration. The results are shown in Figure 5.14. It was found that, after annealing at 950 ^{0}C for a long period, the relationship between the peak wavelength of the FBG and the temperature became quite stable and was no longer changing during all the calibrations carried out later at temperatures below 900 ^{0}C.

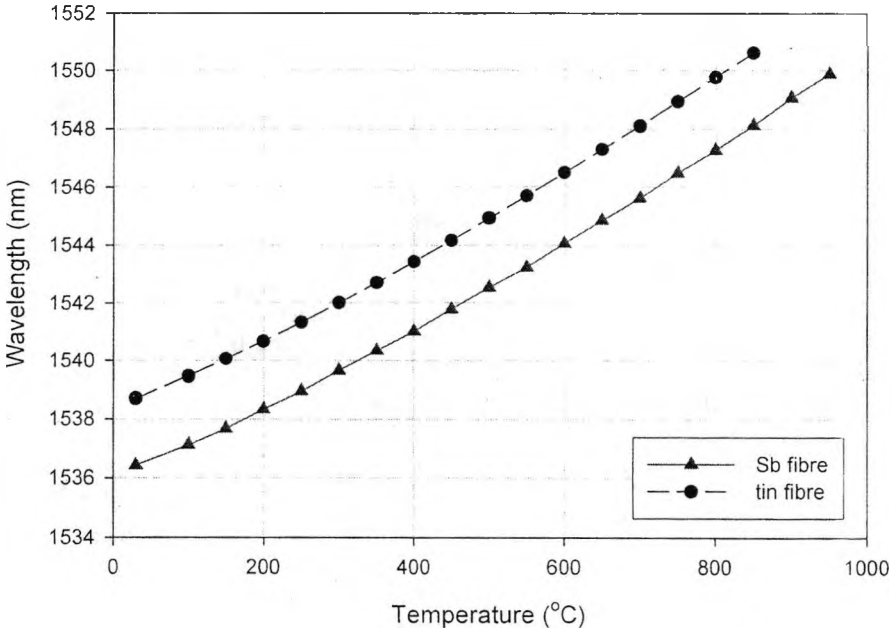

Figure 5.14 Dependence of the peak wavelength in the reflection spectrum of the FBG written into the Sb/Ge fibre on temperature, covering the range from room temperature to 950 ^{0}C

5.4.2 Photosensitive indium doped germano-silica fibre for strong FBGs with high temperature sustainability [23]

In addition to the Sb doping in germanosilicate fibre as presented above, a novel indium codoped germanosilicate fibre was also developed to evaluate the performance in its photosensitivity and the grating stability.

Recent work reported by the authors [13] [22] has indicated that antimony (Sb) doped fibres have not only a good photosensitivity but also a strong temperature sustainability in the gratings written into this fibre. Based on the experimental results obtained from a range of photosensitive fibres in terms of the photosensitivity and the temperature sustainability of FBGs written into them, a so-called cation hopping model was proposed [22] (the cation hopping model will be detailed in Chapter 6), in which the size of the cations responsible for the photosensitivity is considered to be an important factor in determining the temperature sustainability of the FBGs written into the fibre. The bigger the size of the cations doped in the fibre, the stronger the temperature sustainability of the FBGs written into it.

By checking the physical data of the cations, it is easy to find that doping of indium oxide into silica glass may result in a big cation In^{3+} (with a cation size of 80 pm, bigger than 76 pm for

Sb^{3+} and 71 pm for Sn^{4+}) [24]. It is thus expected that doping of In^{3+} into the germano-silicate fibre may result in a photosensitive fibre suitable for fabrication of strong FBGs with high temperature sustainability. Unfortunately, due to the low evaporation temperature of indium oxide (850 ^{0}C), it may be difficult to dope the In^{3+} into the glass host of the fibre as the In_2O_3 will easily evaporate during the fabrication process of the fibre preform, in which the temperature may reach as high as 2200 ^{0}C. The possibility of doping In^{3+} into the fibre and, as a result, the performance of In^{3+} doped fibre then remains a problem. Encouraging as it is, the In^{3+} doped fibre thus developed showed a very good performance in photosensitivity and grating stability.

The In/Ge fibre used in this work was fabricated by means of a modified chemical vapour deposition (MCVD) method, which was similar to that for the fabrication of Sb/Er/Ge fibre, as reported in [13]. The solution concentration of In_2O_3 was controlled to 1% when the powder of In_2O_3 was dissolved in hydrochloric acid and then diluted with de-ionized water. After the solvent was absorbed by the SiO_2—GeO_2 layer within the silica tube, the tube was heated up to 2000 ^{0}C for sintering to convert the loose layer of SiO_2—GeO_2 into a transparent glassy core layer and finally to over 2200 ^{0}C to solidify into the perform. Though there was a phenomenon of In_2O_3 evaporation which existed during such a fabricating process, it was clear that the preform thus developed still had a brown color, which is considered to be the result of In^{3+} doping, implying that some In^{3+} has been doped into the preform. The preform was then drawn into a fibre with core and cladding diameters of 5 μm and 125μm respectively, and a numerical aperture of 0.21 using a normal fibre drawing approach. The GeO_2 concentration in the fibre thus created was about 15wt% while the In_2O_3 composition is about 0.2 wt% (measured by JXA 8800R electron probe micro-analyzer).

Several samples of the In/Ge fibre thus produced were also used to fabricate the FBGs and then test their high temperature performance. The procedures for FBGs writing and testing are similar to those used in Sb/Ge fibres. The performance of the In/Ge fibre was evaluated together with Sb/Ge fibre for ease of comparison.

The reflectivity of the FBGs written into the In/Ge fibres was recorded, with time, during the grating fabrication process and shown in Figure 5.15. The results showed that the FBGs created by the excimer laser when using laser parameters of 12 mJ per pulse and repetition rates of 200 Hz and 300 Hz can reach a high reflectivity of greater than 99.0% and 99.8% respectively,

and these corresponded to a refractive index modulation, dn, of about $2.4x10^{-4}$ and $3.2x10^{-4}$ when considering the grating length of 6.5 mm. No obvious decline of the reflectivity was observed during the FBG writing when a longer exposure time was used, which means the gratings are all in type I form.

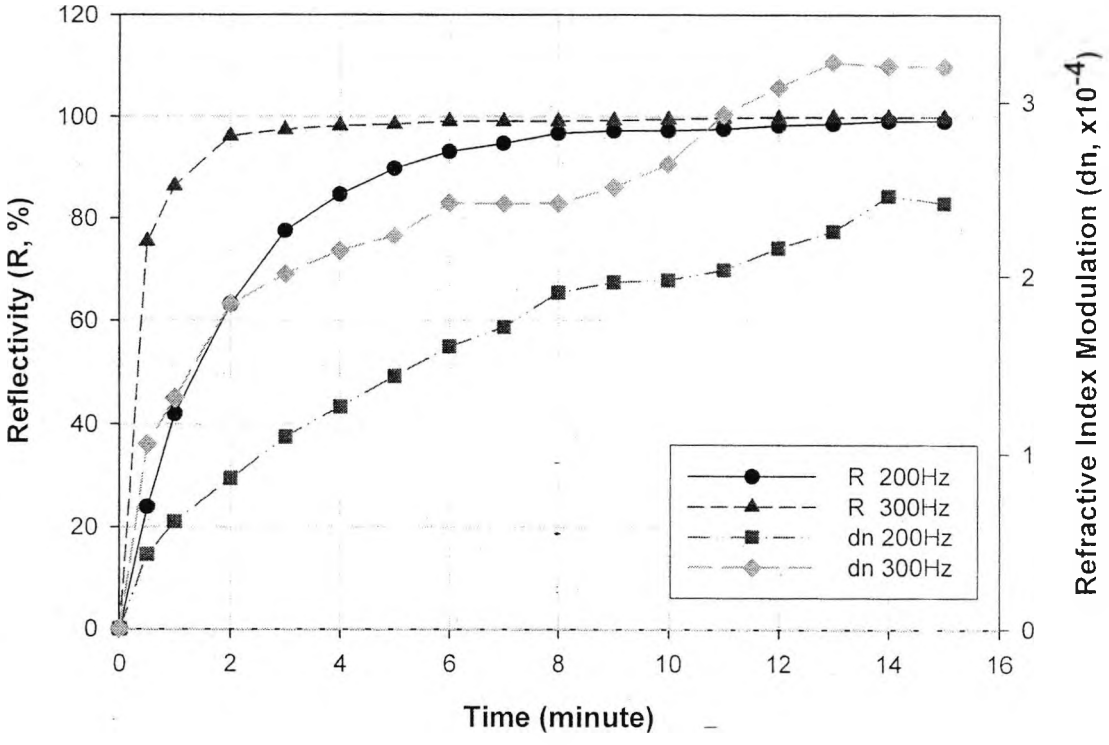

Figure 5.15 Reflectivity and dn increase for FBGs written into In/Ge fibre when using a UV excimer laser with parameters of 12 mJ per pulse, repetition rate of 200 Hz and 300 Hz

The gratings thus produced were also annealed step by step in order to investigate their temperature sustainability. The decay of the reflectivity of the FBGs with time was studied, and the values of reflectivity and the corresponding value of the decay of dn, after annealing at those temperatures for 24 hours, are illustrated in Figure 5.16. It is encouraging to find that after annealing at 900 ^{0}C for 24 hours, the grating still retained a reasonably high reflectivity of 21% (for grating written with 300 Hz repetition rate) and 11% (with 200 Hz repetition rate). These values are still high enough for the gratings to be interrogated by detecting the peak wavelengths in the reflectance spectra and to be used as the sensing probe in a high temperature environment.

The gratings were further annealed at an extremely high temperature of 950 ^{0}C for 8 hours and then 1000 ^{0}C for 2 hours before the temperature of the tube oven was cooled down step by

step to room temperature. The reflectance spectra of the grating written at a repetition rate of 300 Hz were recorded at 950 ^{0}C and 1000 ^{0}C and are illustrated in Figure 5.17. It is obvious that the grating can still be interrogated readily, as the reflectivity is sufficiently high.

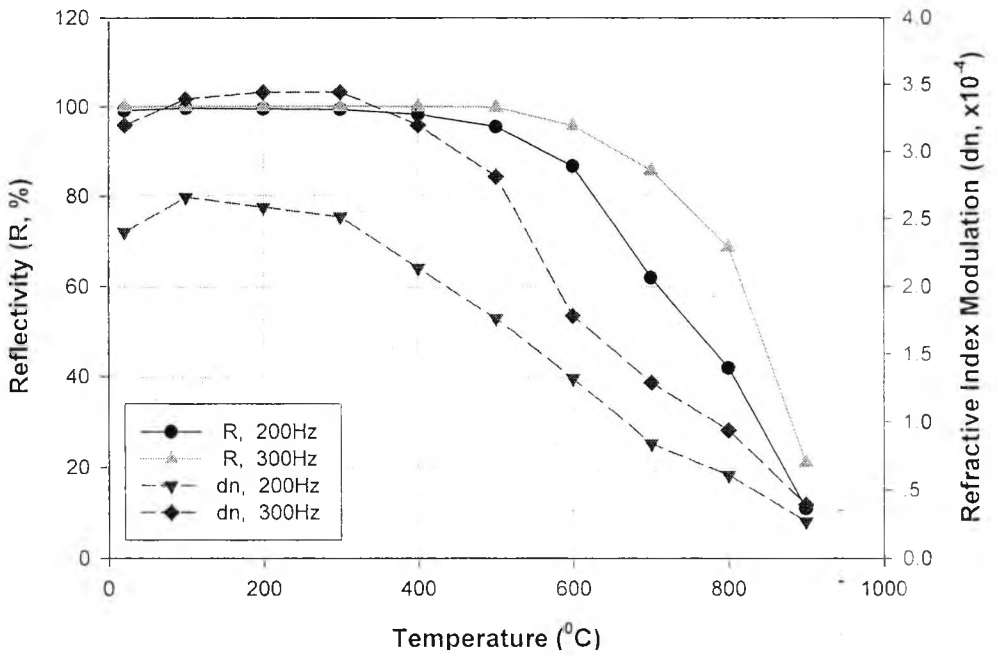

Figure 5.16 Annealing results for FBGs written into In/Ge fibre with temperature from room temperature to 900 ^{0}C, showing the change in reflectivity (R) and the refractive index modulation (dn) with temperature. For each data point in each curve, the annealing period is 24 hours.

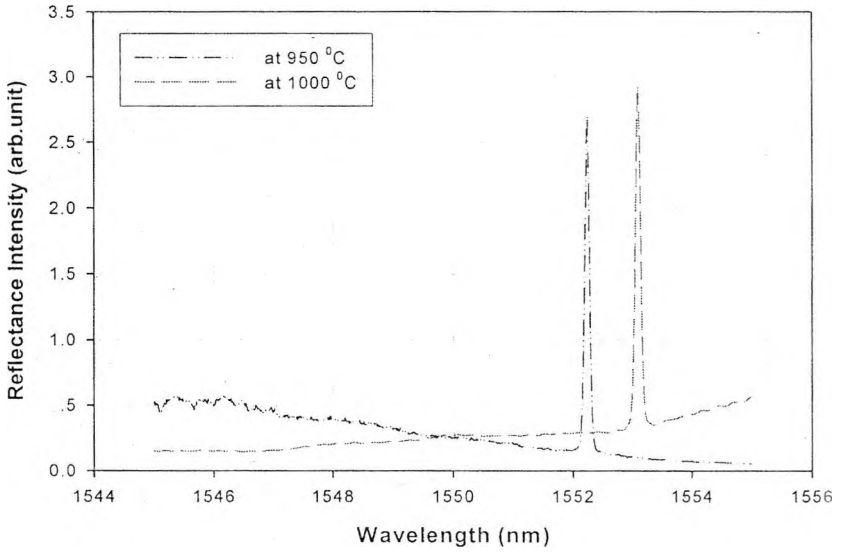

Figure 5.17 Reflectance spectra of the FBG written into the In/Ge fibre with parameters of 12 mJ per pulse, repetition rate of 300 Hz

The relationship between the peak wavelength of the grating and temperature was

calibrated and it is shown in Figure 5.18. As a comparison, a similar calibration curve for Sb/Ge fibre [22] is also shown in the figure.

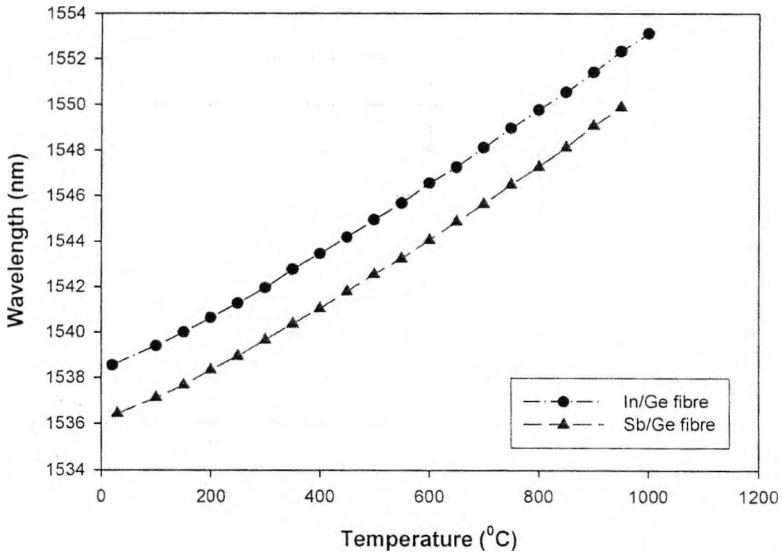

Figure 5.18 Dependence of the peak wavelength in the reflection spectrum for FBGs written into both In/Ge fibre and Sb/Ge fibre with temperature, covering the range from room temperature to 1000 ^{0}C

5.5 Summary

Photosensitive fibres are important components for FBG fabrication. Commercial photosensitive fibres, such as those of B/Ge co-doped fibres, offer high photosensitivity. The gratings can be easily fabricated into the fibres by exposing them to UV laser emission. Unfortunately, the gratings written into the B/Ge fibre feature poor thermal stability and are not suitable for sensing applications covering a wide temperature range.

Compared with this, the gratings written into the tin doped silicate fibre offer much better thermal stability. The photosensitivity of the tin doped silicate fibre is still good though a much longer exposure time is needed for FBG fabrication.

To achieve better performance of FBG-based sensors, several novel photosensitive fibres have been developed and these are Sb/Ge/Er fibres, Sb/Ge fibres and In/Ge fibres. A performance evaluation on the photosensitivity of the fibre and the thermal stability of the gratings confirmed that these fibres are highly photosensitive. The gratings written into them can be strong enough to sustain high temperatures up to 800 or 900 ^{0}C, and thus will be very useful in sensing fields covering a wide temperature region.

5.6 References

[1] K.O. Hill, et al. "Photosensitivity in optical fibre waveguides: Application to reflection filter fabrication," Applied Physics Letters, 32, pp647-649 (1978)

[2] G. Meltz, W.W. Morey and W.H. Glenn, "Formation of Bragg gratings in optical fibres by a transverse holographic method," Optics Letters, 14, pp823-825 (1989)

[3] A. Othonos and K. Kalli, "Fibre Bragg Gratings: Fundamentals and applications in telecommunications and sensing", Artech House, Boston (1999)

[4] R. Kashyap, "Fibre Bragg Gratings", Academic Press, San Diego (1999)

[5] P.J. Lemaire, R.M. Atkins, V. Mizrahi, W.A. Reed, "High-pressure H_2 loading as a technique for achieving ultrahigh UV photosensitivity and thermal sensitivity in GeO_2 doped optical fibres," Electronics Letters, 29, pp1191-1193 (1993)

[6] D.L. Williams, B.J. Ainslie, J.R Armitage, J.R. Kashyap and R. Campbell, "Enhanced UV photosensitivity in boron codoped germanosilicate fibres," Electronics Letters, 29, pp45-47 (1993)

[7] S. R. Baker, H. N. Rourke, V. Baker and D. Goodchild, "Thermal decay of fibre Bragg gratings written in boron and germanium codoped silica fibre," IEEE J. Lightwave Technol., 15, pp1470-1477 (1997)

[8] Y. Shen, S. Pal, J. Mandal, et al, "Investigation on the photosensitivity, temperature sustainability and fluorescence characteristics of several Er-doped photosensitive fibres", Optics Communications, 237, pp301-308 (2004)

[9] L. Dong, J.L. Cruz, J.A. Tucknott, L. Reekie, D.N. Payne, "Strong photosensitivity gratings in tin-doped phosphosilicate optical fibres," Optics Letters, 20, pp1982-1984 (1995)

[10] L. Dong, et al. "Enhanced photosensitivity in tin-codoped germanosilicate optical fibres," IEEE Photonics Technology Letters, 7, pp1048-1050 (1995)

[11] J.E. Townsend, S.B. Poole, and D.N. Payne, "Solution doping technique for fabrication of rare-earth doped optical fibres", Electron. Lett. 23, pp329-331 (1987)

[12] G. Brambilla, V. Pruneri and L. Reekie, "Photorefractive index gratings in SnO_2:SiO_2 optical fibres", Appl. Phys. Lett., 76, pp807-809 (2000)

[13] Y. Shen, T. Sun, K.T.V. Grattan and M. Sun, "Highly photosensitive Sb/ Er/Ge codoped silica fibre for fibre Bragg grating (FBG) writing with strong high-temperature sustainability," Optics Letters, 28, pp2025-2027 (2003)

[14] Y.H. Shen, W.Z.Zhao, J. He, T. Sun, K.T.V. Grattan, "Fluorescence decay characteristic of Tm-doped YAG crystal fibre for sensor applications, investigated from room temperature to 1400 °C", IEEE Sensors Journal, 3, p507-512 (2003)

[15] K.T.V. Grattan, Z. Y. Zhang, Fibre Optic Fluorescence Thermometry, Chapman & Hall (1995)

[16] S.A. Wade, S.F. Collins, and G.W. Baxter, "Fluorescence intensity ratio technique for optical fibre point temperature sensing", Journal of Applied Physics, 94, pp4743-4756 (2003)

[17] D.I. Forsyth, S. A. Wade, T. Sun, X.M. Chen, K.T.V. Grattan "Dual temperature and strain measurement with the combined fluorescence lifetime and Bragg wavelength shift approach in doped optical fibre," Applied Optics, 41, pp6585-6592 (2002)

[18] J. Mandal, S. Pal, T. Sun, et al, Bragg grating-based fibre optic laser probe for temperature sensing, IEEE Photonics Technol. Lett., 16, pp218-220 (2004)

[19] R. S. Quimby, W. J. Miniscalco, B. Thompson, Clustering in Erbium- doped silica glass-fibres analyzed using 980 nm excited-state absorption, J. Appl. Phys., 76, pp4472-4478 (1994)

[20] E. Desurvire, Erbium-doped fibre amplifiers, John Wiley & Sons, Inc. (1994)

[21] K. Arai, H. Namikawa, K. Kumata, T. Honda, Y. Ishii, T. Handa, Aluminum or phosphorus co-doping effects on the fluorescence and structural-properties of Neodymium-doped silica glass, J. Appl. Phys., 59, pp3430-3436 (1986)

[22] Y. Shen, J. He, T. Sun, K.T.V. Grattan, "High temperature sustainability of strong FBGs written into Sb/Ge co-doped photosensitive fibre — decay mechanisms involved during annealing", Optics Letters, 29, p554-556 (2004)

[23] Y. Shen, J. Xia, T. Sun and K.T.V. Grattan, "Photosensitive Indium doped germano-silica fibre for strong FBGs with high temperature sustainability", IEEE Photonic Tech. Lett., 16, pp1319-1321 (2004)

[24] A. M. James and M.P. Lord, Macmillan's Chemical and Physical Data, The MacMillan Press Ltd. (1992)

Chapter 6: Thermal Decay Characteristics of Strong FBGs Showing High Temperature Sustainability

6.1 Thermal decay characteristics of fibre Bragg Gratings

6.1.1 Introduction

As has been discussed in the previous chapters, the fibre Bragg grating (FBG) is particularly important in the fibre-optic sensing field. With the use of FBGs as sensing elements, many physical and chemical parameters, such as temperature, strain and pH value, for example, can be obtained readily by using the scheme of peak-reflection wavelength interrogation. For the optimum application of FBGs, their thermal properties, such as their wavelength stability or the decay characteristics of the peak reflectance have long been an important factor to take into consideration in a range of applications. As some sensors may be expected to work over the long-term, for example for years or even decades at elevated temperatures, it is essential that the performance of the FBGs used is sufficiently stable for this application. However, the performance stability of FBGs fabricated from different types of photosensitive fibres is distinctively different. Thus, the issue of FBG stability remains an important problem to investigate more fully. Many papers have been published over the past ten years on the decay characteristics of FBGs. The so-called power-law or aging decay model presented by Erdogan et al [1] is one of the most important and, based on this, the long-term decay characteristics of several FBGs can be anticipated.

However, the results predicted by the power-law model are only satisfactory when the annealing tests are applied to normal germanium doped silica fibre. The model cannot explain the major difference in the performance stability of FBGs fabricated into different types of photosensitive fibres. It has been confirmed that the thermal decay characteristics of those UV induced FBGs behave very differently from one to another. Such gratings, for example those written into the boron and germanium codoped silicate fibre, can survive only a comparatively low temperature of about 300 ^{0}C and normally disappear after annealing for hours at temperatures over 350 ^{0}C [2]. Compared with these, FBGs written into several Sn, Sb or In codoped germano-silicate fibres can survive much higher temperatures, of up to 800 ^{0}C [3] [4] or even 900 ^{0}C [5][6]. Clearly, the thermal stability of these gratings is strongly dependent on the glass fibre

composition into which the gratings are embedded. Thus, a further investigation on the decay characteristics of the gratings at high temperatures, as well as the mechanism of fibre photosensitivity, is required to obtain a comprehensive understanding of the grating characteristics at high temperatures and thus to develop novel photosensitive fibres suitable for strong FBG fabrication.

6.1.2 Thermal decay of fibre Bragg gratings

As has been presented, the UV induced FBGs actually reflect a metastable state of the glass given the formation process of the grating; as a result, the grating will decay over time. Gratings written into different types of photosensitive fibres under different conditions normally feature different decay characteristics.

In 1994 Erdogan et al. [1] provided the first detailed report on the grating stability and proposed a model to explain the thermal degradation characteristics of fibre Bragg gratings written into germanium and erbium-germanium codoped silica fibres. The model showed that the decay of the UV-induced index change could be described by a power law function of time with a small exponent (<<1), when they are being annealed over a range of elevated temperatures. The power-law decay model, involving the trapping state distribution, seemed quite satisfactory to account for the experimental results for FBGs written into non-H_2-loaded fibres. However, Patrick et al [7], and Baker et al. [2] reported that gratings written into hydrogen-loaded fibres are less stable than those written into normal photosensitive fibres and their thermal degradation characteristics cannot be accurately predicted by the power-law.

The data used in Erdogan's power-law contained an important parameter termed the integrated coupling constant (ICC). This quantity is proportional to the UV-induced refractive index change of the gratings and is defined by

$$ICC = \tanh^{-1}\left(\sqrt{1-T_{min}}\right) \qquad (6.1)$$

where T_{min} represents the transmission coefficient of the grating at the Bragg wavelength.

Furthermore, a quantity η is defined as the ICC normalized to its value at t = 0 and given the proportionality between the ICC and the UV-induced index change, η is essentially a normalized index change, $\Delta n(t)/\Delta n_0$, with the form

$$\eta = \frac{1}{1 + A(t/t_1)^{\alpha}} \qquad (6.2)$$

where t is time, and t_1 is a unit factor (set to 1 minute) that renders the term dimensionless. A and α are dimensionless and temperature-dependent terms.

By fitting the accelerated aging data, for any grating at a given temperature, to Eq.(6.2), the terms of A and α may be obtained for that temperature. Repeating this procedure as a function of temperature leads to the relation between A, α and T, from which the grating stability can be predicted using Eq.(6.2) for a given temperature and time.

In addition to the power-law decay model, a modified model called the aging-decay curve was also presented to predict the decay behavior of FBGs by Erdogan et al [1]. Such a model is similar to that used to describe dispersive carrier transport in amorphous semiconductors. Carriers are excited by the UV irradiation at around the 5 eV spectrum band and are then assumed trapped in a continuous distribution of energy states, rather than at a single trap level. Then, the decay process of the gratings may be interpreted as involving almost all electrons up to a given trap depth, rather than a fraction of electrons at a single trap, being wiped out by the annealing process. Figure 6.1 shows a simplified diagram for this mechanism. E = 0 is the point where the electrons are free. The thermal releasing of electrons results in the reoccupation of the original deep levels occupied prior to UV excitation. The essence of the theoretical picture is the separation of the distribution of trapped carriers into energies above and below a demarcation energy, E_d, that depends on time and temperature. It is therefore convenient to interpret the experimental data in terms of E_d, where $E_d = k_B T \ln(\nu T)$, and ν is obtained by acquiring multiple data sets as a function of temperature and fitting them together. k_B is the Boltzmann coefficient and T the temperature in kelvin

By fitting the data of the so-called aging decay curve [1], the energy distribution of traps can be obtained, where this is normally a one-peak shaped function.

Such a method is normally effective in processing the problem concerned with gratings written into high germanium-doped photosensitive fibres. However, it has been found that the fitting of the aging decay curve with one peak trap distribution was not satisfactory when processing the data of FBGs written into H_2 or D_2 loaded photosensitive fibres [7][2]. In this circumstance, a so-called isochronical annealing method was also presented and used to evaluate

the thermal stability of the gratings [8]. A two-peak shaped trap energy distribution was finally deduced from the experimental results.

Unfortunately, the work mentioned above did not give any explanation on why a two-peak shaped trap energy distribution existed in the gratings written into D_2 loaded fibres.

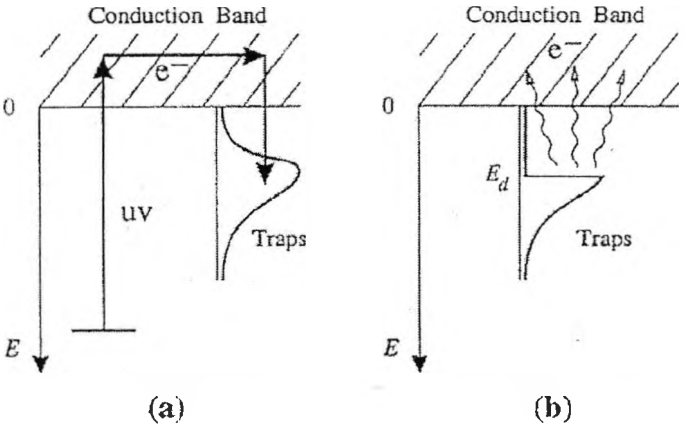

Fig.6.1 Diagram of the proposed physical picture in which (a) electrons excited by UV excitation are trapped in a continuous distribution of traps; and (b) thermal depopulation of the traps at a given time and temperature approximately corresponds to shallower traps ($E < E_d$) being emptied and deeper traps ($E > E_d$) remaining full (After Ref.[1])

6.2 Thermal decay characteristics of strong FBGs showing high temperature sustainability

To meet the requirements of sensing applications at high temperatures, several novel photosensitive fibres have been developed, and further work on the gratings written into these fibres has been carried out recently, as presented in several recent papers [4][5][6] (see Chapter 5 for details). Their thermal decay characteristics have also been investigated and confirmed to be reproducible at high temperatures. It has also been found that the thermal decay characteristics of these gratings, as will be presented in the following section, deviate to a significant extent from those predicted by the aging decay curve when a single-peak trap state distribution was applied [1], which was regarded as applicable to those FBGs written into germano-silicate fibres.

6.2.1 Thermal decay test of FBGs

Three types of photosensitive fibres have been developed for the fabrication of strong FBGs by means of the modified chemical vapour deposition (MCVD) method [4], as detailed in Chapter 5. The fibres were antimony doped germano-silicate fibre [5] (Sb-Ge fibre, with doping

concentrations of 5000 ppm of Sb_2O_3 and 12 wt% of GeO_2), indium doped germano-silicate fibre [6] (In-Ge fibre, with 2000 ppm of In_2O_3 and 15 wt% of GeO_2) and the bismuth doped germano-silicate fibre (Bi-Ge fibre, with 5000 ppm of Bi_2O_3 and 15 wt% of GeO_2).

Several samples of these fibres were used in the experiments to fabricate FBGs by exposing them to the UV emission from a KrF excimer laser (Braggstar-500 supplied by Tuilaser AG) at 248 nm through a phase-mask (pitch period: 1060 nm, supplied by OE-Land Inc., Canada). The parameters of the excimer laser used for FBGs writing were: a repetition rate of 200 Hz or 300 Hz, an energy of 12 mJ per pulse (which corresponded to an energy intensity of about 200 mJ/cm^2). The reflectivity of the FBGs written into these fibres was monitored during UV exposure and the writing time was controlled to achieve the highest reflectivity for each sample.

By using the following equation, the refractive index modulation dn can be calculated [9].

$$dn = [\lambda / \pi L n(V)] \cdot \tanh^{-1}(R^{1/2}) \qquad (6.3)$$

where λ is the operating wavelength for a grating length, L, of reflectivity, R, with an overlap function of the fibre, $n(V) = \{1 - [1/2.405 \cdot (\lambda_{cutoff} / \lambda)]^2\}$.

The change in the reflectivity (R) in these gratings for the Sb-Ge and Bi-Ge fibres, as well as the corresponding values of refractive index modulation (dn), with time, are illustrated in Figure 6.2. It is clear that, when different writing time was used for different types of fibres, the gratings can all reach a high reflectivity (of greater than 99%) with a corresponding value of dn of greater than 2.0 x 10^{-4} (a homogeneous grating with a length of 6.5 mm was considered for this computation for simplicity). A typical transmission spectrum of a fabricated FBG written into the Bi-Ge fibre is presented in Figure 6.3.

The FBGs fabricated in this way were then placed loosely in a silica tube and placed in a tube oven to observe their thermal decay characteristics over a period of time, taking results in a series of isothermal steps, starting from 100 ^{0}C, with increments in temperature steps of 100 ^{0}C and an annealing time of 24 hours at each step. The decay of the reflectivity of two FBGs written into In-Ge fibre (with an exposure time of about 15 minutes to the UV laser emission), after those annealing steps, was recorded and illustrated in Figure 6.4. It can be seen that the FBG written using laser parameters of 200 mJ/cm^2 and 300 Hz can sustain a high temperature of 900 ^{0}C for 24 hours and yet still retain a considerable reflectivity (of about 20%).

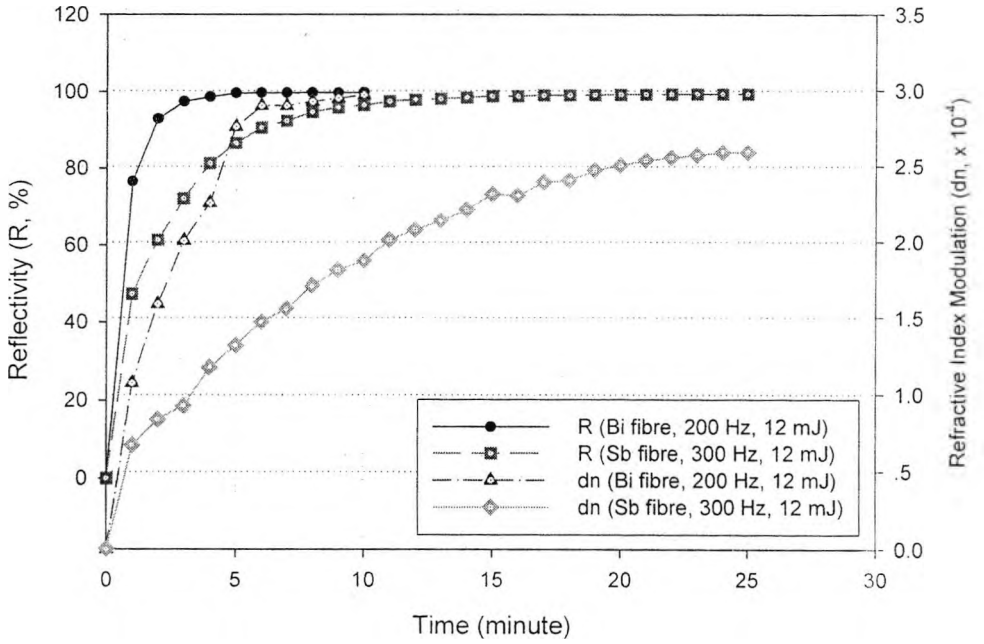

Figure 6.2 Reflectivity (R) and refractive index modulation (dn) increase for FBGs written into Bi-Ge fibre and Sb-Ge fibre when using a UV excimer laser with parameters of 200 mJ/cm^2 per pulse, and repetition rates of 200 Hz and 300 Hz respectively

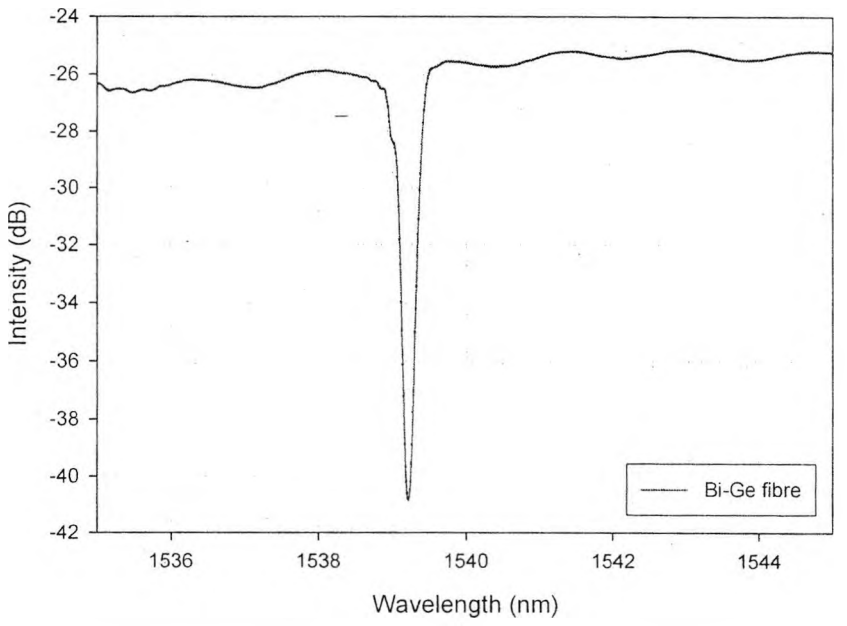

Figure 6.3 Typical transmission spectrum of a fabricated FBG written at 248 nm into Bi-Ge co-doped silica fibre

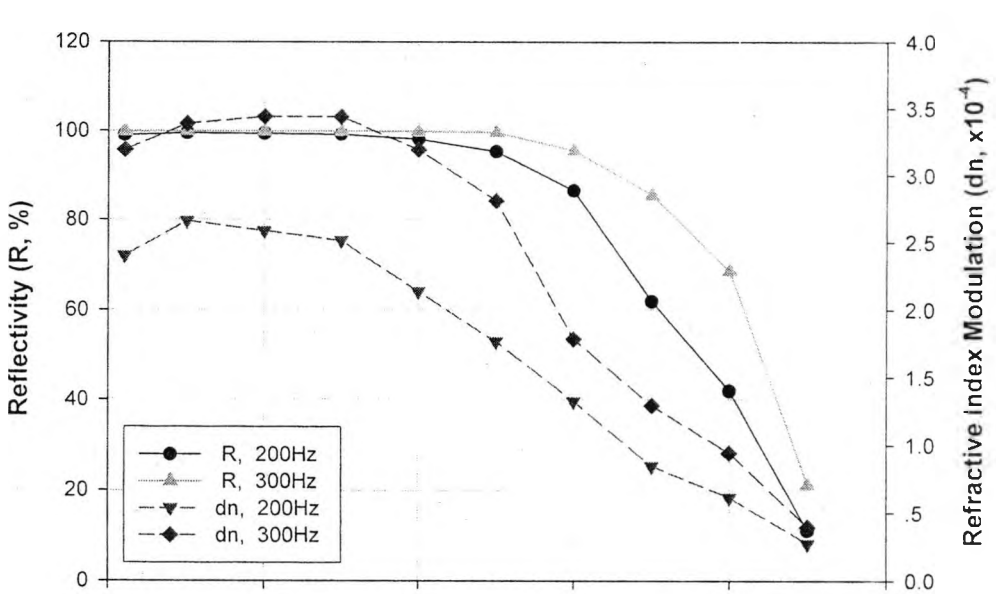

Figure 6.4 Annealing results for two FBGs (with laser parameters of 200 mJ/cm^2 per pulse and repetition rates of 200 Hz and 300 Hz respectively) written into In-Ge fibre, with temperature, from room temperature to 900 ^{0}C, showing the change in reflectivity (R) and the refractive index modulation (dn) with temperature. For each data in each curve, the annealing period is 24 hours.

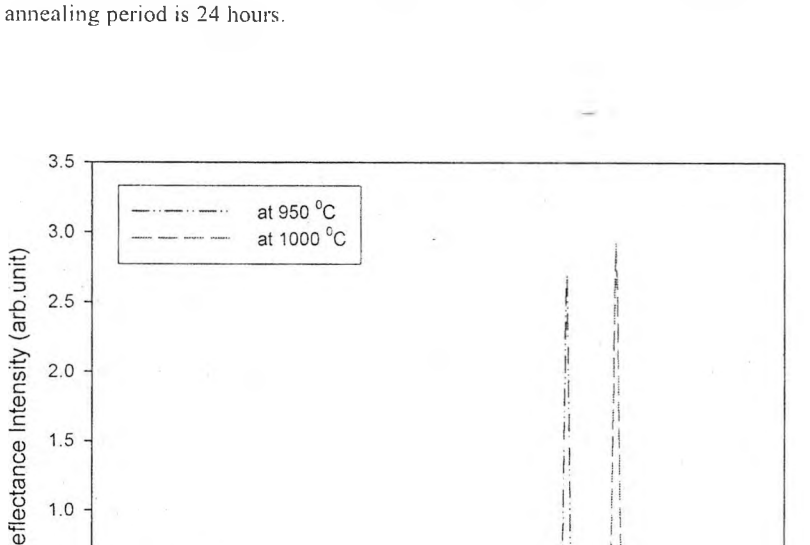

Figure 6.5 Reflectance spectra of an FBG written into In-Ge fibre with parameters of 200 mJ/cm^2 per pulse and a repetition rate of 300 Hz, at temperatures of 950 ^{0}C and 1000 ^{0}C

The experimental results on the tests carried out on the FBGs shown above clearly indicated that the gratings fabricated in Bi-Ge, In-Ge and Sb-Ge fibre had a much high temperature sustainability than those in the Ge doped fibre. They could still retain a particular value of reflectivity after annealing at 900 ^{0}C for over 24 hours [5][6], while similar tests on the FBGs from high germanium doped silica fibre (Ge fibre) showed a highest temperature of only 700 ^{0}C [10]. The reflection spectrum of the FBG written into the In-Ge fibre (the same gratings as mentioned above), after annealing at 950 ^{0}C and 1000 ^{0}C, is illustrated in Figure 6.5. It is clear that the peak wavelength of the reflection (essential for use in sensor systems) can readily be determined.

The annealing results for the gratings shown above clearly indicate that the doping of several Bi^{3+}, In^{3+} and Sb^{3+} ions is highly relevant to the temperature sustainability of the gratings written into the corresponding photosensitive fibres. In addition to this, the writing conditions of the gratings also play an important role in determining their high temperature sustainability.

In Figure 6.6, the decay characteristics of three gratings written into Sb-Ge codoped fibre are illustrated. The gratings were fabricated by exposing the fibre to the excimer laser emission through a phase mask in a condition of energy density 200 mJ/cm^2 per pulse and repetition rates of 100, 200 and 300 Hz respectively. The temperature sustainability of the gratings was then tested by putting them into a silica tube and placing them in a tube oven for annealing. Results were taken in a series of isothermal steps with an annealing time of 24 hours at each step. For comparison, results for a grating written into tin doped fibre are also illustrated.

It is found that the temperature sustainability of these gratings written into the Sb/Ge fibre was especially good. Even after annealing at 900 ^{0}C for 24 hours, a large value of reflectivity (18.5%) still remained for the grating written at a 300 Hz repetition rate, compared to 11.0% and 3.9% for the FBGs written at 200 Hz and 100 Hz repetition rate respectively.

The gratings were then further annealed at 950 ^{0}C to test their performance. The reflectivity of the grating written at 300 Hz repetition rate was recorded over a period of 8 hours, showing a reflectivity of 3.4% still remained. After annealing at 950 ^{0}C for 20 hours, the reflection peak could still be interrogated readily.

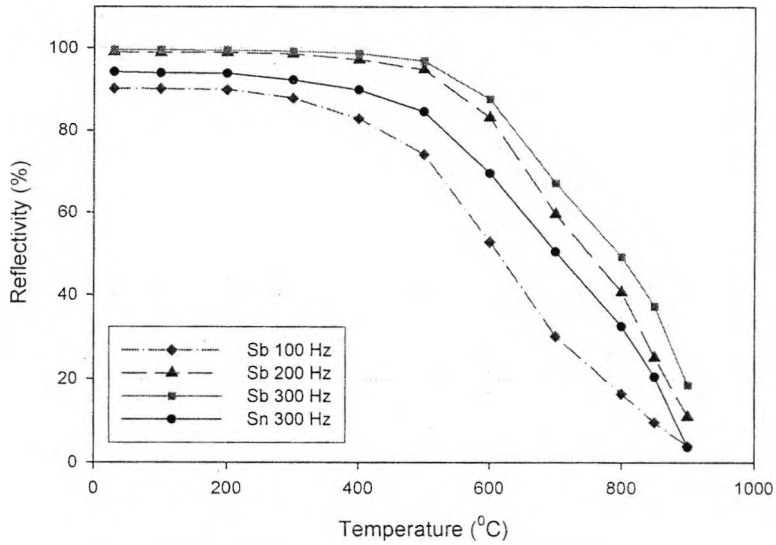

Figure 6.6 Annealing results for FBGs written into Sb/Ge fibre with temperature, in an oven operating from room temperature to 950 ^{0}C, compared with a FBG written into a Sn doped silica fibre under the same experimental conditions. For each data in each curve, the annealing period is 24 hours

6.2.2 Discussion on temperature sustainability of the gratings

In light of the results obtained above, several possible mechanisms for the annealing decay of the FBGs were analyzed. In Figure 6.7(a), the decay of the value of dn, corresponding to these FBGs written in a condition of energy density 200 mJ/cm^2 per pulse and repetition rates of 100, 200 and 300 Hz respectively is demonstrated, and it is clear that the "stronger" the initial grating, the greater the value of dn after annealing. Dividing the values of dn for the FBGs written at 300 Hz and 200 Hz by the corresponding dn of the FBG written at 100 Hz at the same temperature, yields the ratios illustrated in Figure 6.7(b). The curves are almost flat at temperatures below 800 ^{o}C, but deviate upward at 800 ^{o}C and higher temperatures. Assuming the decay model of distributed trap states [1] is applicable here, these results indicate that there are more deep-trap states involved with the FBG written at a higher repetition rate, while the distribution of low-trap states is almost the same. By further comparing the results obtained from the Sn fibre in this work and the Sb/Er/Ge fibre previously reported (with Ge concentration of about 15 wt% [4]), the following conclusions could be reached. The higher the Ge concentration involved in the fibre, the poorer is the temperature sustainability of an FBG written into that fibre; and the bigger the cation size in the doping composition creating the photosensitivity, the greater is the temperature sustainability of the FBG written into the fibre (the cation sizes of B^{3+}, Ge^{4+}, Sn^{4+} and Sb^{3+} are 23

pm, 53 pm, 71 pm and 76 pm respectively [11]). Further, the higher the repetition rate of the laser light used for writing the grating (with the same energy per pulse), the "stronger" is the FBG created and the better is the high temperature sustainability of the FBG, and the higher the laser energy per pulse, the "stronger" is the FBG and the better is the temperature sustainability of the FBG.

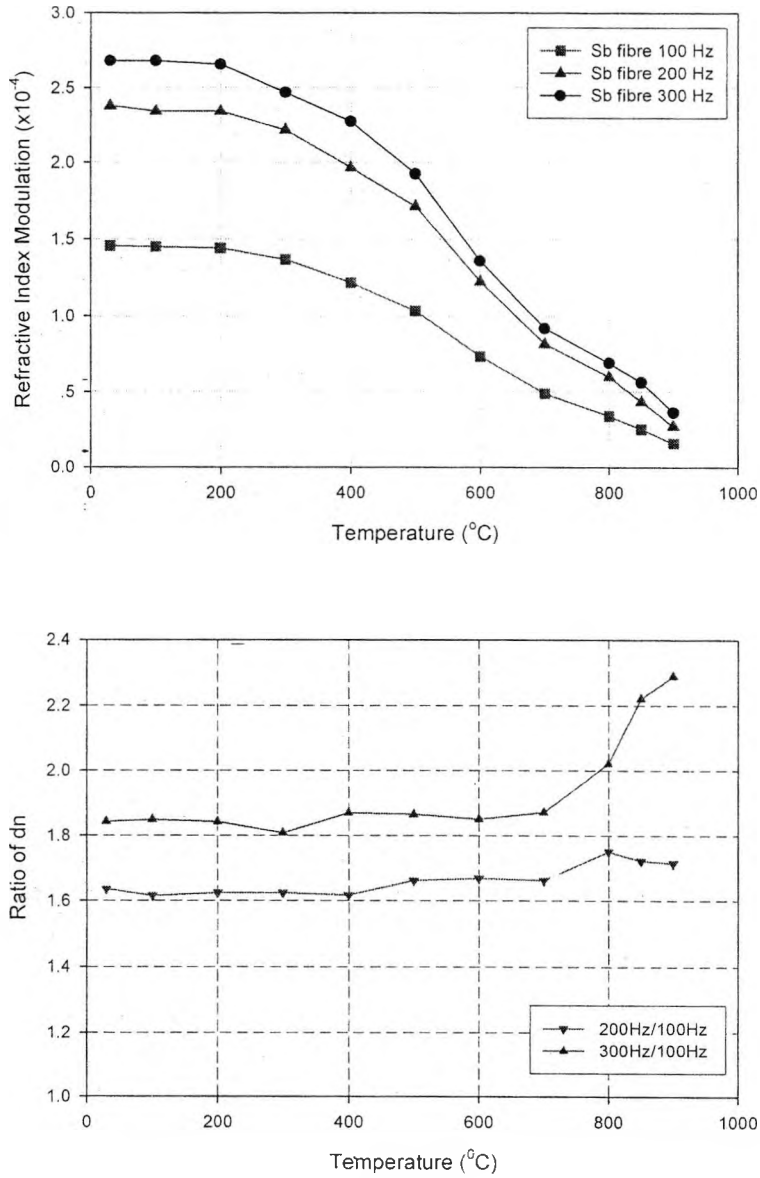

Figure 6.7 (a). Decay of the refractive index modulation (dn) of FBGs written into the Sb/Ge fibre after annealing at different temperatures. The annealing time was 24 hours at each temperature. (b) Ratio of dn after annealing. The ratio was obtained for dn in the FBGs written at 300 Hz and 200 Hz when divided by dn for the FBGs written at 100 Hz

6.3 Decay mechanism of the high temperature sustainable FBGs during annealing at high temperature ------ Cation Hopping Model

6.3.1 Cation-hopping model

By further analysis of the experimental results from the FBG writing and annealing as shown above, and comparing the results of the FBG decay characteristics of different types of photosensitive fibres, a model involving so-called *cation hopping* has been presented to account for the superior high temperature sustainability of these gratings written into Sb/Ge and In/Ge fibre.

That means, the so-called trapping states reported in [1] may mainly be concerned with cations and the distribution of trap states may result from the distribution of the cations "hopping away" from their original positions during FBG writing. During annealing, the decay of the FBG occurs due to the effect of cation diffusion that leads the cations to return to their initial places, under high temperature excitement. In such a model, the hopping of cations occurs through a defect mechanism. These defects can be vacant lattice sites or interstitial ions not in a normal site. Obviously, the cation hopping model can be used to explain the significant differences in the temperature sustainability of the FBGs written into those different types of fibres, if it is noted that the different sizes of the cations doped in the fibres would result in a different hopping movement in each case (the cation sizes of B^{3+}, Ge^{4+}, Sn^{4+}, Sb^{3+}, In^{3+} and Bi^{3+} are 23 pm, 53 pm, 71 pm, 76 pm, 80 pm and 104 pm, respectively [11]). The bigger the cation size, the more difficult the hopping movement would happen. Also, the effect of Ge concentration on the photosensitivity of the fibre may result from the fact that a higher Ge concentration always results in more defects and thus a higher level of photosensitivity. For the difference in dn with FBGs written using different laser repetition rates, the rise of temperature due to the absorption of the laser emission may possibly be an important factor affecting the characteristics of the FBGs written as there would exist more defect sites in the fibre at higher temperatures.

It is clear that the decay mechanism of the FBG during annealing is closely related to the formation mechanism of the UV-excited FBG. Thus the hopping of cations during UV exposure seems likely to be a main factor in FBG fabrication, which relates closely to the viewpoint of the ionic migration model explaining the formation of FBG, as presented by Lawandy [12]. Such an explanation is not inconsistent with the widely accepted compaction/densification model [13,14]

as the process of cation hopping may result in compaction and then the photoelastic-induced index changes in fibre Bragg gratings.

6.3.2 Cation-oriented trap distribution model for the aging decay analysis of gratings

As is mentioned earlier, the aging decay analysis with one-peak shaped trap energy distribution is not satisfactory for the gratings written into In^{3+}, Sb^{3+} or Bi^{3+} codoped germano-silicate fibres, similar to the situation for gratings written into D_2 loaded fibres [8]. To address this problem more clearly, a cation–oriented trap distribution model is proposed in this work and then applied to account for the experimental results obtained in the thermal decay analysis of these gratings in this section. The simulation based on this model gives better agreement between the experimental data and those computed from the model, when compared with the results obtained using the model as presented by Erdogan et al [1]. This will give us a better understanding of the physical mechanisms involved during annealing of the gratings, as well as the formation of UV induced fibre gratings.

In accordance with the *cation hopping* model outlined above, the refractive index modulation (dn) of the FBGs should be related to the cations responsible for the photosensitivity of the fibres, for example, the Sb^{3+} and Ge^{4+} dopants in Sb-Ge fibre. Using the aging decay curve method (as presented by Erdogan et al [1]), the trap distribution of the gratings written into these fibres can be computed by simulating the decay data of the gratings recorded during annealing if a single-peak trap state distribution is assumed. This distribution can then be used to anticipate the possible decay characteristics of the gratings. Unfortunately, when the parameters of the actual annealing process (the duration time of annealing at each temperature) are used, the decay of the grating computed from simulation is found to match the actual decay results rather poorly (as discussed later in Section 6.3.3). This situation is especially evident with the Bi-Ge fibres.

Being consistent with the *cation-hopping* model in physical essence, a simulation based on the cation-oriented trap distribution model gives better agreement with the experimental data, as follows. In the model, it is assumed that the traps concerned with the photosensitivity of the fibres are directly related to the cations doped in the host. For the Sb-Ge fibre, for example, there are two groups of trap distributions related to the Sb^{3+} or Ge^{4+}; while for the Bi-Ge fibre, the two groups of trappings are related to Bi^{3+} and Ge^{4+}.

Referring to the approach used by Erdogan et al [1], the integrated coupling constant (ICC) is also used in this work and is normalized (as η) to its initial value at t = 0. Because the value of ICC is proportional to the UV-induced index change, η can also be thought of as the normalized index change.

By further defining the trap distribution as $g_1(E)$ and $g_2(E)$ with $g_1(E)$ representing the Ge^{4+} related traps and $g_2(E)$ the Sb^{3+} or Bi^{3+} related traps, and the mean occupation number at energy E, and time t, as $f_1(E,t)$ and $f_2(E,t)$ respectively, the traps are thermally depopulated in an exponential fashion and this can be written as

$$f_1(E,t) = f_1(E)\exp[-\nu_1(E)\cdot t] \quad \text{and} \quad f_2(E,t) = f_2(E)\exp[-\nu_2(E)\cdot t] \tag{6.4}$$

where $\nu_1(E)$ and $\nu_2(E)$, and the release rates from the state of energy E, are given by

$$\nu_1(E) = \nu_1 \exp\left(-\frac{E}{k_B T}\right) \qquad \text{and} \qquad \nu_2(E) = \nu_2 \exp\left(-\frac{E}{k_B T}\right) \tag{6.5}$$

in which k_B is the Boltzmann constant, T the absolute temperature in kelvin.

In a similar way to the approach shown in reference [1], two demarcation energies E_{d1} and E_{d2} can be used to divide the trap distribution states. When $E > E_{d1}$ (or $E > E_{d2}$), the trap states remain occupied; otherwise they are thermally depopulated. The two energies involved are $E_{d1} = k_B T \ln(\nu_1 t)$ and $E_{d2} = k_B T \ln(\nu_2 t)$ if the traps are divided approximately by $\nu_1(E_{d1})t = 1$ and $\nu_2(E_{d2})t = 1$, according to equation (6.5).

In this way, the total number of trapped cation charges remaining, at time t, is given by

$$N(t) = N_1(t) + N_2(t) = \int_0^\infty g_1(E) f_1(E,t) dE + \int_0^\infty g_2(E) f_2(E,t) dE \tag{6.6}$$

where $N(t)$, the total numbers of cation charges, is assumed to be proportional to the UV-induced refractive index change.

When E_{d1} and E_{d2} are used, $N(t)$ can be rewritten as

$$N(t) = N_1(t) + N_2(t) = \int_{E_{d1}}^\infty \bar{g}_1(E) dE + \int_{E_{d2}}^\infty \bar{g}_2(E) dE \tag{6.7}$$

where $\bar{g}_1(E) = g_1(E) f_1(E,t)$, $\bar{g}_2(E) = g_2(E) f_2(E,t)$

Thus, it is clear that by computing the $\bar{g}_1(E)$ and $\bar{g}_2(E)$ distributions at an activation

energy E, the sum of the normalized refractive index modulation η can be computed.

6.3.3 Simulation of the experimental data by means of the cation-oriented trap distribution

By using the cation-oriented trap distribution model as outlined in section 6.3.2, the experimental data measured from a series of FBG annealing tests were used to simulate the FBG performance during annealing. This was carried out by computing two sets of cation-oriented trap energy distributions separately, with one set corresponding to Ge^{4+} and another to Sb^{3+} or Bi^{3+}.

For convenience in the computation, the following assumption is made. The Ge^{4+} oriented trap distribution will be recovered or vanish after annealing over 800 ^{0}C for several hours. Such an assumption is reasonable if it is noted that the FBGs written into germano-silicate fibre (including type I and type IIA gratings) will inevitably disappear after annealing at 750 ^{0}C for several hours. Thus, the dn value which remains after such an annealing is entirely attributed to the Sb^{3+} or the Bi^{3+} ions. The procedure for the aging decay analysis of the FBGs written into the Bi-Ge fibre can be seen in Figure 6.8. The first step in this was to compute the Bi-oriented trap distribution by considering the aging decay of the FBG at temperatures over 800 ^{0}C (using only the data obtained at temperatures above 800 ^{0}C, after annealing at 800 ^{0}C for several hours). Then, according to this, the corresponding components of the refractive index modulation at lower temperature, which is considered to be Bi^{3+} oriented, can be computed (as shown in the dotted extend curve in Figure 6.8). Because the refractive index modulation is attributed to two groups of trap distributions at low temperature as depicted in Equation (6.7), the components corresponding to the Ge^{4+} ions can be obtained by subtracting these components from the combined aging decay curve obtained from the experimental data. This can, in turn, be used for the computation of the Ge^{4+} related trap energy distribution.

Thus in this way, the cation-oriented energy distributions, as presented in Figure 6.9a for the Sb-Ge fibre and in Figure 6.9b for the Bi-Ge fibre, can be obtained. It should be pointed out that the same value of 1.0 x 10^{15} was used for parameters ν_1 and ν_2 in Equation (6.4) for these computations. The use of same ν_1 and ν_2 values is mainly for the scaling consideration, which gives a more readable picture in trap energy scale and enables the same demarcation energy E_d be used (that is $E_{d1} = E_{d2} = E_d$). This is also reasonable if the same silica host involved with the doped cations is used in photosensitive fibres. As some change in ν_1 and ν_2 value will not significantly

change the relative shape of trap energy distribution computed and have little effect on the results of simulation, such a choice in ν_1 and ν_2 value is suitable. In this way, the trap energy distribution of Ge^{4+} and Bi^{3+} (or Sb^{3+}) can then be put together for comparison.

Using the energy distribution obtained as shown in Figure 6.9, the decay process of the FBGs can be simulated and the results are illustrated in Figures 6.10a and 6.10b, for FBGs written into the Sb-Ge fibre and the Bi-Ge fibre, respectively. For comparison, several different methods were also used in the simulation. They are the normal simulation method, using the aging decay when considering the trap distribution as a whole single-peak shaped and between them, the first utilized the data over the whole temperature range (from room temperature to 900 ^{0}C — denoted as "whole T simulation") while the second only utilized the data below 600 ^{0}C (denoted as "lower T simulation"). It is clear that the first method has taken into consideration the combined effect of both the lower and the higher temperature region, while the second has only shown the effect of the lower temperature region.

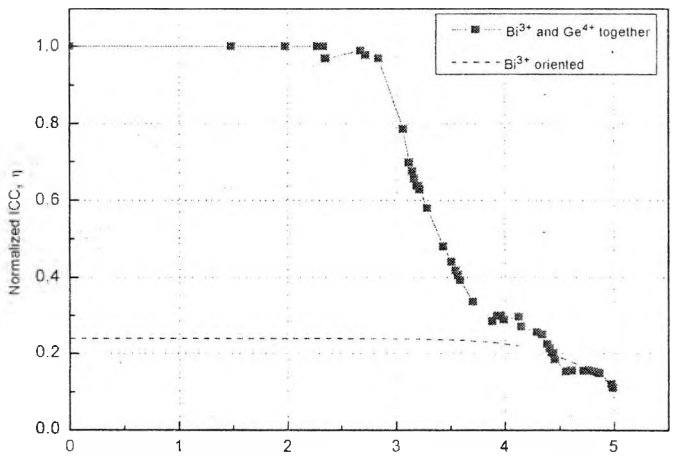

Figure 6.8 Demonstration of the two-stage aging decay curve for the computation of cation-oriented trap distributions. The aging decay curve at temperature over 800 ^{0}C was considered to be only related to Bi^{3+} while that at lower temperatures consisted of two parts, corresponding to Ge^{4+} and Bi^{3+} respectively.

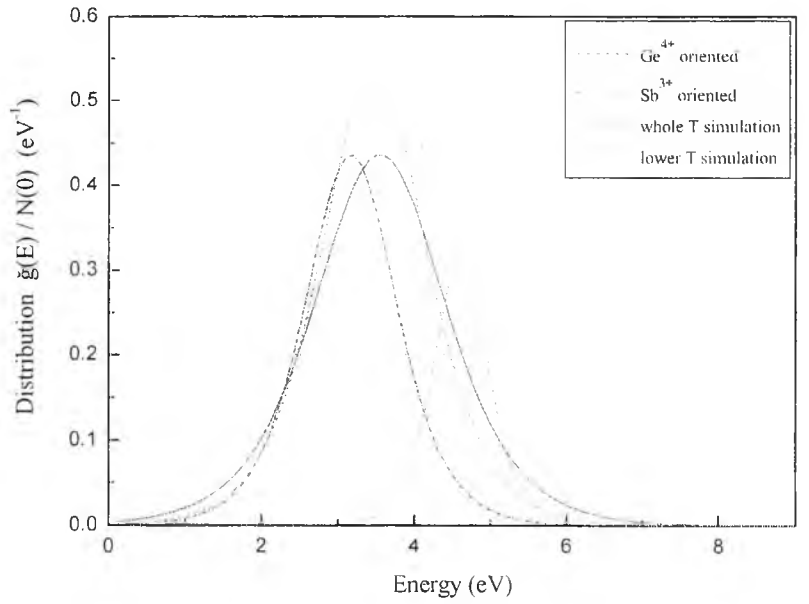

(a)

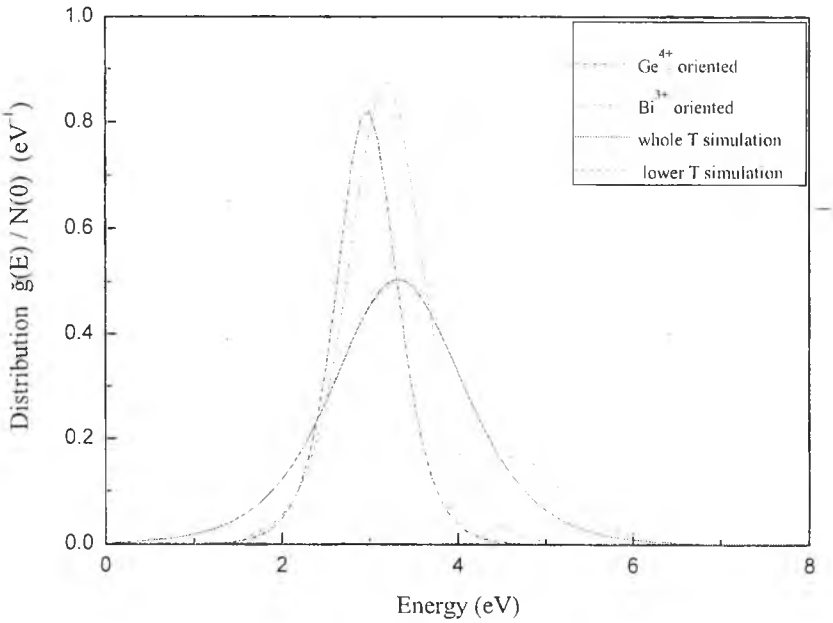

(b)

Figure 6.9 Cation-oriented trap energy distribution for FBGs written into Sb-Ge fibre and Bi-Ge fibre.. For comparison, the trap energy distributions of the FBG when simulated by use of the normal aging decay approach are also illustrated. The curve labeled "the whole T" stands for the result simulated with data for all temperatures, while the curve labeled "the lower T" stands for that obtained by using only data obtained below 600 ^{0}C, with (a) Sb-Ge fibre and (b) Bi-Ge fibre

From the simulation curve presented in Figure 6.10, several important points can be observed. The first is that the cation-oriented simulation gives the best fit to the experimental data. This is especially obvious for the case of the Bi-Ge fibre. The second point is that "the lower T simulation" fits the experimental data very well at temperatures below 600 ^{0}C, but deviates significantly at higher temperatures. This is thought reasonable as the annealing effect at lower temperature is considered to result mainly from the Ge^{4+} oriented distribution. The third point is that all the simulation curves significantly deviate from the experimental data at temperatures around 700 ^{0}C and 950 ^{0}C – a phenomenon for which an explanation is not readily forthcoming and this is the subject of on-going work.

Using the same method presented above, the applicable lifetime of some FBGs at specific temperatures can be easily predicted. In Figure 6.11, the anticipated decay process of an FBG written into Bi-Ge fibre is shown when the grating is annealed at 500 ^{0}C for over 150 hours. In this case, a similar cation-oriented trap distribution is assumed as shown above. As expected, it is clear that the simulated data fit the experimental results quite well.

Because the computation for the cation-oriented trap distribution requires only the data both above 800 ^{0}C and below 800 ^{0}C, thus, for ease of practical operation, only two stages of annealing processes are required to predict the sustainable lifetime of these types of strong FBGs at certain temperatures. One stage should be above 800 ^{0}C while another can be lower than 600 ^{0}C.

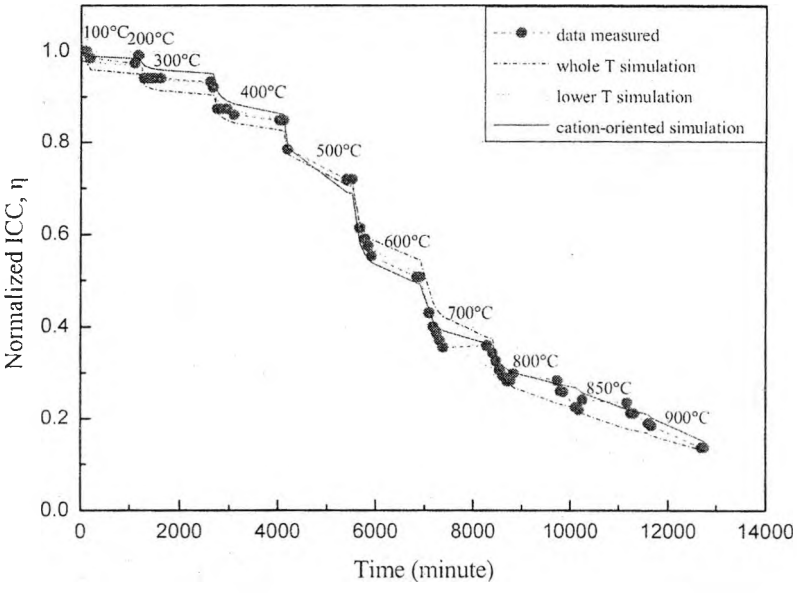

(a)

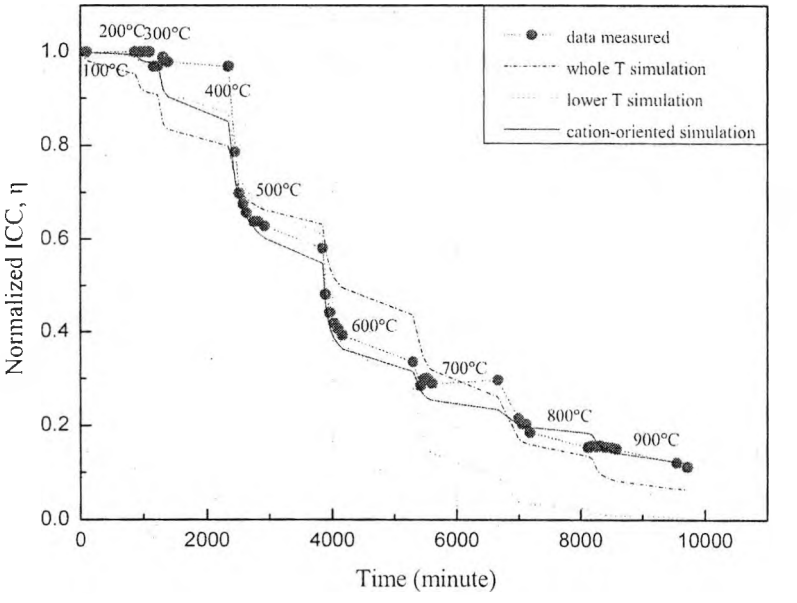

(b)

Figure 6.10 Simulation results of the FBGs when annealed step by step. When compared with the actual decay data, it can be seen that the cation-oriented simulation gives a better fit over the whole temperature range, (a) for FBGs written into Sb-Ge fibre and (b) for FBGs written into Bi-Ge fibre

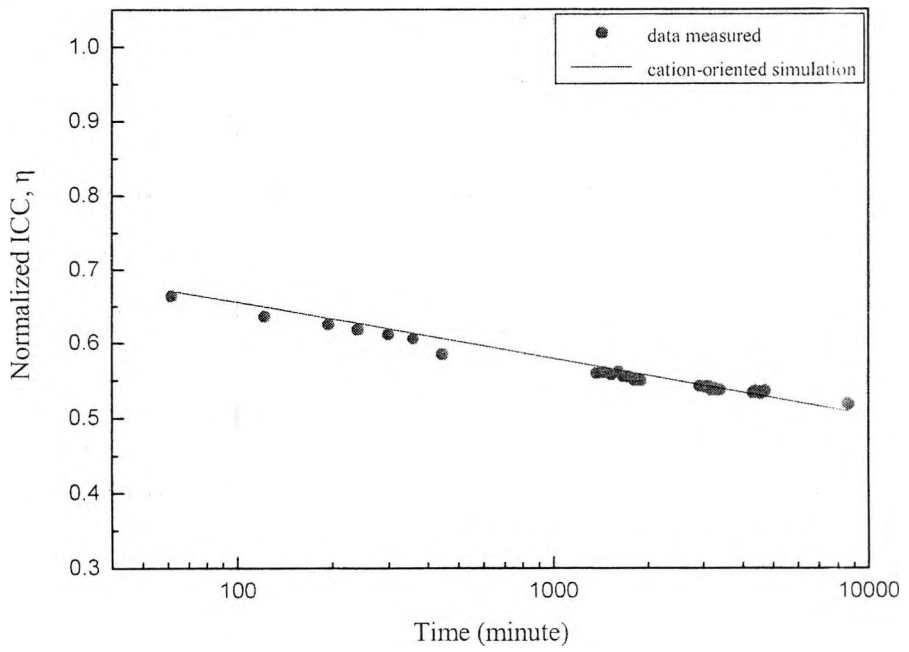

Figure 6.11 Annealing decay of a grating written into Bi-Ge fibre at 500 ^{0}C for over 150 hours, showing the consistency between the anticipated data and the experimental results

6.3.4 Discussion

The results obtained and shown in Sections 6.3.2 and 6.3.3 indicate that the simulation based on the cation-oriented trap distribution model can provide a better fit to the experimentally-observed decay curves than before. This is especially evident where the Bi-Ge fibre is concerned, in which the cation, Bi^{3+}, is as large as 104 pm [11]. Clearly, such a result is consistent with the cation hopping model, associated with the photosensitivity of the fibre and the corresponding decay of the FBGs written into it.

It should be noted that deviations were seen between the simulation and the measured decay curves, at temperatures of about 700 ^{0}C and 900 ^{0}C. As these two temperatures are actually the upper limit temperatures for FBGs written into Ge fibre and Sb-Ge fibre (or Bi-Ge fibre) to survive, it is believed they are related to a particular mechanism involved in the decay of FBGs. In the tests performed in this work, the fibres all include Ge^{4+}, in addition to another cation, so these deviations may also be contributed by the decay of the cation-oriented grating components. A full understanding of these phenomena is being sought to enable the development of higher

temperature sustaining fibres.

In light of this, it should be valuable to reconsider the decay behaviour of the FBGs written into other photosensitive fibres, such as boron codoped germano-silicate fibres or even hydrogen loaded fibres, as cation-oriented traps may play a similar role in the FBG decay and thus lead the decay to deviate from the characteristic of a power-law decay process described by other researchers [2][7]. It is possible to believe that the dual-peak shaped trap energy distribution of the gratings written into D_2 loaded fibres [8] may be regarded as D^+ and Ge^{4+} oriented traps respectively.

Based on this work, it should be possible to design and develop several advanced photosensitive fibres with a better performance in their photosensitivity characteristics and thus to fabricate several superior FBGs with excellent high temperature sustainability, using such fibres. A promising candidate material is Bi^{3+} doped fibre and the optimization of the parameters of such photosensitive fibre is continuing with this purpose.

6.4 Summary

The high temperature sustainability of FBGs is especially important in applying FBGs to the sensing fields covering a wide range of temperatures. It is clear now that this sustainability is strongly dependent on the compositions of the photosensitive fibre into which the FBG is embedded. Doping of several large cations with an unfilled shell charge structure seems beneficial to the sustainability of the FBG fabricated. In addition to this, the fabricating conditions of the FBG also play an important role in creating a strong FBG.

To explain the decay characteristics of gratings written into several recently developed photosensitive fibres, a theoretical model, named Cation Hopping, has been proposed. Based on this model, it is possible to develop some better photosensitive fibres with higher photosensitivity while the gratings written into them can sustain a substantial high temperature up to 800 ^{0}C or 900 ^{0}C. By using the cation-oriented trap-distribution model, the long-term performance of the gratings may be better anticipated. It is also expected that the co-doping of more Bi_2O_3 into the silica host while decreasing the GeO_2 concentration simultaneously may result in a novel photosensitive fibre with better performance.

6.5 References

[1] T. Erdogan, V. Mizrahi, P.J. Lemaire and D. Monroe, "Decay of ultraviolet-induced fibre Bragg gratings," J. Appl. Phys., 76, pp73-80 (1994)

[2] S. R. Baker, H. N. Rourke, V. Baker and D. Goodchild, "Thermal decay of fibre Bragg gratings written in boron and germanium codoped silica fibre," IEEE J. Lightwave Technology, 15, pp1470-1477 (1997)

[3] G. Brambilla, V. Pruneri and L. Reekie, "Photorefractive index gratings in SnO_2:SiO_2 optical fibres", Appl. Phys. Lett., 76, pp807-809 (2000)

[4] Y. Shen, T. Sun, K.T.V. Grattan and M. Sun, "Highly photosensitive Sb/ Er/Ge codoped silica fibre for fibre Bragg grating (FBG) writing with strong high-temperature sustainability," Optics Letters, 28, pp2025-2027 (2003)

[5] Y. Shen, J. He, T. Sun and K.T.V. Grattan, "High temperature sustainability of strong FBGs written into Sb/Ge co-doped photosensitive fibre — decay mechanisms involved during annealing", Optics Letters, 29, pp554-556 (2004)

[6] Y. Shen, J. Xia, T. Sun and K.T.V. Grattan, "Photosensitive Indium doped germano-silica fibre for strong FBGs with high temperature sustainability", IEEE Photonic Tech. Lett., 16, pp1319-1321 (2004)

[7] H. Patrick, S.L. Gilbert, A. Lidgard and M.D. Gallagher, "Annealing of Bragg gratings in hydrogen-loaded optical fibre," J. Appl. Phys., 78, pp2940-2945 (1995)

[8] J. Rathje, M. Kristensen, and J.E. Pedersen, "Continuous anneal method for characterizing the thermal stability of ultraviolet Bragg gratings", J. Appl. Phys., 88, pp1050-1055 (2000)

[9] A.Othonos and K. Kalli, "Fibre Bragg Gratings: Fundamentals and applications in telecommunications and sensing", Artech House, Boston (1999)

[10] Y. Shen, S. Pal, J. Mandal, et al, "Investigation on the photosensitivity, temperature sustainability and fluorescence characteristics of several Er-doped photosensitive fibres", Optics Communications, 237, pp301-308 (2004)

[11] A. M. James and M.P. Lord, Macmillan's Chemical and Physical Data, The MacMillan Press Ltd. (1992)

[12] N.M. Lawandy, "Light induced transport and delocalization in transparent amorphous systems," Optics Communications, 74, pp180-184 (1989)

[13] M. Douay, W.X. Xie, T. Taunay et al, "Densification involved in the UV-based photosensitivity of silica glasses and optical fibres," IEEE J. Lightwave Technology, 15, pp1329-1342 (1997)

[14] H.G. Limberger, P.Y. Fonjallaz, R.P. Salathe and F. Cochet, "Compaction- and photoelastic-induced index changes in fibre Bragg gratings," Appl. Phys. Lett., 68, pp3069-3071 (1996)

Chapter 7: Industrial Applications of the Fluorescence-based Fibre Thermometer and FBG-based Thermometer

As were presented in Chapter 2 of this thesis, fibre-optic sensors feature high-sensitivity, immunity to electro-magnetic radiation and long lifetime in harsh environment. The fibre-optic thermometer is one type of modern instrument that can be used to measure temperature accurately in a variety of environments. For most applications, thermocouples are adequate – for some, especially where there are issues of intrinsic safety, high levels of e.m. interference or where thermocouples offer a poor lifetime due to the excessive temperature, a fibre optic probe may be the preferred solution. Such sensors are immune to the interfering effects of electro-magnetic radiation (often not the case with thermocouples) and may be lighter in weight and more durable in use.

Fibre-optic thermometers, based on both the fluorescence characteristics of materials [1] and the wavelength dependence of fibre Bragg gratings (FBGs) [2], are most important in industry and scientific research. The works on the related characteristics of materials and systems have been detailed in the earlier parts of this thesis. Their performance in industrial situations was also evaluated and the related work is reported in this chapter. Furthermore, as an important application of fibre-optic thermometer, heat-flux measurement was carried out by using the fluorescence-based fibre thermometer and the FBGs-based fibre thermometer separately, which shows the possibility and potential of fibre-optic sensors in various types of sensing fields.

7.1 System evaluation of the fluorescence-based fibre thermometer at Corus, UK

Fibre thermometry based on the temperature dependence of the fluorescence lifetime of Tm:YAG garnet has been developed at City University [3][4]. A detailed performance evaluation and calibration has been performed in the laboratory, as reported in Chapter 4 of this thesis. It is clear that the thermometer developed can work stably at high temperatures up to 800 ^{0}C, or even 1200 ^{0}C (when a ceramic tube is used as the probe protector), for a long period. With the help of this characteristic, the system may be suitable in monitoring the performance of several refractory linens in the steel industry, where real-time monitoring and reliable control of steel furnaces is particularly important.

To prove the suitability of this type of fibre thermometer in the practical industrial field, the fibre thermometer developed was evaluated at Corus, Teeside Technology Centre, Middlesborough, Middlesborough, UK. The evaluation was carried out by comparing the performance of the fibre thermometer with a normal K-type thermocouple when they were both inserted into the inside of a refractory brick, which was the same type used currently in steel furnace as lining. The refractory brick was placed in an oven and heated up gradually by the surrounding high temperature environment. With such a configuration, the temperature inside the brick was initially lower than the environment and thus, the heat would flow in from outside due to the temperature difference. As a result, the temperature inside the brick where the probes were situated would gradually rise until an equilibrium state was reached, if sufficient time was given. After that period, the oven power was turned off, the surrounding oven temperature dropped quickly and thus resulted in an opposite heat flux. It means that the heat would gradually flow out from inside of the brick and as a result, the temperature inside the brick would become lower. As a refractory brick with high quality was used in the experiment, the process of heat flowing in or out takes a long time. To expedite the evaluation of the dynamic performance of the system, both the probes of the fibre thermometer and the thermo-couple were taken out from the brick and then put into the brick again quickly on two separate occasions during the whole process. The data obtained from the fibre thermometer and the thermocouple were all recorded in a laptop computer with time for comparison. A photograph of measurement setup is shown in Figure 7.1.

Two separate cycles of tests were performed and the results were recorded. In Figure 7.2, the temperature variations measured from the fibre thermometer and the thermocouple are illustrated with time. It is clear that the curves by the fibre thermometer and the thermo-couple are very similar, showing that the two independent temperature measuring devices respond in the same way to temperature changes.

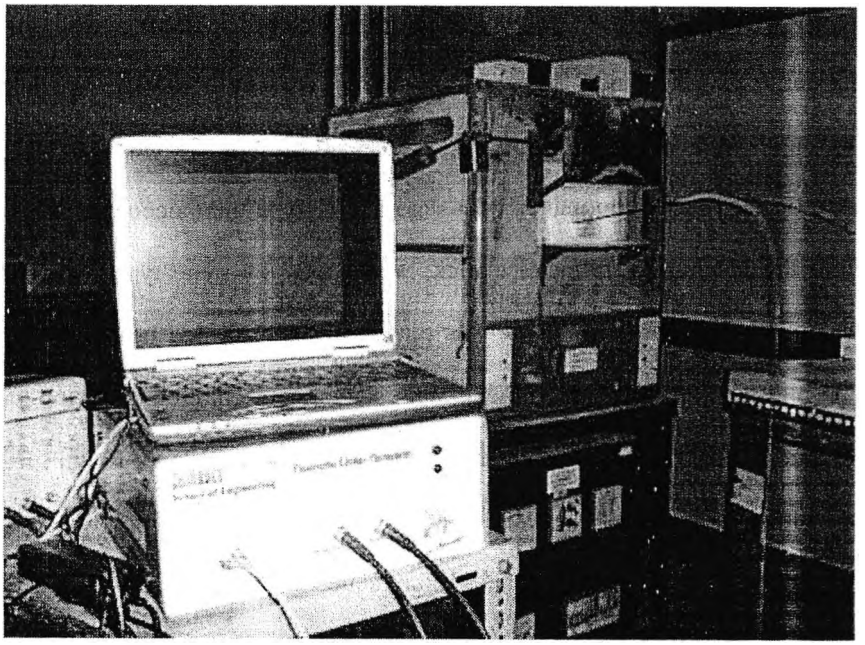

Figure 7.1 Experimental setup of fibre thermometer evaluation in Corus, Teeside Technology Centre

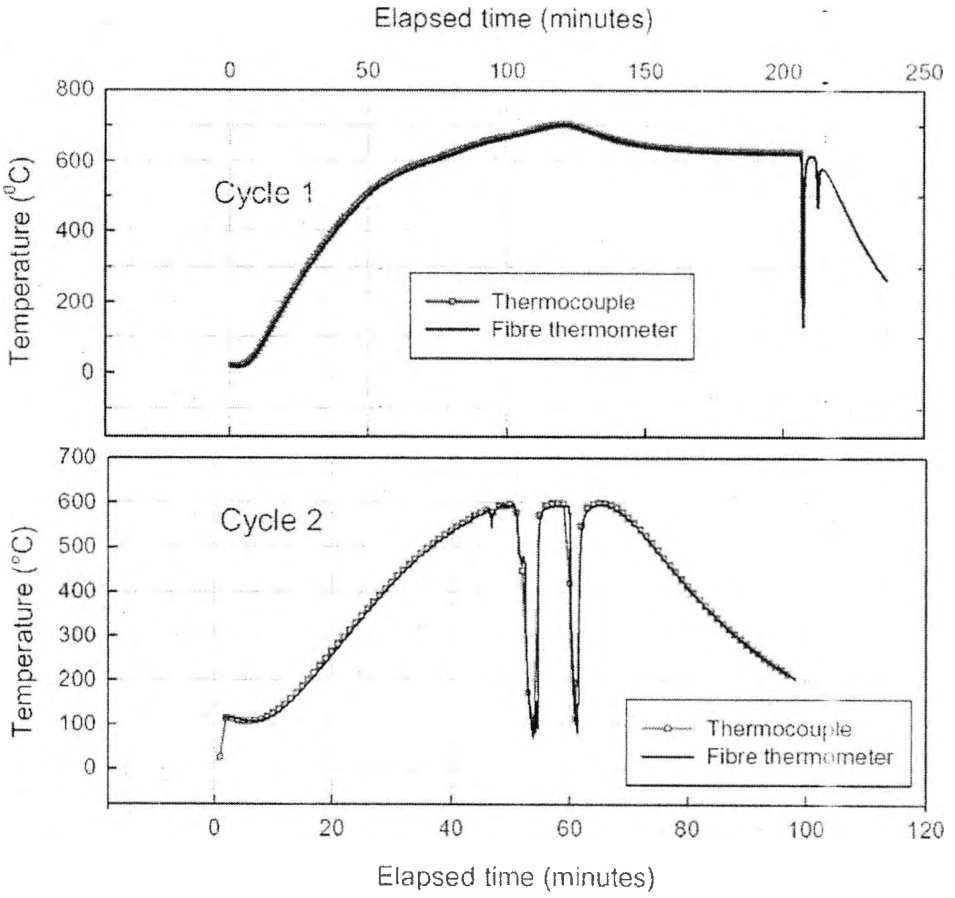

Figure 7.2 Cross-comparison of the output of a fluorescence lifetime-based fibre thermometer with results from a thermocouple (co-located with the optical probe) when they are used for the simultaneous temperature measurement in an insulating refractory brick

7.2 Heat-flux measurement by using the fluorescence-based fibre thermometer and the FBGs-based fibre thermometer

Accurate temperature measurement is important in industry – in chemical plants, in furnaces and kilns, and in a range of situations where the use of higher temperatures enhances a reaction or process. In some circumstances the heat flux, rather than temperature *per se*, is the more important parameter to measure. Heat flux is defined as the energy transition through a unit cross-sectional area normal to the direction of the flux. As it is impossible to measure the energy directly, it is the change in energy that can be monitored by means of the change of its physical state, such as through temperature monitoring. The standard physical method currently available for the measurement of heat flux is based on the monitoring of temperature and many different techniques have been presented and utilized, for example as reviewed by Childs et al [5].

As the research reported in this thesis has concentrated on both FBG-based and fluorescence lifetime-based measurement techniques, the fibre-optic temperature sensors, one based on the fluorescence decay scheme and a second on the scheme involving the peak wavelength interrogation of a fibre Bragg grating (FBG), were both utilized in experiments at the outlet port of a tube oven, to measure the heat flux in the material into which the sensors were placed. The principles of operation of the two sensor types have been discussed in previous chapters. The purpose of these experiments is to test the feasibility of the use of these fibre-optic based sensors for heat-flow measurements in a tube-oven and, further, to simulate their application in the monitoring of the lining of furnaces (for example to monitor the lining lifetime) and in process control such as for cement brick fabrication, where heat flux and energy consumption are critically important.

7.2.1 Introduction to the heat-flux measurement by using fibre-optic sensors

The principle of heat flux measurement used in these experiments involves measuring the temperature difference between two points, separated by a known distance, in a specific medium. The heat-flux can then be calculated by using the following equation

$$Q = - k (T_1 - T_2) A / L \qquad (7.1)$$

where Q is the heat flux, k the conductivity of the medium used, A the cross-sectional area of the medium which conducts heat, L the distance between the two sensing points, and T_1, T_2 are the

temperatures at the two measurement points. The minus sign in equation (7.1) indicates the direction of the heat flux, which is from the high temperature region to the lower temperature region i.e. away from the centre of the oven where the temperature is the highest.

From equation (7.1), for a specific medium with a conductivity k, the heat-flux is directly proportional to the temperature difference between the two points at which the probes are placed. To assess the effectiveness of the medium used, a series of measurements was carried out in experiments using both air and silica powder, and the results obtained were cross-compared.

The apparatus used for the experiments include a Carbolite tube oven, with a maximum achievable temperature of around 1400 ^{0}C, and firstly the use of a fluorescence lifetime-based fibre thermometer system with two fibre-optic probes which can measure the temperature at two positions simultaneously. Secondly a FBG-based probe using a peak wavelength interrogating scheme (with two FBGs of known spacing written into one piece of Sb/Er/Ge co-doped photosensitive fibre [6]), and using an optical spectral analyzer (OSA) for accurate wavelength determination was tested and evaluated.

To monitor the heat-flux across the medium, these two different fibre probe systems were placed in the medium at the same time. The oven was heated up from room temperature to a high temperature (over 1100 ^{0}C) and, after several hours of stabilization, cooled step by step to temperatures of 1000 ^{0}C, 900 ^{0}C, 800 ^{0}C and 700 ^{0}C etc, and back to room temperature. The temperature changes were recorded from these probes using both systems, with time, and the temperature difference thus obtained was used to calculate the heat flux.

7.2.2 Working principle of the fibre optic sensing systems involved

In the experiments carried out in this work, two different types of fibre optic sensors were used, these being the fluorescence lifetime based fibre thermometer [1] and the FBG-based fibre-optic thermometric sensor [2].

A. Fibre-optic fluorescent sensor-based system ? System A

The principle of the fluorescence lifetime based fibre thermometer used here is essentially similar to that previously reported by Shen et al [3], except that there are two probes interfaced with the sensing system in this work, so that the temperatures at two separate points could be measured simultaneously. A schematic of the fibre heat flux sensor (System A) is illustrated in

Figure 7.3. This shows that there were two sets of the phase-locked-detection (PLD) [1] units used in the system, with two fibre pigtailed laser diodes operating at 785 nm and controlled separately by the PLD. The two units worked independently, before their modulation signals were inputted to a mono-chip micro-processor (AT80C51) for the measurement of the modulation frequency (or period), from which the fluorescence lifetimes of the probes (the temperature sensitive factors) were obtained and which were calibrated against temperatures. The mono-chip microprocessor was connected to a PC via a RS-232 serial port for data transmission. The changing temperature values were recorded, with time, automatically in the computer. The probes used were based on those reported previously [3] where the sensing fluorescence material used was a Tm-doped YAG crystal which was coupled into a silica optical fibre. Two Y-shaped fibre bundles were also used to transmit the exciting laser light to the probes and to collect the fluorescence emission from them. The construction of the probe is shown schematically in Figure 7.4. In this system, the relationship between the fluorescence lifetime and the temperature recorded by the two fluorescent probes used (termed probe 1 and probe 2) has been carefully calibrated over the temperature range from room temperature to 800 ^{0}C.

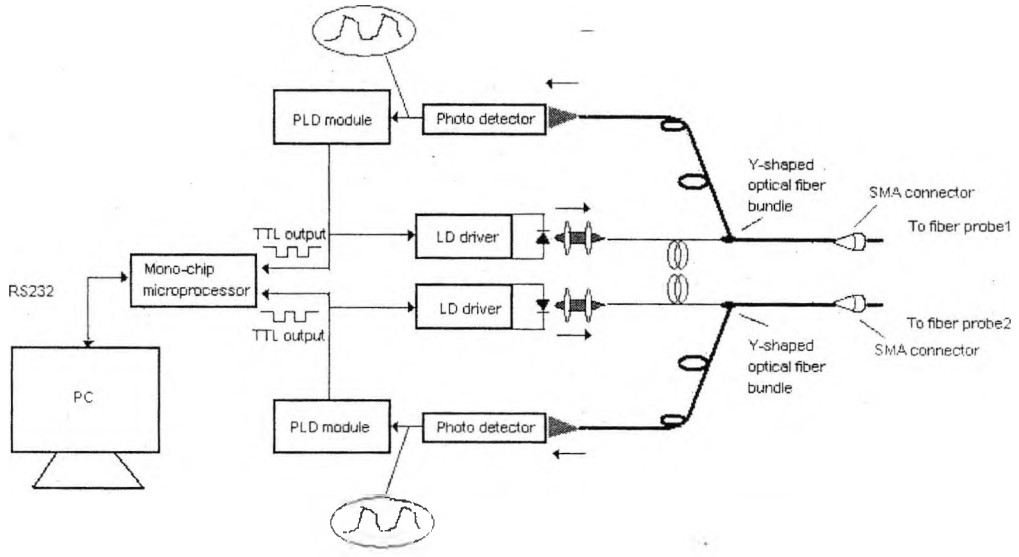

Figure 7.3 Schematic diagram of the fluorescence lifetime based fibre sensor system (System A), in which two PLD units were incorporated (PLD- phase locked detection, LD-laser diode, PC- computer)

A cross-comparison between the performance of a single probe fluorescence lifetime based

fibre thermometer and a K-type thermocouple had been carried out repeatedly in the laboratory, as reported by Shen et al [3], and also performed at Corus, UK [7] in tests on refractory materials. It is clear that the temperature data obtained using the fibre-optic sensor scheme closely matches that obtained from the thermocouple, except that the response time of the fibre-optic sensor is somewhat faster than that of the thermocouple used.

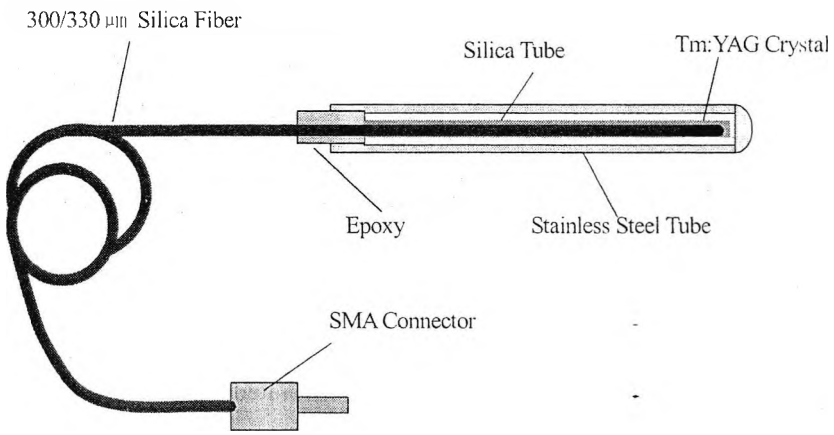

Figure 7.4 Schematic diagram of one of the Tm:YAG crystal based fibre-optic sensing probes used in System A

B. FBG-based fibre-optic thermometer system ? System B

The principle of the FBG-based fibre sensor used in these experiments has been discussed in reference [8]. However it is important to note that the fibre used was carefully chosen to have a high sustainability of the FBGs written into it at the high temperature at which the measurement [6] was carried out. The availability of such gratings in specialized fibre has opened up the potential for this type of experiment using a FBG-based measurement system. By inscribing two gratings into a Sb/Er/Ge co-doped photosensitive fibre by means of exposure via a phase-mask with UV light [2], two peaks in the reflection spectrum could be readily identified and interrogated with the use of an OSA. When the fibre probe was loosely placed in a stainless steel tube, the effect of strain on the FBGs could be neglected. Thus, the full wavelength shift of the peak reflectance in the spectrum obtained could be attributed only to the temperature change at the position of the FBG. The gratings were ~ 6.5 mm in length, effectively a point sensor and approximately the same size as the active medium of the fluorescent sensor. Using prior calibration, these values of the

wavelength shift could be used to measure the temperature accurately. The wavelength values of the gratings were recorded, with time, every two minutes. The calibration curve of the peak wavelength of the FBG written into the Sb/Er/Ge fibre via temperature is illustrated in Figure 7.5, and a systematic illustration of the FBG sensing system is presented in Figure 7.6.

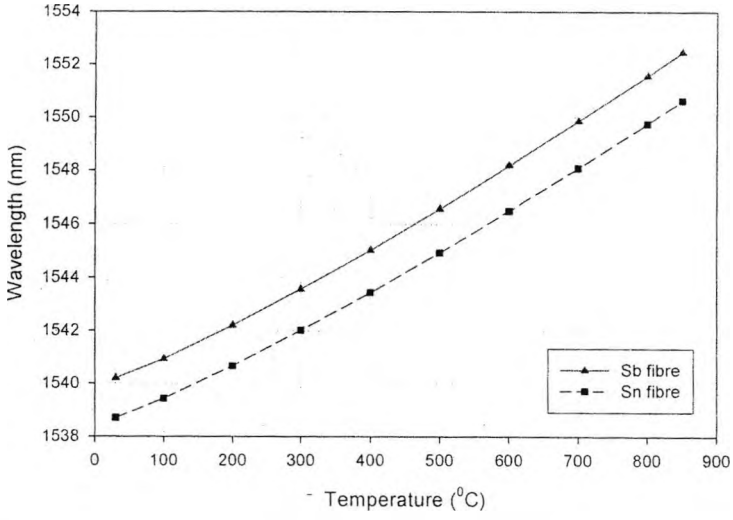

Figure 7.5 Calibration curve of the peak wavelength in the reflection spectrum with temperature for the FBGs written into the Sb/Er/Ge fibre, and for comparison using Sn/Ge fibre with temperature.

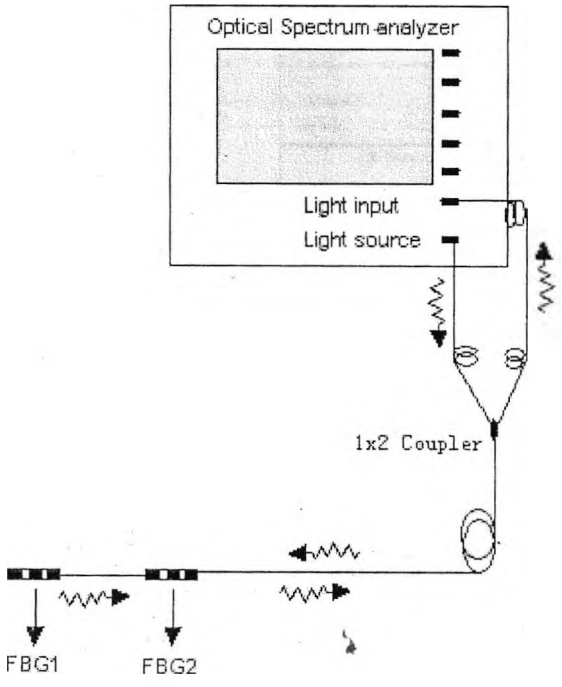

Figure 7.6 Schematic diagram of the operation of the FBG based fibre-optic sensor system, System B

7.2.3 Probe installation

A Carbolite tube-oven with a highest working temperature of 1400 ^{0}C was used as the heat source. The tube was cylindrical in shape and of even diameter of 30 mm along its length of 1100 mm. This cylindrical configuration is well suited to the calibration of the sensor systems and to the measurement of heat flux along the axis of the oven.

The two probes from the fluorescence based fibre thermometer system were installed separately in the outlet tube of the Carbolite tube-oven to measure the temperature of two points separated by a chosen distance of 85 mm, determined from the oven dimensions. The probe with two FBGs written into the fibre was also placed into the tube beside the two fluorescence lifetime sensing probes, with the same distance between the two sensing points – the gratings are also 85 mm apart. However, it should be mentioned that the position of the FBG probe was displaced when compared with that of fluorescence based fibre-probes, by 20 mm overall, as illustrated in Figure 7.7.

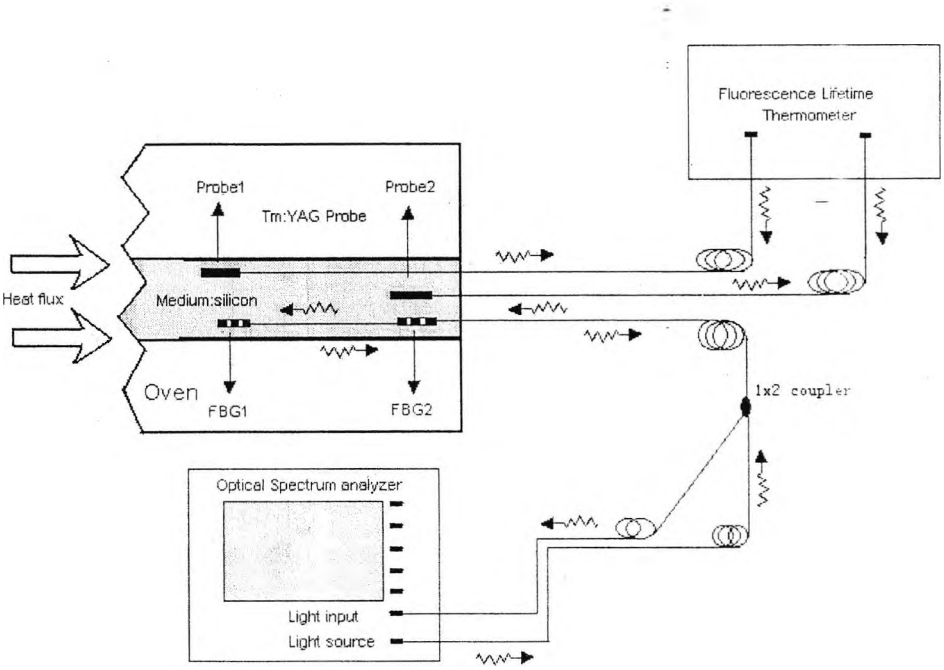

Figure 7.7 Schematic of the installation of System A and System B for the heat flux measurements. The two probes used in the fluorescence scheme based were installed separately at a distance one from the other of 85 mm, and the probe with the two FBGs written into the fibre was placed beside the fluorescence-based

Two types of media were used, and their heat flow characteristics compared. These media were air (i.e. no other medium involved inside the tube except the probes themselves) and silica powder (with a conductivity of about 0.012 W/cm.K at room temperature [9]).

These two configurations were used in an experiment to monitor the heat-flux from the centre of the tube-oven through the probes. The temperature change during the temperature rise, stabilization and cooling down will be different for the two probes, separated as they are by a significant distance (85 mm), and this indeed was confirmed by the experimental results (which are detailed in the next section). It should be noted that in the case of air as the medium, the diffusion and the convection activity of the air will cause some error in the heat flux measurement, compared with the effect of conduction, but these effects are minimized in a tube oven design of this type.

7.2.4 Results and their analysis

Monitoring was carried out continuously over several days, with the air and the silica powder used as the conductive media, in separate experiments. The results of the temperature change with time are illustrated in Figure 7.8 and Figure 7.9 for the air and the silica media respectively, where the temperature difference between the two points being monitored is also seen.

From the results obtained, it is clear that the temperature change of each probe in each sensor system followed the same trend, reflecting the temperature of the oven at those points, away from the peak, centre temperature. For the case where air is the medium, the temperature difference between the two probes in both Systems A and B was comparatively small, when compared with the situation with the silica medium. As discussed above, this has mainly resulted from the fact that the air in the tube would be more diffusing and convective, in addition to having a different thermal characteristic for conduction, and thus the heat flux measured would be different from that for the powder material. If equation (7.1) is considered, it would appear that the heat flux is directly proportional to the temperature difference, T_1-T_2, and that a small value of T_1-T_2 would be associated with a small heat flux. However, if the effect of diffusion and convection is also considered, it can be understood that the term k in equation (7.1) was large and

thus the equation should still result in a large value of heat flux. As the effect of diffusion and convection on the heat flux measurement, and thus the value of k, was quite difficult to be determined precisely in this work, it is more difficult to compute the heat flux precisely. However, the cylindrical geometry of the oven helps to minimize the other losses and give a closer value for k for the case of air, and these problems are minimized for the silica powder measurement.

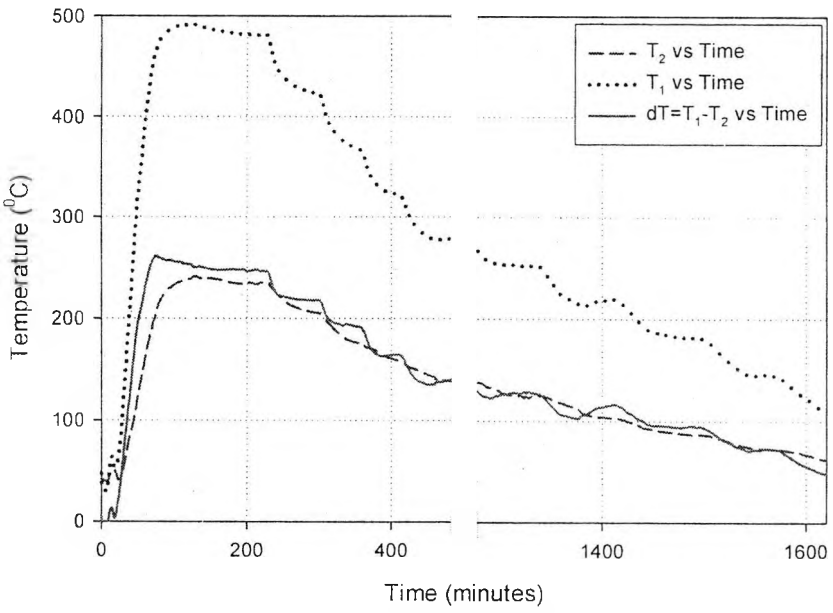

(a)

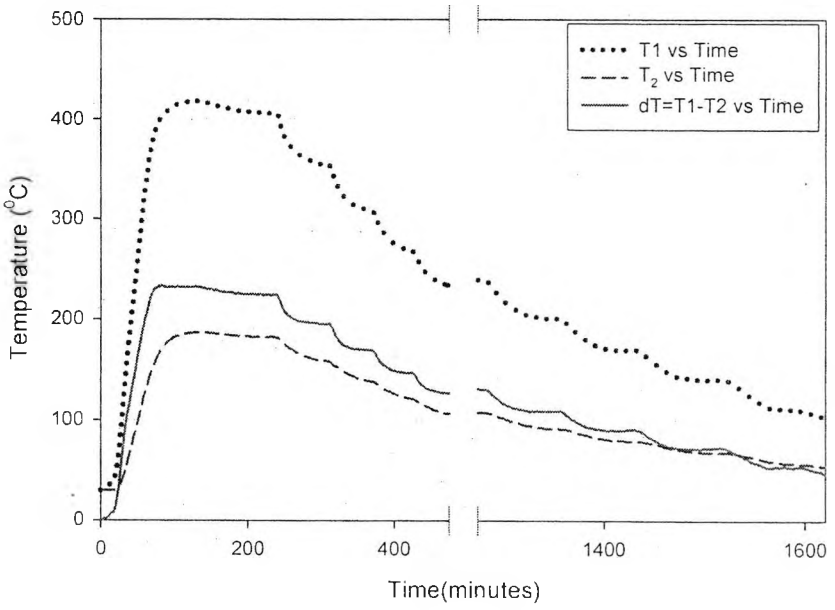

(b)

Figure 7.8 Temperature changes of the probes with time when the medium was air. (a). using the fluorescence lifetime based fibre thermometer, System A (b). with the FBG-based fibre-optic sensor, System B

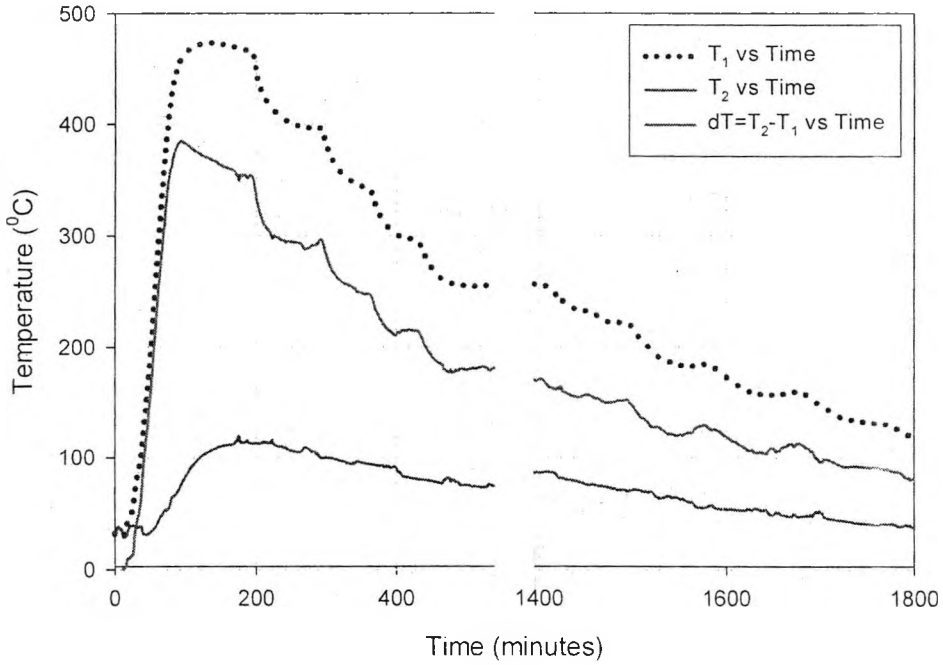

(a)

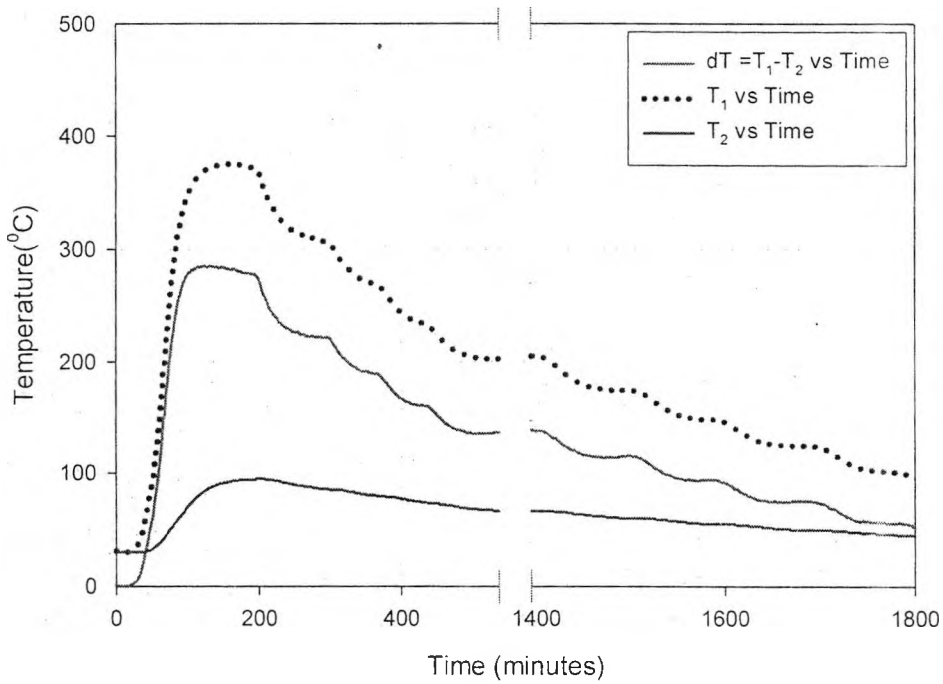

(b)

Figure 7.9 Temperature changes of the probes with time when silica powder was used as the medium, (a) with the fluorescence lifetime based fibre thermometer, System A and (b) with the FBG-based fibre-optic sensor, System B

The data, in Figure 7.9, show a number of interesting features. The first point to note is that during the heating of the oven, the two fluorescent probes (or the two gratings) reached their highest temperatures separately and in sequence. It was faster for the probe 1 and slower for probe

2 for both Systems A and B. This is simply a reflection of the flow of heat from the centre of the oven and it means that the heat flux was from the hotter point registered by probe 1 and then, after some time, the second probe experienced the heat flux traveling from the centre of the oven. The second point is that the largest value of T_1-T_2 arose before both probe 1 and probe 2 reached their highest temperatures. This is an indication of the specific heating characteristic of the oven used and could be useful for oven temperature control. The third point is that the process of thermal stabilization at different nominal oven temperatures, such as 1000 ^{0}C, 900 ^{0}C etc. all showed a decreasing, followed by a gradually stabilizing, temperature difference, which is consistent with the first point on the nature of the oven heating. However, at lower oven set-temperatures, for example, from 500 ^{0}C to room temperature, the stabilization process showed a large "over-run" phenomenon. Comparing the "over-run" value of T_1-T_2 with the temperature changes recorded by probe 1, shown in Figures 7.8 and 7.9, they are clearly larger. In the process of cooling, it can be seen that the speed of cooling was different with probe 1 and probe 2 in their respective positions of the oven.

When the data, showing the temperature difference in Figure 7.9, were used to compute the heat flux using equation (7.1), it can be seen that the value of k is different for the situation shown in Figures 7.9a and 7.9b respectively. This is due to the fact that the temperature differences in Figure 7.9a and 7.9b were also quite different from each other, but they should give the same value of heat flux, Q, as in both situations the same heating phenomenon is seen in the same tube. By using the published conductivity value given by [9] and making the reasonable assumption that it is constant for this work (it is acceptable to apply such an approximation when the temperature is close to room temperature [10]), the heat flux change with temperature was then computed and this is shown in Figure 7.10. It can be seen that the heat flux values computed from Figure 7.9a and from Figure 7.9b are very similar for both Systems A and B. Based on this result, at temperatures around room temperature, it appears that the conductivity coefficient at higher temperature is a little lower than that at lower temperature. The difference is illustrated in Figure 7.10 and this has mainly resulted from the approximation used for the conductivity coefficient, however, a clear result, showing the same trend for Systems A and B, is seen.

Compared with the heating power of the oven (around 1 kW at a temperature of 1000 ^{0}C), the heat flux values presented in Figure 7.10 shows a relatively small value of power through the

probes. This is reasonable if the geometry of the oven and the small cross section of the probe in the tube, together with the large layer thickness of the silica powder used (over 150 mm) are taken into consideration. The heat produced by the power applied to the oven is mainly dissipated through other outlets and the other surfaces of the oven compared to the small flux monitored through the fibre optic probes.

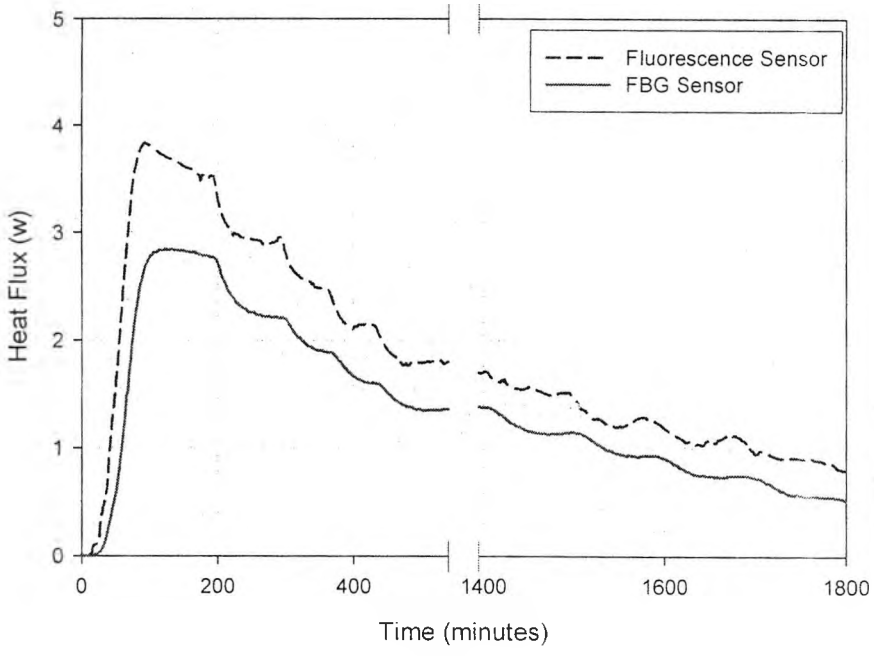

Figure 7.10 Heat flux change with time. The heat flux data reflect the value of energy passing through the probes in the two systems used (placed at 20 mm from each other)

7.2.5 Discussion

The work reported above shows a novel approach to measure the heat flux in an oven by using fibre-optic sensors and employing two different fibre-optic monitoring techniques. The results obtained are quite encouraging and support the simplicity of the approach and the inherent advantages of fibre-optic sensors and especially the ability to multiplex several fibre sensing probes based on a demonstration of the two probes in each system. It would be feasible to apply these fibre-optic sensor systems to the monitoring of the heat flux of a range of materials, e.g., concrete or cement bricks and the lining of ovens and furnaces, especially when the medium concerned does not show significant diffusion and convection as alternative routes for heat loss.

Using either system, it would also be possible to measure the temperature dependence of the conductivity of some specific insulating media using a multi-probe fibre-optic sensor, and such a scheme is proposed in Figure 7.11, using an extended vesion of System B, with several evenly spaced FBGs to monitor the temperature distribution of the medium when the heat flows from one side to another. As the peak wavelength position of each FBG corresponds to a temperature at which the FBG is situated, the temperature difference between any two FBGs (consecutive or otherwise of known spacing) could easily be calculated. By monitoring the temperature between any two gratings, the temperature dependence of the conductivity in the medium studied could be easily determined. In such a system, the FBG based sensor is likely to be more suitable, especially for multiple measurements. In another context, many such sensors have been multiplexed along a single fibre cable, allowing for a simpler installation of the sensor system.

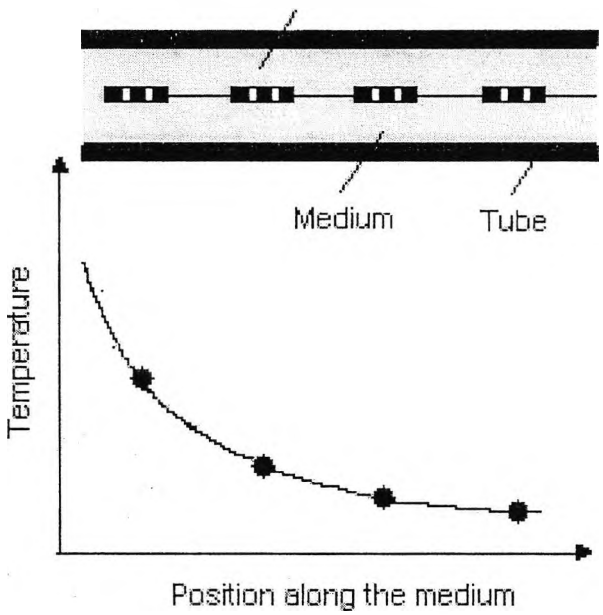

Figure 7.11 Schematic of a proposed system for the measurement of temperature dependence of the conductivity coefficient

The two types of fibre-optic sensors used in the recent experiments have both shown themselves effective and they are both capable of performing multi-point temperature measurements simultaneously. The disadvantage of the FBG-based System B is that there is a greater strain uncertainty than for System A using fluorescence, and as the fibre is subject to strain, separate measurements must be made and a correction is applied. However, for multipoint measurements, System B is easier to configure as many gratings can readily be written along the

same fibre probe used. The results obtained from the experiments using System A or B are very encouraging for heat flux monitoring and work is continuing to explore different possibilities.

7.3 Summary

In this chapter, performance evaluations in a heat flow application of a fibre optic thermometer using fluorescence lifetime scheme and an FBG-based thermometer in an industrial field were presented. The cross-referencing experiment of process temperature measurement in a refractory cement brick showed good long-term system stability and dynamic response when compared with the result from a K-type thermocouple.

Both the fibre optic thermometer based on the fluorescence lifetime and the fibre-optic sensing system using the peak wavelength interrogation of fibre Bragg gratings have been applied to test the heat flux of tube oven in an attempt to explore this application of fibre-optic sensors. The preliminary results obtained also showed very promising prospect for these fibre sensors to be used in such applications in industry.

7.4 References

[1] K.T.V. Grattan, Z. Y. Zhang, Fibre Optic Fluorescence Thermometry, Chapman & Hall (1995)

[2]A.Othonos and K. Kalli, "Fibre Bragg Gratings: Fundamentals and applications in telecommunications and sensing", Artech House, Boston (1999)

[3] Y.H.Shen, W.Z.Zhao, T. Sun, K.T.V. Grattan, "Characterization of an optical fibre thermometer using Tm^{3+}:YAG crystal, based on the fluorescence lifetime approach", Sensors and Actuators: A. Physical, 109, pp53-59 (2003)

[4] Y.H. Shen, W.Z.Zhao, J. He, T. Sun, K.T.V. Grattan, "Fluorescence decay characteristic of Tm-doped YAG crystal fibre for sensor applications, investigated from room temperature to 1400 ^{0}C", IEEE Sensors Journal, 3, p507-512 (2003)

[5] P.R. Childs, J.R. Greenwood and C.A. Long, "Heat flux measurement techniques", Proc. Instn. Mech. Engrs., 213, part C, pp655-677 (1999)

[6] Y. Shen, T. Sun, K.T.V. Grattan and M. Sun, "Highly photosensitive Sb/ Er/Ge codoped silica fibre for fibre Bragg grating (FBG) writing with strong high-temperature sustainability", Optics Letters, 28, pp2025-2027 (2003)

[7] W. Zhao,Y.H. Shen, S.Pal, et al, "Optical fibre systems for measurement of high temperature," Conference on On-Line Measurements for Quality in the Metals Industries, October 2003, London, UK (IOM Communications, London, 2003)

[8] S.A.Wade, D.I. Forsyth, K.T.V. Grattan, Q. Guofu "Fibre optic sensor for dual measurement of temperature and strain using a combined fluorescence lifetime decay and fibre Bragg grating technique", Review of Scientific Instruments, 72, pp3186-3190 (2001)

[9] G.E. Childs, L.J. Ericks and R.L. Powell, "Thermal conductivity of solids at room temperature and below", NBS Monograph 131 (1973)

[10] L. R. Ingersoll, O. J. Zobel and A. C. Ingersoll, Heat conduction with engineering and geological applications, McGRAW-HILL Book Company, INC. (1948)

Chapter 8 Conclusions

8.1 Summary of major achievements

8.1.1 Review of the achievements of the work

The main work of this thesis has been focused on the following two major aspects: novel fibre thermometry based on the fluorescence lifetime of the sensing materials and strong FBGs and the related novel photosensitive fibres. Several major achievements have been made on both aspects and these are briefly reviewed again as follows:

1. Tm doped YAG crystal was selected as the sensing material of a fluorescence lifetime based fibre thermometer developed. Its strong fluorescence and long lifetime value from room temperature to above 1200 ^{0}C enabled the thermometer based on this crystal to cover a wide temperature with a relatively high resolution over the whole region [1].

2. After a comprehensive investigation of the fluorescence characteristics of Tm:YAG crystal, a novel fibre thermometer was constructed. The phase-locked-detection (PLD) signal processing scheme reported by previous authors [2] for the fluorescence lifetime measurement has also been improved to compensate the strong background radiation at high temperatures. As a result, the fibre thermometer developed can operate successfully over a temperature range from room temperature to 1200 ^{0}C. Good repeatability and long term stability has been confirmed [3].

3. Novel photosensitive fibres with dopants of Sb, In and Bi have been developed for strong FBG fabrication by use of the MCVD technique. Tests on the FBG fabrication showed that these fibres are all photosensitive to varying degrees and suitable for strong FBG fabrication. Annealing tests on the FBGs written into these fibres revealed that the gratings embedded in these fibres could sustain higher temperatures, up to 800 ^{0}C or even 900 ^{0}C for substantial periods and are thus valuable for sensing application at high temperatures [4][5][6][7].

4. Based on the annealing experimental results for FBGs written into Sb, In and Bi co-doped photosensitive fibres, a theoretical model, termed the Cation-Hopping model, was presented to account for the extremely satisfactory high temperature sustainability of these gratings, as well as the large photosensitivity of the fibres thus developed. Simulation based on the cation-oriented trap energy distribution has demonstrated better agreement with the experimental data than that achieved using the previously reported model [8].

5. Both the fluorescence lifetime based fibre thermometer and FBG based sensing systems were employed to measure the heat-flux in a tube oven. Tests carried out and results obtained have shown promising prospect for fibre sensor applications in the industrial fields [9].

6. Arising from the work, eight journal and four international conference papers have been produced and all have now been published.

8.1.2 Outline of the major innovation of this work

Arising form the achievements reviewed above, the major innovative aspects of the work are outlined as follows.

1. For the first time, the Tm:YAG crystal was used as the sensing material in a fluorescence -based fibre thermometer. The fibre thermometer thus developed has shown to cover a wide range of temperature with a distinctively high resolution, much better than that in the former published works [1][3].

2. Novel Sb, In or Bi doped fibres with very good photosensitivity have been developed for the first time for strong FBG fabrication. The gratings written into these fibres were able to sustain high temperatures, up to 900 ^{0}C over a substantial period, much higher than that with gratings in other materials also fabricated by means of UV exposure[4][5][6].

3. A theoretical model, termed Cation Hopping, was proposed to account for the extremely good temperature sustainability of the gratings written into the photosensitive fibres developed. The model can be effectively used to inform the design and development of novel photosensitive fibres with superior performance [5].

4. Fibre thermometers based on the fluorescence lifetime scheme and the FBG scheme have both been applied to test the heat flux in a tube oven for the first time and results have been obtained in the industrial context [9].

8.2 Suggestions for further work

Based upon the results reported in this thesis, further work may possibly be important in the field of fluorescence lifetime based fibre thermometry. For example, a detailed investigation of the concentration effects of Tm dopant in the YAG crystal would be valuable in obtaining a fuller knowledge of the concentration dependence of the fluorescence lifetime and the fluorescence

intensity, and thus to provide a means of optimizing the probe by a suitable choice of dopant concentration. Further improvement of the voltage-frequency unit in PLD processing circuit is necessary so that it can cover a wider range of fluorescence lifetime and thus monitor the corresponding temperature.

In the field of FBG related fibre-optic sensors, further work should be performed on novel devices. The first is to develop some more photosensitive fibres with the help of the Cation Hopping model. Fibres with heavy Bi dopant and low Ge concentration would appear to be especially important. The second is to test the performance of the gratings over a longer term at some specific temperatures. Such tests may give further information on the potential of these gratings or fibres in fibre optic sensors to cover a wider temperature region. The third is to employ further efforts to investigate the nucleating and crystallizing phenomena in the doped silica fibres which may possibly happen at temperatures above 900 ^{0}C. That will be essential for the development of novel photosensitive fibres with better high temperature performance. The work has shown the importance of the different compositions of dopants in photosensitive fibres and the potential for a range of further applications.

8.3 References

[1] Y. Shen, W.Z. Zhao, J. He, et al, "Fluorescence decay characteristic of Tm-doped YAG crystal fibre for sensor applications, investigated from room temperature to 1400 °C", IEEE Sensors Journal, 3, pp507-512 (2003)

[2] K.T.V. Grattan, Z. Y. Zhang, Fibre Optic Fluorescence Thermometry, Chapman & Hall (1995)

[3] Y. Shen, W.Z. Zhao, T. Sun and K.T.V. Grattan, "Characterization of an optical fibre thermometer using Tm^{3+}:YAG crystal, based on the fluorescence lifetime approach", Sensors and Actuators: A. Physical, 109, pp53-59 (2003)

[4] Y.Shen, T. Sun, K.T.V. Grattan and M. Sun, "Highly photosensitive Sb/ Er/Ge codoped silica fibre for fibre Bragg grating (FBG) writing with strong high-temperature sustainability," Optics Letters, 28, pp2025-2027 (2003)

[5] Y. Shen, J. He, T. Sun and K.T.V. Grattan, "High temperature sustainability of strong FBGs written into Sb/Ge co-doped photosensitive fibre — decay mechanisms involved during annealing", Optics Letters, 29, pp554-556 (2004)

[6] Y. Shen, J. Xia, T. Sun and K.T.V. Grattan, "Photosensitive Indium doped germano-silica fibre for strong FBGs with high temperature sustainability", IEEE Photonics Technology Letters, 16, pp1319-1321 (2004)

[7] Y. Shen, S. Pal, J. Mandal, et al, "Investigation on the photosensitivity, temperature sustainability and fluorescence characteristics of several Er-doped photosensitive fibres", Optics Communications, 237, pp301-308 (2004)

[8] T. Erdogan, V. Mizrahi, P.J. Lemaire and D. Monroe, "Decay of ultraviolet-induced fibre Bragg gratings," J. Appl. Phys., 76, pp73-80 (1994)

[9] Y. Shen, J. He, W. Zhao, T. Sun and K.T.V. Grattan，"Fibre-optic sensor system for heat flux measurement"，Review of Scientific Instruments, 75, pp1006-1012(2004)

Relevant Publications by the Author

A. papers published in Journals

1. J. Mandal, **Y. Shen**, S. Pal et al, "Bragg grating tuned fibre laser system for measurement of wider range temperature and strain", **Optics Communications**, 244, pp111-121 (2005)

2. **Y. Shen**, S. Pal, J. Mandal, et al, "Investigation on the photosensitivity, temperature sustainability and fluorescence characteristics of several Er-doped photosensitive fibres", **Optics Communications**, 237, pp301-308 (2004)

3. **Y. Shen**, J. Xia, T. Sun and K.T.V. Grattan, "Photosensitive Indium doped germano-silica fibre for strong FBGs with high temperature sustainability", **IEEE Photonics Technology Letters**, 16(5), pp1319-1321 (2004)

4. **Y. Shen**, J. He, W. Zhao, T. Sun and K.T.V. Grattan, "Fibre-optic sensor system for heat flux measurement". **Review of Scientific Instruments**, 75(4), pp1006-1012 (2004)

5. **Y. Shen**, J. He, T. Sun and K.T.V. Grattan, "High temperature sustainability of strong FBGs written into Sb/Ge co-doped photosensitive fibre — decay mechanisms involved during annealing", **Optics Letters**, 29(6), pp554-556 (2004)

6. **Y. Shen**, W.Z. Zhao, T. Sun and K.T.V. Grattan, "Characterization of an optical fibre thermometer using Tm^{3+}:YAG crystal, based on the fluorescence lifetime approach", **Sensors and Actuators: A. Physical**, 109(1-2), pp53-59 (2003)

7. **Y. Shen**, T. Sun, K.T.V. Grattan and M. Sun, "Highly photosensitive Sb/ Er/Ge codoped silica fibre for fibre Bragg grating (FBG) writing with strong high-temperature sustainability," **Optics Letters**, 28(21), pp2025-2027 (2003)

8. **Y. Shen**, W.Z. Zhao, J. He, et al, "Fluorescence decay characteristic of Tm-doped YAG crystal fibre for sensor applications, investigated from room temperature to 1400 °C", **IEEE Sensors Journal**, 3(4), pp507-512 (2003)

B. Papers presented in Conferences

1. W. Z. Zhao, **Y. Shen**, T. Sun, et al. "Precision free electron laser materials adhesion monitoring using an optical fibre temperature sensor system", Technical Digest, P248-251, 16th international conference on optical fibre sensors, (OFS-16), Oct., Japan Technical Digest

2. W. Z. Zhao, **Y. Shen**, et al. "Optical fibre systems for measurements of high temperature", Conference on "On-line measurements for quality in the metals industries", October 2003, London, UK

3. **Y. Shen**, T. Sun, K.T.V. Grattan and M. Sun, "High-temperature sensor potential and sustainability of fibre Bragg gratings written in highly photosensitive Sb/Er/Ge codoped silica fibre", Paper presented at Sensors and their Applications XII, September 2003, Limerick, Ireland

4. **Y. Shen**, W. Zhao, J. He, T. Sun, K.T.V. Grattan, "Fibre thermometer based on the cross detection of the fluorescent decay of Tm:YAG crystal fibre and background radiation", SPIE Proceedings, V4920, pp16-24 (2002)